

**LIVER-TARGETED TRANSCRIPTION
ACTIVATOR-LIKE EFFECTOR
REPRESSORS THAT INACTIVATE HBV
CCCDNA**

Haajira Kaldine

A dissertation submitted to the Faculty of Health Sciences, University of the
Witwatersrand, in fulfillment of the requirements for the degree
of
Master of Science in Medicine

Johannesburg, 2017

Declaration

I, Haajira Kaldine (student number: 395158) declare that this dissertation is my own work.

It is being submitted for the degree of Master of Science in Medicine at the University of the Witwatersrand, Johannesburg. It has not been submitted before for any degree or examination at this or any other University.

.....

.....day of, 2017

Dedication

To my son Isma'eel

A tribute for providing me with the motivation to follow through.

Publications and presentations

Conference Proceedings

1. Kaldine H, Ely A, Arbuthnot P. (2016). Liver-targeted Transcription Activator-Like Effector repressors for the transcriptional inhibition of HBV cccDNA. DST-NRF Nanotechnology Symposium poster presentation, 27-28 June 2016, Pretoria, South Africa.

Abstract

The hepatitis B virus (HBV) continues to be a global health threat as chronic infection may lead to cirrhosis and hepatocellular carcinoma (HCC). Current treatments are limited in efficacy and do not target the stable HBV covalently closed circular DNA (cccDNA) minichromosome which forms the template for viral replication and is responsible for persistence of the infection. Using gene editing technologies to disable cccDNA presents a potential approach for treating HBV infection. Transcription activator-like effector (TALE) proteins provide specific and adaptable DNA binding modules, which can be used to generate engineered proteins capable of modifying DNA. Transcription activator-like effector nuclease (TALEN) mediated cleavage of cccDNA has been shown to effectively inhibit HBV replication. However, the approach to transcriptionally silence cccDNA, instead of cleaving it, may overcome the risk of unwanted host DNA cleavage. Repressor transcription activator-like effectors (rTALEs), which target and transcriptionally silence genes, have shown potential as antiviral agents. Here we generated Krüppel-associated box (KRAB)-based rTALEs targeted to the *surface* open reading frame (ORF) and HBx promoter region of HBV cccDNA to inhibit transcription. The rTALEs were placed under the transcriptional control of the liver-specific modified murine transthyretin (mTTR) promoter, to restrict activity to hepatocytes thereby reducing the potential for off-target activity. *In vitro* the mTTR-driven rTALEs were shown to tissue specifically decrease secreted HBV surface antigen (HBsAg) levels by 63 - 92 %. Additionally, the mTTR-driven rTALEs were shown to tissue specifically decrease *surface* mRNA levels by 65 – 81 % and pregenomic RNA levels by 60 - 76 %. These results indicate that the KRAB domain was able to effectively suppress transcription from the basic core, Pre-S1 and/or

Pre-S2 promoters which otherwise regulates HBV transcription. Furthermore, the observed inhibition was not associated with cytotoxicity or off-target effects. The work presented here is a proof-of-concept study demonstrating that highly specific transcriptional repressors designed to target and inhibit HBV viral replication without altering the genetic sequence or causing mutations in the host genome may be a promising antiviral approach. The capabilities of this technology to directly target cccDNA and inhibit its transcription, could contribute to addressing a global health problem.

Acknowledgements

I would like to extend my immense gratitude to my supervisors Dr Abdullah Ely and Prof. Patrick Arbuthnot, for their patience and providing me with unfailing support, assistance and continuous encouragement throughout my research and dissertation writing.

I am thankful to Toni Cathomen for supplying the rTALE plasmids and Kristie Bloom for supplying the TALEN plasmids.

Thank you to Dr Musa Marimani for his assistance on challenging aspects of my project.

I am also grateful for all the members of the Antiviral Gene Therapy Research Unit (AGTRU) for their assistance.

I wish to extend my heartfelt gratitude to my family for their limitless and unwavering support. Special thanks to my parents Zainodine and Jawahier for their continuous love, support, patience, and prayers without which the completion of this work would not be possible. I am also grateful to my siblings Fatheela (and her husband Oleg), Abduragheem, Moegammad, Abdunnoer and Thaakirah, for their assistance and encouragement, and to my aunts Chrissie and Shouline for their support.

A special thank you to my dear friend Yamnkela for his assistance, support, and words of encouragement when I needed it the most.

Finally, I am grateful for the funding from the National Research Foundation (NRF) of South Africa.

Table of Contents

Declaration.....	ii
Dedication.....	iii
Publications and presentations.....	iv
Conference Proceedings.....	iv
Abstract.....	v
Acknowledgements	vii
List of Figures.....	xii
List of Abbreviations	xv
1. Introduction	1
1.1 Epidemiology and transmission of hepatitis B virus	1
1.2 HBV molecular biology and replication	2
1.3 HBV management.....	8
1.4 Gene editing technologies.....	11
1.5 Engineering TALE proteins	13
1.6 Transcriptional repression of HBV	16
1.7 Aims.....	21
2. Materials and Methods	22
2.1 Plasmids	22
2.1.1 pCH-9/3091	22
2.1.2 pCI-neo-eGFP	22

2.1.3 pTZ57R	22
2.1.4 pRK5-CMV-rTALE plasmids	23
2.2 Plasmids constructed in this study	26
2.2.1 Construction of mTTR-driven KRAB-based rTALEs targeted to the HBV ORF	26
2.3 Plasmid preparation	36
2.4 Mammalian cell culture	36
2.5 Determination of rTALE expression in cell culture	37
2.5.1 Transient transfection of cultured mammalian cells with rTALE expression vectors	37
2.6 Assessing rTALE-mediated HBV gene knockdown	38
2.6.1 Transient transfection of cultured mammalian cells with rTALE expression vectors	38
2.4 Assessment of potential cellular toxicity	42
2.4.1 Examining potential rTALE-mediated cell toxicity	42
2.4.2 Examining potential off-target binding	43
2.5 Statistical analysis	45
3. Results	46
3.1 Successful generation of mTTR-driven rTALE vectors	46
3.2 Liver-specific expression of mTTR rTALEs <i>in vitro</i>	50
3.3 Anti-HBV rTALEs mediate efficient transcriptional silencing of viral gene expression	57

3.3.1 rTALE-mediated inhibition of HBsAg expression <i>in vitro</i>	57
3.3.2 rTALE-mediated repression of HBV transcription <i>in vitro</i>	60
3.4 Evaluation of potential rTALE-mediated cytotoxicity	64
3.4.1 rTALE expression does not alter cell viability.....	64
3.4.2 rTALEs do not interfere with expression of potential off-target genes	66
4. Discussion.....	71
4.1 Tissue-specificity	71
4.2 Anti-HBV activity.....	72
4.3 Cytotoxicity.....	76
4.4 Challenges facing anti-HBV gene therapy	77
4.5 Potential antiviral combinatorial therapy.....	80
4.6 Conclusion	81
5. Appendix	82
5.1 Additional figures	82
5.2 Laboratory techniques.....	94
5.2.1 Gel Electrophoresis	94
5.2.2 Gel extraction	95
5.2.3 Preparation and transformation of chemically competent <i>E. coli</i>	96
5.2.4 High Pure Plasmid Isolation.....	98
5.2.5 Plasmid Maxi preparation	99
5.2.6 Mycoplasma detection.....	100
5.2.7 jetPRIME® transfection.....	100

5.2.8 Lipofectamine® 3000 transfections	101
6. References:	103

List of Figures

Figure 1.1: Hepatitis B virus genomic organisation	4
Figure 1.2: Hepatitis B virus replication cycle	7
Figure 1.3: Schematic diagram of a naturally occurring TAL effector	15
Figure 1.4: Schematic representation of the rTALE design and rTALE mediated transcriptional repression.....	20
Figure 2.1: Schematic diagram of the promoter insert fragment	25
Figure 2.2: Schematic diagram of the cloning strategy used to generate the pRK5-mTTR-control plasmid	27
Figure 2.3: Schematic diagram of the cloning strategy used to generate the pRK5-mTTR-plasmids.....	32
Figure 3.1: Confirmation of complete pRK5-mTTR-rTALEs assembly	44
Figure 3.2: Confirmation of rTALE identity	45
Figure 3.3: Immunofluorescence detection of rTALEs <i>in vitro</i>	48
Figure 3.4: Immunofluorescence detection of control rTALEs <i>in vitro</i>	49
Figure 3.5: Immunofluorescence detection of S1 rTALEs <i>in vitro</i>	50
Figure 3.6: Immunofluorescence detection of S2 rTALEs <i>in vitro</i>	51
Figure 3.7: Immunofluorescence detection of X1 rTALEs <i>in vitro</i>	52
Figure 3.8: Immunofluorescence detection of X2 rTALEs <i>in vitro</i>	53
Figure 3.9: Assessment of rTALE-mediated knockdown of HBsAg in Huh 7 (A) and HEK293T (B) cells	57
Figure 3.10: Assessment of rTALE-mediated knockdown of HBV mRNA <i>in vitro</i>	60

Figure 3.11: Assessment of rTALE-mediated knockdown of HBV mRNA <i>in vitro</i>	61
Figure 3.12: Assessment of cell viability	63
Figure 3.13: Evaluation of rTALE off-target activity	68
Figure 5.1: CMV-driven rTALE plasmid map	82
Figure 5.2: mTTR-driven rTALE plasmid map	83
Figure 5.3: Agarose gel electrophoresis of the digested plasmids for backbone preparation	84
Figure 5.4: Agarose gel electrophoresis of <i>Bpi</i> I digested pUC57-mTTR	85
Figure 5.5: Agarose gel electrophoresis of digested pRK5-CMV-X2-rTALE for insert extraction	86
Figure 5.6: Agarose gel electrophoresis of digested pRK5-CMV-S1-rTALE and pRK5-CMV-S2-rTALE for insert extraction	87
Figure 5.7: Agarose gel electrophoresis of the digested plasmids for backbone extraction	88
Figure 5.8: Transfection efficiency of Huh 7 and HEK293T cells (ELISA)	89
Figure 5.9: Transfection efficiency of Huh 7 and HEK293T cells (HBV RT-qPCR)	90
Figure 5.10: Transfection efficiency of Huh 7 cells (MTT assay)	91
Figure 5.11: Transfection efficiency of Huh 7 cells (Off-target RT-qPCR)	91
Figure 5.12: Melting curve analysis from qPCR of the <i>prostate androgen-regulated transcript 1 (PART1)</i> gene	92
Figure 5.13: Agarose gel electrophoresis of qPCR products	93

List of Tables

Table 2.1: Amino acid sequences of the S1 and S2- rTALEs and their target viral DNA sequence.....	31
Table 2.2: Amino acid sequences of the X1 and X2- rTALEs and their target viral DNA sequence.....	41
Table 2.3: Sequences of the primers used in q-PCR to amplify the HBV and h <i>GAPDH</i> genes.....	31
Table 2.4: Sequences of the primers used in q-PCR to amplify the potential rTALE off-target binding sites	41
Table 3.1: Potential rTALE binding sites.....	66
Table 5.1: The DNA transfection amounts used for the different culture plates based on the jetPRIME® transfection guidelines	101
Table 5.2: The DNA transfection amounts used for the different culture plates based on the Lipofectamine® 3000 transfection guidelines.....	102

List of Abbreviations

1. AAV	-	Adeno-associated virus
2. AD	-	Activation domain
3. Ad	-	Adenovirus
4. ALT	-	Alanine aminotransferase
5. BD	-	Binding domain
6. bp	-	Base pair
7. BSA	-	Bovine serum albumin
8. cccDNA	-	Covalently closed circular DNA
9. Cas 9	-	CRISPR-associated protein 9
10. C/EBP	-	CCAAT/enhancer binding protein
11. CMV	-	Cytomegalovirus
12. CRISPR	-	Clustered Regularly Interspaced Short Palindromic Repeat
13. DBD	-	DNA binding domain
14. DMEM	-	Dulbecco's Modified Eagle Medium
15. DNA	-	Deoxyribonucleic acid
16. dTALE	-	Designer TALE
17. eGFP	-	Enhanced green fluorescent protein
18. ELISA	-	Enzyme Linked Immunosorbent assay
19. FCS	-	Foetal calf serum
20. GAPDH	-	Glyceraldehyde-3-phosphate dehydrogenase
21. GFP	-	Green fluorescent protein
22. gRNA	-	Guide RNA
23. HA	-	Haemagglutinin epitope

24. HBeAg	-	HBV e antigen
25. HBV	-	Hepatitis B virus
26. HBx	-	Hepatitis B virus X protein
27. HCC	-	Hepatocellular carcinoma
28. HIV	-	Hepatocyte nuclear factor
29. HNF	-	Hepatocyte nuclear factor
30. HP1	-	Heterochromatin protein 1
31. HSPG	-	Heparan sulphate proteoglycan
32. IFN- α	-	Interferon alpha
33. KAP 1	-	KRAB-associated protein 1
34. KRAB	-	Krüppel-associated box
35. MTT	-	3-(4,5-Dimethylthiazol-2-yl)-2,5-diphenyltetrazolium bromide
36. mTTR	-	Modified murine transthyretin
37. NAs	-	Nucleos(t)ide analogues
38. NLS	-	Nuclear localisation signal
39. Nm	-	Nanometres
40. NTCP	-	Sodium taurocholate co-transporting polypeptide
41. NuRD	-	Nucleosome-remodelling and histone deacetylation
42. OD	-	Optical density
43. ORF	-	Open Reading Frame
44. PAM	-	Protospacer Adjacent Motif
45. PBS	-	Phosphate buffered saline
46. PEG-IFN- α	-	PEGylated IFN- α
47. pgRNA	-	Pregenomic RNA
48. qPCR	-	Quantitative PCR

49. rcDNA	-	Relaxed circular DNA
50. RISC	-	RNA induced silencing complex
51. RNA	-	Ribonucleic acid
52. RNAi	-	RNA interference
53. rTALE	-	Repressor TALE
54. RT-qPCR	-	Reverse transcriptase quantitative PCR
55. RVD	-	Repeat variable di-residue
56. shRNA	-	Short hairpin RNA
57. siRNA	-	Small interfering RNA
58. TALEN	-	Transcription activator-like effector nuclease
59. TALE	-	Transcription activator-like effector
60. ZFN	-	Zinc Finger Nuclease
61. ZFP	-	Zinc Finger Protein

Chapter 1

1. Introduction

1.1 Epidemiology and transmission of hepatitis B virus

The hepatitis B virus (HBV) is a partially double stranded DNA virus that causes both acute and chronic infection of the liver (1). HBV continues to be a major health threat globally, with an estimated 240 million people chronically infected and more than 686 000 HBV-related deaths annually (2). The life-threatening consequences of chronic HBV infection include advanced liver diseases such as cirrhosis and hepatocellular carcinoma (HCC) (2, 3). Despite an available effective HBV vaccine, chronic infection remains a global medical problem as vaccination coverage is not complete (4). Furthermore, the vaccine does not benefit the millions of people already infected (5, 6). HBV is endemic across the world, with developing regions such as sub-Saharan Africa and Asian countries classified as hyper-endemic areas (2, 7). To date, ten HBV genotypes have been identified (genotype A-J), each having a distinct geographical distribution including a role in determining the severity of disease and treatment outcome (8).

HBV can be spread through percutaneous or mucosal exposure to infected body fluids (horizontal transmission) (9, 10). Additionally infants can also contract the virus percutaneously from the mother during child birth (vertical transmission), with the risk of the infant developing chronic infection being as high as 90% (9, 11). Most adults can readily clear an infection and thus do not require treatment, but a fraction (<5%) do continue to develop chronic infection (11, 12). However, management of chronic HBV infection has been shown to reduce the patient's risk of disease progression and death (13).

Current treatments available for HBV infection include the use of nucleos(t)ide analogues (NAs) and immune system modulators (14). These treatments have significant drawbacks such as the development of viral drug resistance to the NAs over a period of time, the severe side effects and poor efficacy associated with immune system modulators (15). Furthermore, variation between the HBV genotypes leads to variation in the response to treatment of these genotypes adding to the difficulty of treating HBV infection (16, 17). For this reason, the development of novel therapeutic strategies to combat HBV is needed. Of critical importance to the development of novel therapeutics is the persistence of the episomal viral covalently closed circular DNA (cccDNA), which is not diminished by current therapeutic strategies (18). Formed in the nucleus of infected hepatocytes, cccDNA is important for virus replication and since it is not diminished during treatment, there is viral rebound upon treatment withdrawal (18, 19). Therefore, an ideal approach for combating HBV may be through the direct inactivation of HBV cccDNA. With the advances made in the field of gene therapy, genome editing technologies developed from zinc finger proteins (ZFP), transcription activator-like effectors (TALEs) and the clustered regularly interspaced palindromic repeat (CRISPR)-associated genes (CRISPR-Cas) system, has provided a platform for developing new therapeutic strategies. *In vitro* and *in vivo* experimental studies have successfully exploited these technologies for targeting various viral genomes, highlighting that gene therapy strategies can provide a direct approach at targeting HBV cccDNA (20-24).

1.2 HBV molecular biology and replication

Belonging to the *Hepadnaviridae* family, HBV is a hepatropic DNA virus and thus primarily infects hepatocytes (25). The virion is measured to be 42 nanometres (nm) in

diameter and consists of an outer bilayered lipoprotein envelope which surrounds the viral nucleocapsid containing the viral genome. (1, 26). The HBV genome is a roughly 3.2 kb partially double stranded DNA which comprises a full length minus strand and an incomplete plus strand (1, 27). The virus replicates by reverse transcription of an RNA intermediate that yields relaxed circular DNA (rcDNA) (28). In the nucleus rcDNA is converted to cccDNA, which is the template for viral transcription and subsequently is important for viral replication (28).

The HBV genome contains four overlapping open reading frames (ORFs); the *surface* (*S*), *precore/core* (*C*), *polymerase* (*P*) and *X* ORFs, which together code for the 7 viral proteins (Figure 1.1) (26). The *S* ORF contains three translation initiation codons functionally dividing the ORF into the *pre S1*, *pre S2* and *S* regions which encode the large (L), middle (M) and small (S) surface antigens respectively (26, 29). The hepatitis B virus surface antigens (HBsAgs) are embedded in the viral envelope and additionally the L protein is responsible for the attachment of the virus to the hepatocyte (30). Similar to the *S* ORF, the *C* ORF contains two translational start codons functionally dividing the ORF into the *precore* and *core* regions (31). RNA translated from the *precore* start codon yields precore proteins which are proteolytically processed by the Golgi apparatus and secreted as HBV e antigen (HBeAg) (32). The role of HBeAg in the HBV life cycle is not yet fully understood but is thought to be involved in inducing immune tolerance to HBV (33). Translation from the *core* start codon yields core proteins that are used for capsid formation (31).

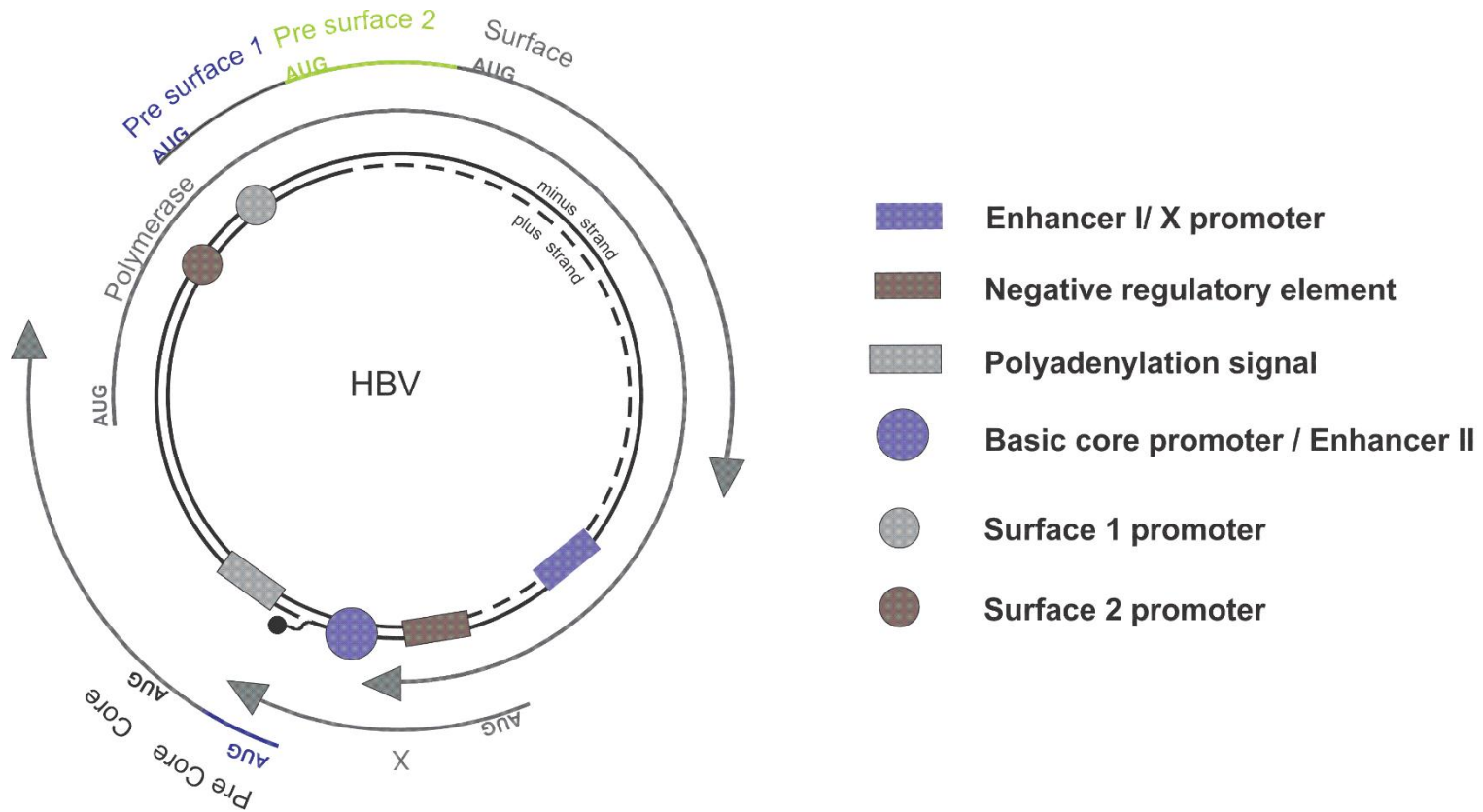


Figure 1.1: Hepatitis B virus genomic organisation. The centre of the schematic diagram represents the partially double stranded HBV rcDNA. During HBV replication rcDNA is repaired to cccDNA which serves as the template for viral transcription. The compact HBV genome contains four overlapping ORFs, as illustrated by the arrows. The *polymerase*, *X*, *precore/core*, and *surface* ORFs encode for polymerase, X, core and HBeAg, and the three surface proteins respectively. HBV DNA transcription regulatory elements are illustrated by the different geometric shapes. Image adapted from (34).

The *P* ORF yields the viral polymerase protein which has DNA-dependent DNA polymerase, reverse transcriptase, and RNase H activities (31). Lastly translation of the *X* ORF yields the hepatitis B virus X protein (HBx) which promotes viral gene expression. HBx achieves this by degrading the Smc5/6 complex which functions to suppress expression from episomal DNA such as cccDNA (35).

Having a narrow host range and liver tropism, HBV primarily infects the livers of humans and some great apes (36). During the first steps of infection the virion attaches to heparan sulphate proteoglycan (HSPG) receptors expressed on the surface of hepatocytes (Figure 1.2) (37). Subsequently, the virion binds to the hepatocyte-specific sodium taurocholate co-transporting polypeptide (NTCP) surface receptor, which has only recently been identified as the corresponding receptor to the Pre-S1 domain of the large surface antigen (38). After binding to the NTCP receptor, the virion is able to enter the cell via endocytosis and is uncoated in the cytoplasm (38). The nucleocapsid is subsequently directed to the nucleus of the cell via active transport mediated by microtubules (39, 40). The viral capsid is disassembled and the rcDNA released within the nucleus (40). The rcDNA is then repaired to cccDNA which in turn is used as a template by host RNA polymerase II to transcribe viral RNAs (1, 41). Within the cccDNA, there are four viral promoters; the basic core, pre-S1, pre-S2, and X promoters, and two enhancer sequences; enhancers I and II, which initiate transcription of the cccDNA by host RNA polymerase II (26). The viral pgRNA and the surface and X mRNAs are then transported to the cytoplasm to be translated into proteins essential for production of new virions (29). Once the viral polymerase is translated from pgRNA, it binds to the encapsidation signal on the pgRNA. The polymerase-bound pgRNA is subsequently encapsidated by core proteins and reverse transcribed by viral polymerase to produce the minus DNA strand of HBV (28). As the polymerase moves along the minus strand to synthesise the plus strand, the polymerase

degrades the pgRNA (28). The core particle with the HBV DNA, known as the nucleocapsid, can either be directed to the nucleus to deliver its DNA thus increasing the cccDNA pool or it can be directed to the secretory pathway and enveloped with a lipid bilayer embedded with surface proteins and then released into the blood stream (26, 42). In addition to releasing infectious virions the infected cell also secretes non-infectious HBsAg subviral particles composed of empty envelopes embedded with HBsAg (43). HBV-infected cells also secrete HBeAg which is a variant of the core protein (43).

Unravelling the life cycle of HBV has facilitated various developments in managing and treating HBV infection (18, 44, 45). HBsAg was identified as a marker for HBV infection and has been used in the development of an HBV infection screening assay called the HBsAg enzyme linked immunosorbent assay (ELISA) (46, 47). The first available HBV vaccines were also produced from plasma-derived HBsAg (5). Furthermore, different stages of the life cycle are used as potential target sites for HBV therapy as demonstrated by the development of inhibitors for HBV entry, replication, nucleocapsid formation and secretion inhibitors (48-52). However these do not impact the persistent pool of cccDNA within infected hepatocytes and therefore strategies that would target the formation, replication or elimination of cccDNA may be a better option for treating HBV infection (53).

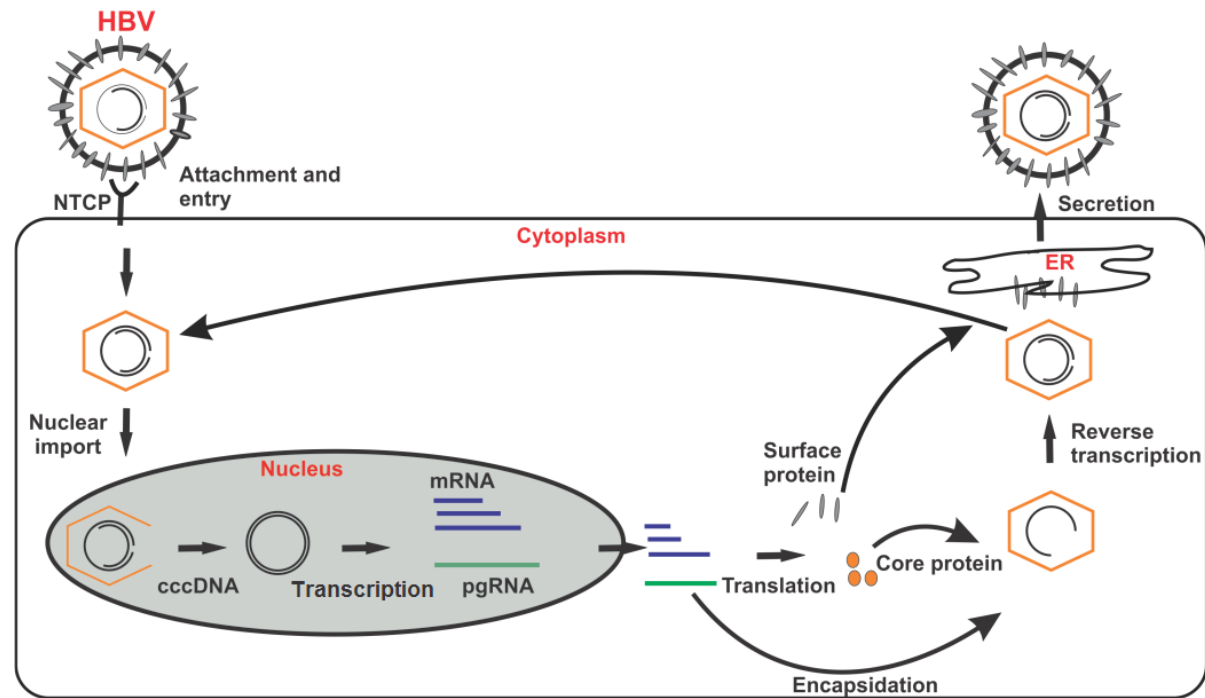


Figure 1.2: Hepatitis B virus replication cycle. HBV virions attach to the NTCP receptor on hepatocytes and enter the cell through endocytosis. After uncoating the viral capsid is translocated to the nucleus where the rcDNA is released and repaired to cccDNA. The cccDNA is used as a template to transcribe pgRNA and subgenomic RNAs which are then transported to the cytoplasm. The viral RNAs are translated into viral proteins, whereby the core and surface protein are required for new virion assembly. Once the polymerase is translated from the pgRNA the two are encapsidated by core proteins forming the nucleocapsid. Subsequently the polymerase reverse transcribes the pgRNA and ultimately produces the partially double-stranded rcDNA. The nucleocapsid is either recycled to the nucleus to maintain the cccDNA pool or enveloped with a lipid bilayer, embedded with surface proteins, and secreted into the blood stream. Image adapted from (54).

1.3 HBV management

To control the burden of the disease, an effective recombinant vaccine is currently used in approximately 180 countries as part of their routine universal HBV vaccination of newborns and adults (5, 55). Despite the success of the vaccine in reducing the incidence of HBV infection, it cannot treat established infections. Furthermore, in adults administered with the vaccine, about 5 % do not acquire significant anti-HBs antibody levels and thus remain unprotected (56). In addition, the number of non-responders is increased under circumstances of immunosuppression (57-59). Factors that lead to immunisation failure include improper storage of vaccine, old age, male gender, obesity, renal failure, impaired immune system, genetic factors and certain diseases such as celiac disease, diabetes mellitus, chronic liver disease, Crohn's disease and cancer (60-62). Another limiting factor is the emergence of HBV S-gene mutants that cannot be neutralised by vaccine induced anti-HBs antibodies (63, 64).

There are currently seven licensed therapeutic agents available for treating chronic HBV infection which fall in the categories of either immunomodulators or NAs (14). The immunomodulators includes interferon alpha (IFN- α) and a more potent form, PEGylated IFN- α (PEG-IFN- α), which act by aiding the host's immune system in mounting an immune response against the virus (65, 66). The use of standard IFN- α was replaced with PEG-IFN- α due to its improved pharmacokinetic properties and decreased dosages (67, 68). IFN- α treatment is given via subcutaneous injection and exerts its effect by engaging cell surface receptors to stimulate intracellular signalling pathways, which then regulates the transcription of IFN-stimulated genes that ultimately inhibit viral replication (69). IFN therapy has been used successfully in chronically infected patients to achieve a decrease in HBsAg, HBeAg, and normalised alanine aminotransferase (ALT) levels (70-73).

Furthermore, a decreased incidence in HCC was also observed following IFN- α administration (74). Compared to NAs, the major benefits of IFN therapy include the finite duration of treatment, greater loss of HBsAg and a lack of drug resistance (65, 75). Despite the benefits and success rates of IFN therapy it is only effective in about 30% of treated patients and has an overall weaker antiviral activity compared to NAs (76, 77). To improve the efficacy of treatment, combination therapy was explored where patients were treated with a NA and PEG-IFN- α , but no improvement in response to this treatment strategy was observed (78). IFN therapy is associated with several side effects such as bone marrow suppression, influenza-like symptoms, depression, aggravation or unmasking of autoimmune diseases, renal failure and heart failure (79). The more efficient PEG-IFN- α produces similar side effects as the standard IFN (79). Another disadvantage of IFN therapy is the high cost associated with treatment (80).

Licensed NAs include lamivudine, adefovir, dipivoxil, entecavir, telbivudine and tenofovir and act by inhibiting viral polymerase activity thus inhibiting viral replication. The various NAs function to suppress replication by a similar mechanism but differ in their clinical efficacy (80). NAs are chemically produced and are structurally similar to endogenous nucleotides and are therefore incorporated into the growing DNA strand during viral DNA synthesis causing termination of chain extension, thus ultimately inhibiting viral replication (80, 81). Lamivudine, the first licensed oral anti-HBV agent, proved to be successful as it was able to reduce HBV DNA levels, normalised ALT levels and also improved liver histology in patients (82-84). However, a major drawback of lamivudine therapy is emergence of lamivudine drug resistant HBV strains (85). Compared to lamivudine, adefovir dipivoxil and entecavir achieve a superior virological response including a much lower incidence of resistance (86-88). Despite the improved viral suppression observed with telbivudine, compared to lamivudine, it is not often used due to the high rate of

resistance associated with this NA (80). Tenofovir was initially licensed as treatment for the human immunodeficiency virus (HIV), but was later found to be a potent therapy option against HBV infection and for treating patients co-infected with HBV and HIV (80, 89). Tenofovir has been chosen as a first line therapy due to its improved efficacy compared to the other analogues and no resistance has been reported for up to 144 weeks of treatment (80, 90). Although successful at inhibiting the viral polymerase activity, these NAs do not suppress viral replication completely and consequently residual virions are still produced which are able to infect new cells (91-93). Since reactivation will occur if treatment is stopped, it necessitates prolonged use of NAs, which in turn increases the chance of emergence of drug resistant strains (80).

Despite the anti-HBV activity of currently available therapeutic agents, efficacy is only partial and is coupled with various limitations such as cost, life-long treatment regimens, the emergence of resistance, severe side effects and importantly the reactivation of HBV replication once treatment is stopped (65, 80, 94). These issues highlight the need for novel therapeutic agents with improved efficacy and safety.

Therapeutic strategies that employ gene therapy have shown potential as an approach to combat HBV infection and have modes of action that overcome challenges faced by current treatment strategies (54, 95). Several anti-HBV gene therapy strategies targeted to viral RNA have been explored and include antisense DNA and RNA, ribozymes, DNazymes and RNA interference (RNAi) (96-99). The use of RNAi has proved to be most efficient in silencing gene expression and has gained attention as one of the leading strategies of targeting and suppressing viral RNA (100). RNAi is a naturally occurring process where specific mRNA is targeted for degradation by a 21 nucleotide guide RNA and its associated silencing complex, RISC (RNA induced silencing complex) (100, 101). Guide RNA, produced from synthetic small interfering RNA (siRNA) or expressed RNA

sequences (microRNA mimics), have been successfully used to target and induce viral mRNA degradation (102-104). Although the aforementioned approaches were able to silence gene expression, since these strategies function at a post-transcriptional level the pool of persistent cccDNA remains undiminished (105).

1.4 Gene editing technologies

Using gene editing technologies to target viral genomes can, theoretically, be applied to edit and disrupt vital viral genes thereby clearing the virus. Prominent nuclease technologies for gene modification include zinc finger nucleases (ZFNs), transcription activator-like effector nucleases (TALENs) and the CRISPR/Cas system, each of which has been investigated for its ability to disrupt cccDNA and inhibit viral replication (106).

Zinc finger proteins (ZFPs) belong to a class of naturally occurring transcription factors and are able to bind specific DNA sequences via their Cys₂His₂ zinc finger motifs (107). In a modular arrangement of ZFPs, the amino acids on the tip of the α helix of each finger binds to a specific DNA triplet within the major groove of DNA (108, 109). Varying the amino acids at the finger tips enables the manipulation of sequence specificity of the zinc fingers, therefore ZFPs can be constructed to bind any sequence of interest (110, 111). Furthermore, fusing an effector domain, such as a nuclease domain, a transcription activator domain or repressor domain, to the re-engineered zinc finger domain creates a protein capable of cleaving (ZFN), activating expression (ZF transcription factor) or suppressing expression (ZF repressor) of a specific gene in a variety of cells and organisms (112-114).

A more promising alternative to ZFPs are TALEs which are DNA binding proteins produced by gram negative plant pathogenic bacteria of the genus *Xanthomonas* (115, 116). Using their type III secretion system *Xanthomonas* bacteria inject the TALEs into plant cells, and upon reaching the nucleus, the TALEs bind to specific promoter sequences on the host genome, to initiate transcription of genes that favour bacterial colonisation (115, 116). The central DNA binding domain (DBD) comprises tandem repeats of 34 amino acid residues, with the 12th and 13th amino acid residues (called repeat variable di-residues (RVDs)) determining DNA binding specificity (115). The repeats in the TALE DNA-binding domain has no context dependence and confers specificity for a single nucleotide, thereby creating a straightforward protein-DNA binding code (117). The specific and adaptable modules of TALEs render it a favourable molecular tool for modifying DNA as it can be fused to different effector domains. TALEs fused to effector domains such as nucleases (20), transcription repressors (118) and transcription activators (119) have been demonstrated to be functional in mammalian cells.

With the recent functional elucidation of the CRISPR/Cas system, research displaying its utility for targeted genome modification has emerged (120-122). The CRISPR/Cas system is naturally found in bacteria and acts as a defence tool against foreign nucleic acids through its RNA guided endonuclease activity (123). A certain sequence of the foreign nucleic acid is captured and incorporated in the CRISPR locus (124). CRISPR RNAs (crRNA) are produced which contain a segment of the CRISPR repeat and a protospacer sequence transcribed from the captured foreign nucleic acid (125). In the most commonly used CRISPR system, the type II system, the crRNA hybridises to transactivating RNA, which is also encoded by the CRISPR system, forming a guide RNA (gRNA) complex, that associates with a Cas9 protein (126, 127). The gRNA then binds to a target sequence, which is complementary to a portion of the gRNA, and found next to a protospacer

adjacent motif (PAM) represented by the sequence NGG (124, 125). The Cas9 protein then cleaves the target sequence thus destroying the invading species (127). The CRISPR/Cas system relies on RNA-DNA complementary base pairing rules and therefore targeting a sequence of interest can be achieved by modifying the DNA target-binding sequence in the gRNA (127, 128).

Overall these designer endonucleases are able to target the cccDNA directly, overcoming a challenge that has made current therapeutic options inefficient (20, 54, 95, 129, 130). However, a major concern for this type of technology is its ability to cleave HBV DNA integrated into the host genome or cleave off-target genes (131, 132). This would cause insertions or deletions (indels) and possibly chromosomal translocations in the host genome, resulting in cytotoxicity (133, 134). Methods capable of epigenetically altering the expression of cccDNA may be a more favourable approach to cccDNA gene editing (135). Therefore, the use of highly specific DNA-binding domains, to direct a repressor effector protein to the cccDNA, may be an alternative method to nuclease mediated gene disruption.

1.5 Engineering TALE proteins

As a result of the predictable DNA binding code, specificity, and the modular design of TALE proteins, it has become a popular tool in synthetic biology studies. Advances made with TALE technology derived from the *Xanthomonas* sp has enabled the construction of designer TALEs fused to a variety of effector domains for effective use in a broad range of applications (20, 118, 119). The predictable and programmable specificity of the TALE protein is as a consequence of the unique recognition mode of the central binding domain, where the RVD specifies the DNA base to be bound on the sense strand (Figure 1.3) (115).

The crystal structure of a TALE bound to a DNA reveals that each repeat consists of two helices bound to a RVD-containing loop (116, 136). The amino acid repeats associate with each other forming a right handed super helical structure that wraps around the major groove of DNA where residue 13 binds to its specific nucleotide and residue 12 is responsible for stabilising the RVD loop (116, 136). Of the 25 natural RVDs known, the ones mostly used are HD, NI, NK and NG which strongly binds to C,A,G and T bases respectively (117). However, some RVDs can recognise more than one base, such as the RVD NN which recognises guanine bases but also to a lesser extent recognises adenine (117). This allows targeting of multiple genomic sites that vary in the degree of specificity for each site, thus making TALEs a flexible tool compared to other gene editing strategies (137). Characterisation studies revealed that TALE derivatives can vary in their efficiency depending on RVD composition and that the presence of strong RVDs HD and NN is necessary for efficient activity (138). Additionally using a DNA-binding domain with longer repeats makes the TALE more specific (137). Further characterisation revealed that a thymine base (T0) preceding the target sequence was required for TALE activity (117). Structural studies revealed that the N terminal portion of the TALE protein recognises and interacts with the T0 and that by mutating the N terminal domain, novel N terminal domains are created which prefer other bases (N0) (139).

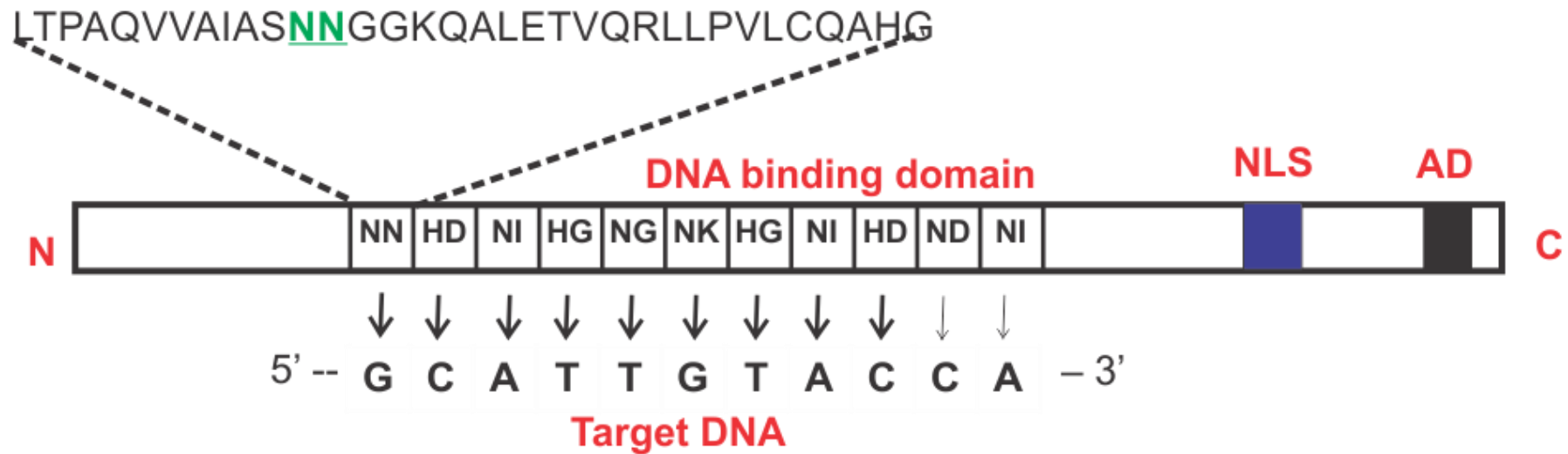


Figure 1.3: Schematic diagram of a naturally occurring TAL effector, illustrating the N-terminal translocation signal (N), repeat region, and a C-terminal region (C) consisting of a nuclear localisation signal (NLS) and a transcriptional activation domain (AD). The repeat region is the DNA-binding domain composed of tandem repeats of 34-35 amino acid residues, where the 12th and 13th amino acid residues (underlined) determine the specificity of the target sequence. The RVDs and their major nucleotides for binding are also depicted. Reproduced from (116).

1.6 Transcriptional repression of HBV

Cells regulate the expression of genes to control the amount and the time when a specific gene is expressed (140). Transcription factors are the molecular machinery that regulate gene expression through interactions with transcription regulatory elements such as promoters, enhancers, silencers, insulators and locus control regions (141-144). Transcription repressors have binding sites within silencers or can directly act on the promoter thereby disrupting the transcription initiation process (142). Transcriptional repression can be achieved by a repressor through competition with transcriptional activators for binding sites thereby inhibiting the recruitment of co-activators or by masking the activator domain inhibiting its function (145). Another mechanism of repression is through inhibiting transcriptional machinery activity. This is achieved by preventing the formation of the pre-initiation complex, thereby preventing the initiation of transcription or by binding at a site which prevents the transcriptional elongation process (145). Transcriptional repression can also be achieved through repressive heterochromatin formation which sterically prevents transcription factor binding and transcription initiation (145). Heterochromatin is brought about by chromatin remodelling through histone modifications and through the methylation of CpG islands (145). Based on this natural phenomenon, the use of artificially designed transcription factors to repress gene activity has been explored. Artificial transcription factors are typically constructed by fusing a repressor domain to the DNA-binding domain of ZFPs (146), TALEs (147) or an inactive Cas9 (dead Cas9 or dCas9) of the CRISPR/Cas system (148).

The Krüppel-associated box (KRAB) repressor domain is one of the most commonly used repressor domains in artificial transcriptional repressors and functions by recruiting heterochromatin forming complexes to a target site making the chromatin inaccessible to

transcription machinery (149, 150). By fusing a KRAB repressor domain to a dCas9, Gilbert *et al.* was able to achieve at least 90% repression of the various endogenous genes tested in a mammalian cell line (148). While the CRISPR/Cas system has been successfully repurposed to transcriptionally repress endogenous and exogenous gene activity in a variety of cell lines (148, 151-153), no attempts to target HBV cccDNA has been reported as yet. Several studies have also demonstrated that an artificial transcription factor consisting of a KRAB transcriptional repressor domain fused to a ZFP DBD was able to inhibit expression of viral target genes (146, 154, 155). A proof-of-concept study demonstrated that designing a ZFP DNA-binding domain to target a sequence in the enhancer 1 region found upstream of an integrated *HBx* sequence was capable of specifically binding the target and causing a 57.2% decrease in *HBx* transcription (154). The adaptable modules of a TALE protein allow the TALE DNA-binding domain to be fused to a repressor domain to achieve silencing of a gene. Several studies have successfully re-engineered TALEs as repressor TALEs (rTALEs) capable of targeted endogenous or exogenous gene silencing in a variety of cell lines (118, 147, 156-158).

Based on these studies the potential of highly specific transcriptional repressors designed to target and inhibit HBV viral replication without altering the genetic sequence or causing mutations in the host genome may be a promising antiviral approach. Given the high level of specificity observed with engineered TALEs and their efficiency in regulating genes in mammalian cells makes TALEs a favourable molecular tool for creating artificial transcription factors (118, 159, 160).

To design rTALEs for use as therapeutics against HBV, certain technical considerations must be taken into account such as the type of gene modifier to be incorporated. For rTALE construction, the well-studied and efficient KRAB domain has been a popular choice as a repressor domain (118, 135, 147, 161). The highly conserved KRAB repression

domain is a DNA binding-dependent transcriptional repressor naturally found as part of the zinc finger transcriptional regulatory proteins (162, 163). The KRAB domain is a powerful repressor and therefore, most eukaryotic KRAB-ZFPs are known to be involved in important processes such as cell differentiation, embryonic development, cell cycle regulation, and apoptosis amongst other cellular functions (164, 165). The KRAB domain functions by interacting with transcriptional co-repressor proteins or other transcriptional factors (165, 166). An important universal co-repressor needed for KRAB domain transcriptional repression is the KRAB-associated protein 1 (KAP 1) (163, 166). Bound to the target promoter, the KRAB repressor domain recruits and binds KAP1 at its Ring-box-coiled-coil (RBCC) motif (163, 166). KAP1 in turn recruits and binds heterochromatin-inducing factors to the target promoter, like the heterochromatin protein 1 (HP1), the histone methyltransferase SETDB1, the nucleosome-remodelling and histone deacetylation (NuRD) complex and the nuclear receptor corepressor complex 1 (149, 165, 167, 168). As a result, the chromatin is modified through compaction and increased DNA methylation events which create facultative heterochromatin that is inaccessible to RNA polymerase II (165, 169). Additionally the KRAB/KAP1 complex has the ability to cause induced heterochromatin spreading over long ranges of DNA, further demonstrating the advantage of using a KRAB repressor domain as the choice of a gene modifier (168).

An essential feature for anti-HBV rTALEs would be the incorporation of a nuclear localisation signal which would mediate the process of rTALE import into the nucleus to bind targeted DNA (170). Furthermore, an important factor in therapeutics is the spatial control of exogenous gene expression to restrict unintended adverse effects from activity in non-targeted cells. Since HBV primarily affects hepatocytes (1), designing the rTALEs to be liver-specific is of prime importance.

This project entails the construction of rTALEs, which comprise of a KRAB repressor domain fused to a TALE DBD. In contrast to previous studies where rTALEs were designed to incorporate the repressor domain at the C terminus end (118, 147) here the KRAB domain is incorporated at the N terminus end of the rTALE vector, analogous to repressor proteins found naturally (165). The TALE DBD should specifically bind to the target HBV sequences and the KRAB repressor should mediate heterochromatin formation at the site (169). As a result the target site should be inaccessible to transcription machinery and hence transcription of the target HBV DNA should be inhibited (Figure 1.4) (169). The well-characterised modified transthyretin (mTTR) promoter will drive expression of these rTALE proteins to permit hepatocyte-specific expression (171). The tissue-specific rTALE activity was intended to restrict unwanted transgene expression and activity in other cell types. Additionally, the rTALE vectors were designed to contain a NLS signal that will enable the rTALE to be transported into the nucleus of the cell after it has been translated in the cytoplasm.

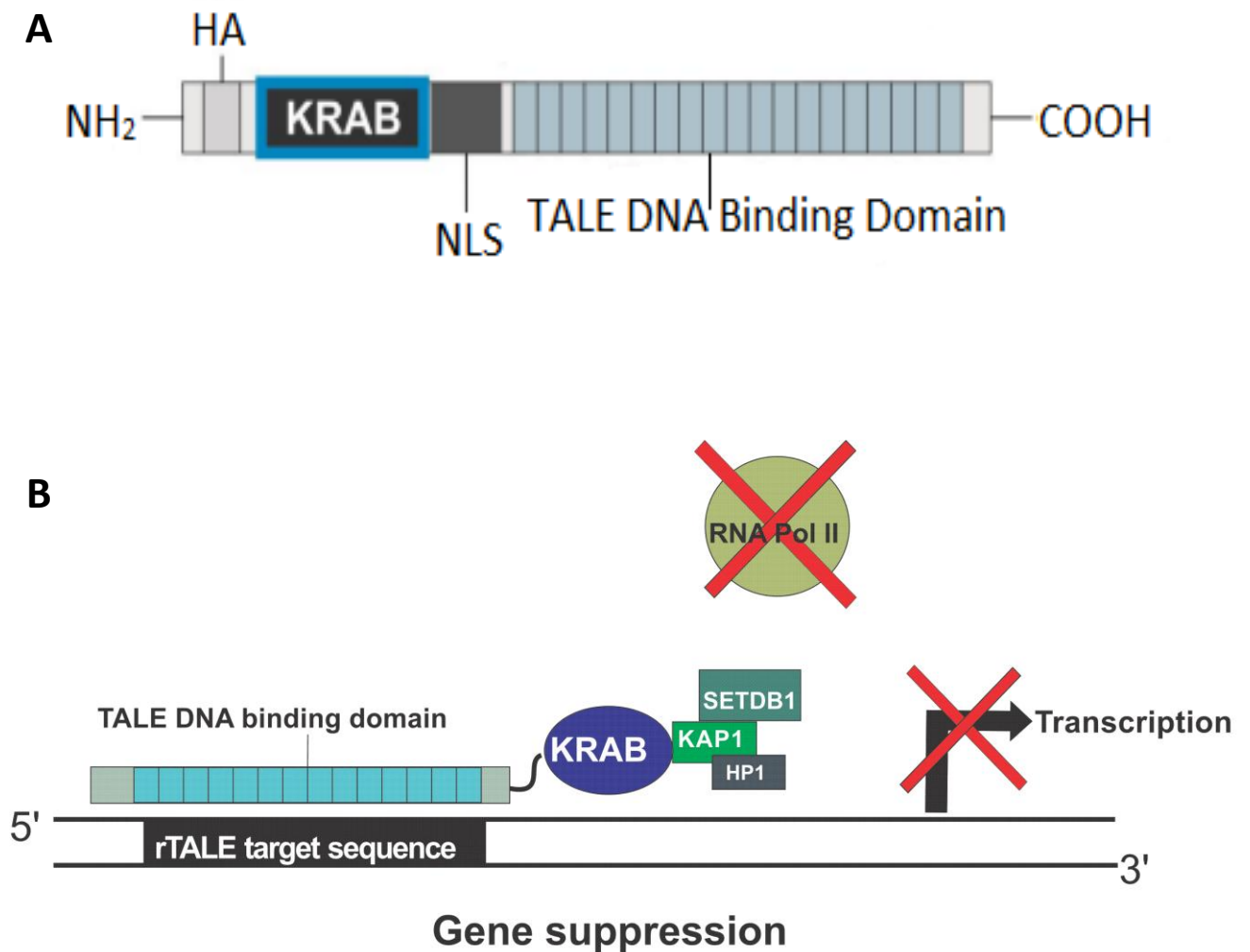


Figure 1.4: Schematic representation of the rTALE design and rTALE-mediated transcriptional repression. (A) The rTALE consists of a KRAB repressor domain fused to a TALE DNA-binding domain (DBD). A nuclear localisation signal (NLS) is incorporated to facilitate transport back to the nucleus once translated. A haemagglutinin epitope (HA) tag is included which acts as a protein tag to detect rTALE expression. (B) The TALE DBD specifically binds to its target sequence and the KRAB repressor recruits co-repressors and heterochromatin-inducing factors which forms a heterochromatin state at the target site. Thus, the target site is inaccessible to transcription machinery leading to inhibition of viral transcription.

1.7 Aims

The aim of the current study was to construct KRAB-based rTALEs and assess their anti-HBV potential. The rTALEs were designed to be under the transcriptional control of a mTTR promoter and to target the HBV *surface* and *polymerase* ORFs, including the viral enhancer *I/X* promoter region of cccDNA, to achieve chromatin-based repression of HBV gene expression. The transcriptional repression activity of the rTALEs on HBV cccDNA, off-target effects and cytotoxicity were assessed in cell culture.

Chapter 2

2. Materials and Methods

2.1 Plasmids

2.1.1 pCH-9/3091

pCH-9/3091 was used in this study as a target plasmid to assess the anti-HBV efficacy of the rTALEs. pCH-9/3091 is a replication-competent plasmid and is therefore able to mimic the HBV replication process *in vitro* and *in vivo*. Developed by Nassal and colleagues (172), pCH-9/3091 contains a greater-than-genome-length genotype D HBV sequence under the transcriptional control of the CMV promoter. The plasmid contains two terminal repeats thereby facilitating the transcription of the greater-than-genome-length pgRNA as would normally occur from the circular HBV genome. The pgRNA is sufficient for initiation of viral replication.

2.1.2 pCI-neo-eGFP

The pCI-neo-eGFP reporter plasmid is a convenient measure of transfection efficiency when co-transfected with any other plasmid. The plasmid expresses enhanced green fluorescent protein (eGFP) under the control of the CMV promoter (173).

2.1.3 pTZ57R

The pTZ57R (Thermo Scientific, USA) plasmid does not contain any extraneous sequences capable of expressing in mammalian cells and was used to ensure an equivalent amount of DNA was transfected between cell culture experiments.

2.1.4 pRK5-CMV-rTALE plasmids

The previously described anti-HBV TALEN-expressing plasmids (174) were used to construct the CMV-driven rTALEs (unpublished data). These rTALEs consists of a TALE DBD, based on the AvrBs4 TALE protein scaffold, fused to a KRAB domain to cause gene repression (Figure 5.1). The TALE DNA-binding arrays were engineered to target the HBV genome. To generate the CMV-driven rTALE expressing plasmids, the sequence encoding the TALE DBD was excised from the anti-HBV TALEN-expressing plasmids and cloned it into a destination vector which contained a KRAB repressor domain (pRK5-HA-KRAB-NLS-TAL). The pRK5-HA-KRAB-NLS-TAL vector sequence encodes the upstream immediate early CMV promoter/enhancer to drive rTALE transcription, a TALE DBD, a haemagglutinin epitope (HA) as a protein tag for rTALE expression, a KRAB repressor domain for gene suppression, and a nuclear localisation signal to facilitate transport into the nucleus once translated. Furthermore, the KRAB domain was designed to be at the N-terminal of the repressor plasmid as would occur naturally in KRAB-ZF proteins. All the CMV-driven rTALE plasmids have the same sequence except for the sequence encoding the TALE DBD. Of the five CMV-driven rTALE plasmids; pRK5-CMV-S1-rTALE and pRK5-CMV-S2-rTALE targets and binds the *surface* and *polymerase* ORFs of the HBV genome whereas pRK5-CMV-X1-rTALE and pRK5-CMV-X2-rTALE targets and binds the *polymerase* ORF and the HBx promoter region of the HBV genome. The final amino acid sequences of the rTALE DBD and the DNA target sequence are shown in Table 2.1 and 2.2. The fifth rTALE, pRK5-CMV-control-rTALE, targeted a sequence unrelated to HBV and served as a negative control.

Table 2.1: Amino acid sequences of the S1 and S2- rTALEs and their target viral DNA sequence.

S1-rTALE	DNA target	S2-rTALE	DNA target
LTPEQVVAIASHDGGKQALETVQALLPVLCQAHG	C	LTPDQVVAIASNIGGKQALETVQRLLPVLCQAHG	A
LTPEQVVAIASHDGGKQALETVQALLPVLCQAHG	C	LTPEQVVAIASHDGGKQALETVQALLPVLCQAHG	C
LIPQQVVAIASNNGGGKQALETVQRLLPVLCQDHG	T	LTPEQVVAIASHDGGKQALETVQALLPVLCQAHG	C
LTPEQVVAIASNKGGKQALETVQRLLPVLCQAHG	G	LIPQQVVAIASNNGGGKQALETVQRLLPVLCQDHG	T
LTPEQVVAIASHDGGKQALETVQALLPVLCQAHG	C	LIPQQVVAIASNNGGGKQALETVQRLLPVLCQDHG	T
LIPQQVVAIASNNGGGKQALETVQRLLPVLCQDHG	T	LTPEQVVAIASNKGGKQALETVQRLLPVLCQAHG	G
LTPEQVVAIASNKGGKQALETVQRLLPVLCQAHG	G	LTPDQVVAIASNIGGKQALETVQRLLPVLCQAHG	A
LTPEQVVAIASHDGGKQALETVQALLPVLCQAHG	C	LIPQQVVAIASNNGGGKQALETVQRLLPVLCQDHG	T
LIPQQVVAIASNNGGGKQALETVQRLLPVLCQDHG	T	LTPDQVVAIASNIGGKQALETVQRLLPVLCQAHG	A
LTPDQVVAIASNIGGKQALETVQRLLPVLCQAHG	A	LTPEQVVAIASNKGGKQALETVQRLLPVLCQAHG	G
LIPQQVVAIASNNGGGKQALETVQRLLPVLCQDHG	T	LIPQQVVAIASNNGGGKQALETVQRLLPVLCQDHG	T
LTPEQVVAIASNKGGKQALETVQRLLPVLCQAHG	G	LTPEQVVAIASHDGGKQALETVQALLPVLCQAHG	C
LTPEQVVAIASHDGGKQALETVQALLPVLCQAHG	C	LTPEQVVAIASHDGGKQALETVQALLPVLCQAHG	C
LTPEQVVAIASHDGGKQALETVQALLPVLCQAHG	C	LTPDQVVAIASNIGGKQALETVQRLLPVLCQAHG	A
LIPQQVVAIASNNGGGKQALETVQRLLPVLCQDHG	T	LTPEQVVAIASNKGGKQALETVQRLLPVLCQAHG	G
LTPEQVVAIASHDGGKQALETVQALLPVLCQAHG	C	LTPDQVVAIASNIGGKQALETVQRLLPVLCQAHG	A
LTPDQVVAIASNIGGKQALETVQRLLPVLCQAHG	A	LTPDQVVAIASNIGGKQALETVQRLLPVLCQAHG	A
LIPQQVVAIASNNGGGKQALETVQRLLPVLCQDHG	T	LTPEQVVAIASNKGGKQALETVQRLLPVLCQAHG	G

Table 2.2: Amino acid sequences of the X1 and X2- rTALEs and their target viral DNA sequence.

X1-rTALE	DNA target	X2-rTALE	DNA target
LTPEQVVAIASHDGGKQALETVQALLPVLCQAHG	C	LTPDQVVAIASNIGGKQALETVQRLLPVLCQAHG	A
LTPEQVVAIASNKGGKQALETVQRLLPVLCQAHG	G	LTPEQVVAIASNKGGKQALETVQRLLPVLCQAHG	G
LTPEQVVAIASHDGGKQALETVQALLPVLCQAHG	C	LTPEQVVAIASNKGGKQALETVQRLLPVLCQAHG	G
LTPDQVVAIASNIGGKQALETVQRLLPVLCQAHG	A	LTPDQVVAIASNIGGKQALETVQRLLPVLCQAHG	A
LTPEQVVAIASNKGGKQALETVQRLLPVLCQAHG	G	LTPEQVVAIASHDGGKQALETVQALLPVLCQAHG	C
LTPEQVVAIASHDGGKQALETVQALLPVLCQAHG	C	LTPDQVVAIASNIGGKQALETVQRLLPVLCQAHG	A
LTPDQVVAIASNIGGKQALETVQRLLPVLCQAHG	A	LTPDQVVAIASNIGGKQALETVQRLLPVLCQAHG	A
LTPEQVVAIASNKGGKQALETVQRLLPVLCQAHG	G	LTPEQVVAIASHDGGKQALETVQALLPVLCQAHG	C
LTPEQVVAIASNKGGKQALETVQRLLPVLCQAHG	G	LTPDQVVAIASNIGGKQALETVQRLLPVLCQAHG	A
LIPQVVAIASNNGGGKQALETVQRLLPVLCQDHG	T	LTPEQVVAIASNKGGKQALETVQRLLPVLCQAHG	G
LTPEQVVAIASHDGGKQALETVQALLPVLCQAHG	C	LTPDQVVAIASNIGGKQALETVQRLLPVLCQAHG	A
LIPQVVAIASNNGGGKQALETVQRLLPVLCQDHG	T	LTPEQVVAIASNKGGKQALETVQRLLPVLCQAHG	G
LTPEQVVAIASNKGGKQALETVQRLLPVLCQAHG	G	LIPQVVAIASNNGGGKQALETVQRLLPVLCQDHG	T
LTPEQVVAIASNKGGKQALETVQRLLPVLCQAHG	G	LIPQVVAIASNNGGGKQALETVQRLLPVLCQDHG	T
LTPDQVVAIASNIGGKQALETVQRLLPVLCQAHG	A	LTPDQVVAIASNIGGKQALETVQRLLPVLCQAHG	A
LTPEQVVAIASNKGGKQALETVQRLLPVLCQAHG	G	LIPQVVAIASNNGGGKQALETVQRLLPVLCQDHG	T
LTPEQVVAIASHDGGKQALETVQALLPVLCQAHG	C	LTPEQVVAIASHDGGKQALETVQALLPVLCQAHG	C
LTPDQVVAIASNIGGKQALETVQRLLPVLCQAHG	A	LTPDQVVAIASNIGGKQALETVQRLLPVLCQAHG	A

2.2 Plasmids constructed in this study

2.2.1 Construction of mTTR-driven KRAB-based rTALEs targeted to the HBV ORF

2.2.1.1 Design of the mTTR-driven rTALE plasmids

To generate the mTTR-driven rTALE plasmids (pRK5-mTTR-rTALEs) (Figure 5.2), the CMV-driven rTALEs were modified by replacing the CMV promoter sequence with that of the liver-specific murine transthyretin (mTTR) promoter. Since the mTTR-driven rTALEs are based on their CMV counterparts pRK5-mTTR-S1-rTALE and pRK5-mTTR-S2-rTALE targets the *surface* and *polymerase* ORFs of the HBV genome whereas pRK5-mTTR-X1-rTALE and pRK5-mTTR-X2-rTALE targets and binds the *polymerase* ORF and the HBx promoter region of the HBV genome. Finally, a pRK5-mTTR-control-rTALE was also generated.

2.2.1.1.1 Design of the mTTR promoter sequence fragment

The promoter insert sequence was designed to include sequences from the pRK5-CMV-control-rTALE vector that flank the 5' and 3' ends of a mTTR promoter (Figure 2.1). This was done to ensure that the mTTR-driven rTALEs match the sequence of their CMV-driven rTALE counterparts, except for the promoter sequences. The 5' flanking sequence (fragment A) extends from the *Pci* I site to the start of the CMV promoter of pRK5-CMV-control-rTALE and is represented by nucleotides 7060 - 14 (Figure 5.1). The 3' flanking sequence (fragment B) extends from the end of the CMV promoter to the *Not* I site of pRK5-CMV-control-rTALE and is represented by nucleotides 597-963 (Figure 5.1). Since the mTTR promoter sequence contains a *Pci* I site, *Pci* I digestion could not be used for the purposes of cloning. Instead the mTTR insert was designed to include *Bpi* I type IIS restriction sites upstream of the *Pci* I and downstream of the *Not* I site. The *Bpi* I sites were

added in such a fashion that digestion with *Bpi* I would cut within the *Pci* I and *Not* I sites to yield the mTTR fragment with a *Pci* I overhang at the 5'-end and a *Not* I overhang at the 3'-end. Furthermore, the insert was designed to contain *Xho* I and *Asc* I restriction sites flanking the mTTR promoter sequence, thus providing an easier cloning option for switching the promoters in this plasmid at a later stage.

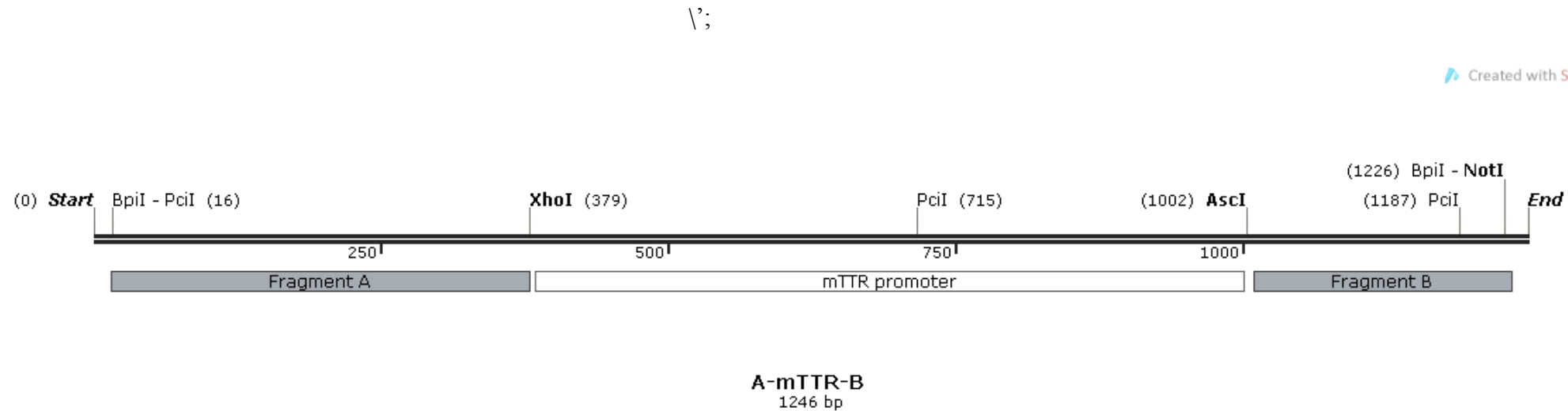


Figure 2.1: Schematic diagram of the promoter insert fragment. The insert was designed to contain the mTTR promoter sequence that would replace the promoter in the CMV-driven rTALEs. Short fragments that flank the CMV promoter in the CMV-driven rTALE vector were added to flank the mTTR promoter (fragment A and B). This ensures that, excluding the promoter sequences, the sequences of the mTTR-driven rTALE vector matches that of the CMV-driven rTALE vector. *Bpi* I restriction sites were included in the sequence such that *Bpi* I digestion would yield *Pci* I and *Not* I overhangs that would be complementary to the overhangs of the rTALE vector backbone. Furthermore, the insert was designed to contain *Xho* I and *Asc* I restriction sites flanking the mTTR promoter sequence. Map was created with SnapGene® software (from GSL Biotech; available at snapgene.com).

2.2.1.2 Construction of pRK5-mTTR-control plasmid.

Construction of pRK5-mTTR-control-rTALE plasmid is illustrated in Figure 2.2. The CMV promoter sequence was excised from the pRK5-CMV-control-rTALE expression vector (Figure 5.1) by a double restriction enzyme digestion reaction using *NotI* and *PciI*. The digestion reactions were carried out in two steps as recommended by the manufacturer (Thermo Scientific, CA, USA). The first digestion was carried out in a 40 µl reaction volume containing 1 µg of pRK5-CMV-control-rTALE, Buffer Tango at a final concentration of 1×, 1 U *Pci I*, and ddH₂O. After an incubation period of 1 hour at 37 °C, 4 U of *Not I* and 10× Buffer Tango to a final concentration of 2× was added, and the reaction was incubated for an additional hour at 37 °C. After the digestion reaction, 1 U of FastAP Thermosensitive Alkaline Phosphatase (Thermo Scientific, CA, USA) was added and incubated at 37 °C for 30 minutes to remove 5' phosphates. An undigested control reaction was included receiving all the components of the digestion except for the enzyme. The restriction digests were resolved on a 0.5 % agarose gel containing 0.5 µg/ml ethidium bromide and the resulting DNA bands were viewed with a GBOX UV transilluminator (Syngene, Cambridge, UK) (Appendix 5.2.1). The pRK5-CMV-control-rTALE vector backbone represented by the 6097 bp fragment (Appendix, Figure 5.3), was excised from the gel and purified using the MinElute™ Gel Extraction Kit (Qiagen, Hilden, Germany) according to the manufacturer's instructions (Appendix 5.2.2). DNA recovery was confirmed through gel electrophoresis (Appendix 5.2.1). The purity and concentration of the recovered DNA was assessed by spectrophotometry. This rTALE backbone fragment now lacked the CMV promoter and still contained the TALE DBD and KRAB repressor domain sequences.

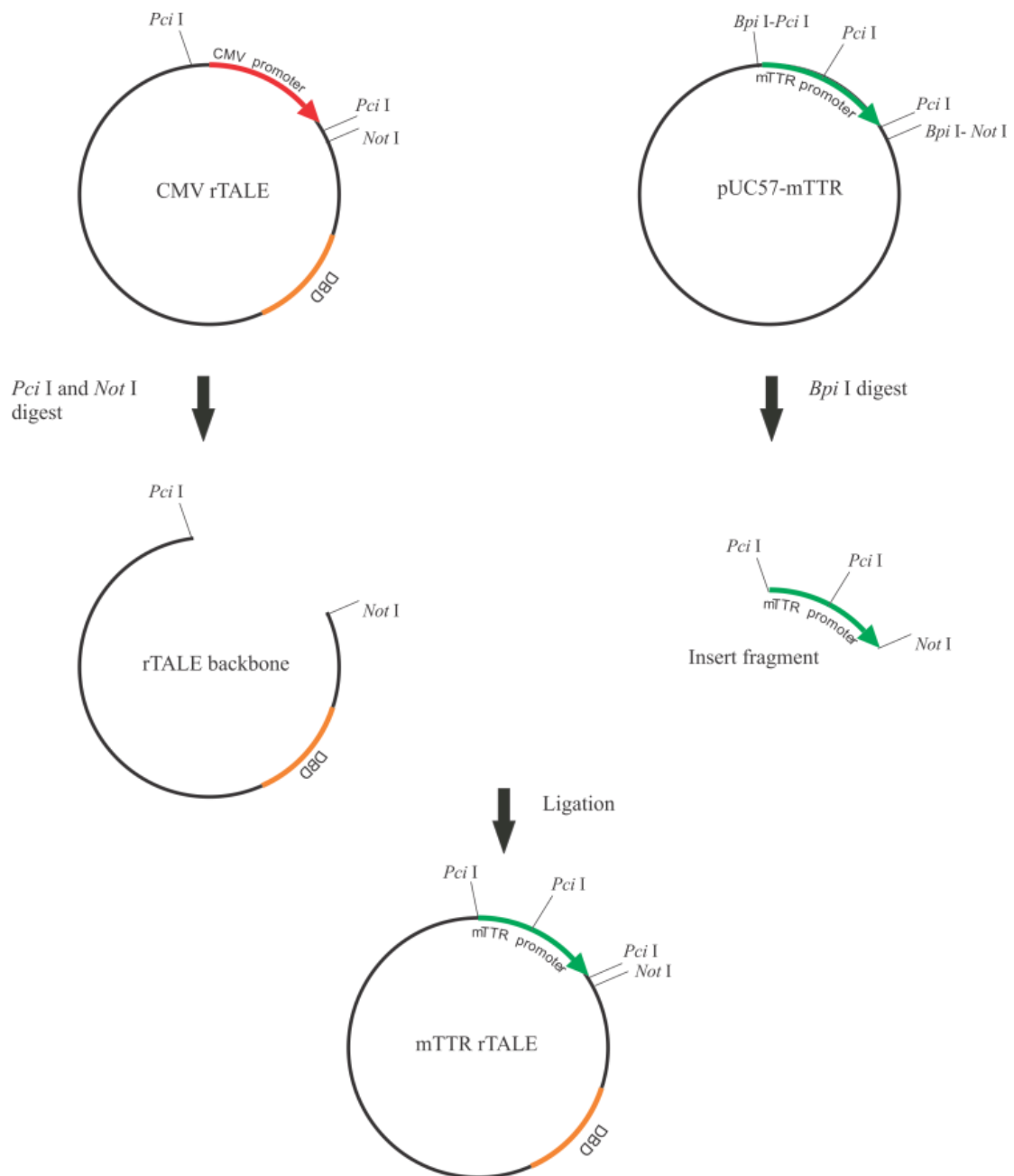


Figure 2.2: Schematic diagram of the cloning strategy used to generate the pRK5-mTTR-control plasmid. The pUC57-mTTR plasmid was digested with *Bpi I* to excise the mTTR promoter sequence. *Bpi I* restriction digest would produce a mTTR fragment with a *Pci I* overhang upstream of the promoter sequence and a *Not I* overhang downstream of the promoter sequence. The pRK5-CMV-control-rTALE plasmid was double digested with *Not I* and *Pci I* to remove the CMV promoter region from the rTALE backbone sequence. Finally, the mTTR promoter sequence was ligated into the rTALE backbone to create the pRK5-mTTR-control-rTALE plasmid.

The mTTR fragment to be cloned into the rTALE vector backbone was synthesised and inserted into the pUC57-Mini plasmid to produce the pUC57-mTTR plasmid (GenScript, NJ, USA). The fragment was excised from the pUC57-mTTR plasmid by *Bpi* I restriction enzyme digestion at 37 °C for 2 hours (Thermo Scientific, CA, USA). The digestion reactions contained 1 µg of pUC57-mTTR plasmid DNA, Buffer G at a final concentration of 1×, 1 U of *Bpi* I enzyme and ddH₂O made to a final volume of 20 µl. Additionally, an undigested control reaction was included that did not contain the restriction enzyme. The restriction digests were resolved on a 1% agarose gel stained with 0.5 µg/ml ethidium bromide and viewed with a GBOX UV transilluminator (Syngene, Cambridge, UK) (Appendix 5.2.1). The 1210 bp insert fragment (Appendix, Figure 5.4), was excised from the gel and purified using the MinElute™ Gel Extraction Kit (Qiagen, Hilden, Germany) (Appendix 5.2.2). DNA recovery was confirmed through agarose gel electrophoresis and quantified by spectrophotometry (Appendix 5.2.1).

The insert was ligated into the pRK5-control-rTALE backbone fragment using T4 DNA Ligase at a 1:3 vector to insert ratio (New England Biolabs, NJ, USA). The ligation reaction was carried out at 16 °C overnight and consisted of 100 ng of the rTALE vector backbone, 59.16 ng of insert fragment, 2 µl of 10× T4 DNA Ligase Reaction Buffer, 1 U of T4 DNA ligase made to a final volume of 20 µl with ddH₂O. After an overnight incubation period, the ligase was heat inactivated at 65 °C for 10 minutes. Ten microlitres of the ligation mix was used to transform 100 µl of chemically competent *E. coli* cells (XL10-Gold, Thermo Scientific, CA, USA) (Appendix 5.2.3). The transformed *E. coli* cells were plated on Luria Bertani (LB) agar plates supplemented with 100 µg/ml ampicillin (Appendix 5.2.3) and incubated at 37 °C overnight. Additionally, a sample of untransformed *E. coli* cells was also plated as a transformation control. Single colonies from the experimental plates were inoculated in 10 ml LB media supplemented with

100 µg/ml ampicillin and cultured at 37 °C in a shaking incubator overnight. Plasmid DNA from the bacterial cultures was isolated and purified using the High Pure Plasmid Isolation Kit (Roche Applied Science, Mannheim, Germany) according to the manufacturer's instructions (Appendix 5.2.4). The purified plasmids were screened by restriction enzyme digestion using *Bam* HI (Thermo Scientific, CA, USA). The successfully cloned plasmid is hereafter referred to as pRK5-mTTR-control-rTALE.

2.2.1.3 Construction of pRK5-mTTR-X1 plasmid

The construction of the pRK5-mTTR-X1 plasmid was achieved in a similar manner as described above for the pRK5-mTTR-control plasmid. The CMV promoter sequence was excised from the pRK5-CMV-X1 plasmid by a *Not* I and *Pci* I double restriction enzyme digestion reaction according to the manufacturer's instructions (Thermo Scientific, CA, USA) for 2 hours at 37 °C. The digested fragments were then resolved on a 1% agarose gel (Appendix 5.2.1) and the pRK5-CMV-X1-rTALE vector backbone was excised and purified from the agarose gel using the MinElute™ Gel Extraction Kit (Qiagen, Hilden, Germany) (Appendix 5.2.2). The mTTR fragment was excised from the pUC57-mTTRplasmid by *Bpi* I (Thermo Scientific, CA, USA) restriction enzyme digestion for 2 hours at 37 °C. The digested fragments were subsequently resolved on a 1% agarose gel (Appendix 5.2.1) and the insert fragment was excised and purified from the agarose gel using the MinElute™ Gel Extraction Kit (Qiagen, Hilden, Germany) (Appendix 5.2.2). Thereafter, the insert was ligated into the vector using T4 DNA ligase (New England Biolabs, NJ, USA) as described above. The ligation reactions were performed at 16 °C overnight and 10 µl of the ligation mix was used to transform 100 µl of chemically competent *E. coli* cells (XL10-Gold, Thermo Scientific, CA, USA) (Appendix 5.2.3). Positive clones containing the insert were screened by *Bam* HI restriction enzyme digestion.

2.2.1.4 Construction of pRK5-mTTR-S1, pRK5-mTTR-S2 and pRK5-mTTR-X2 plasmid

The remaining three mTTR rTALEs were cloned by replacing the TALE sequence from pRK5-mTTR-control-rTALE with the TALE sequence from each of the pRK5-CMV-rTALEs (Figure 2.3). The binding domains from pRK5-CMV-S1-rTALE, pRK5-CMV-S2-rTALE and pRK5-CMV-X2-rTALE were used to generate pRK5-mTTR-S1-rTALE, pRK5-mTTR-S2-rTALE and pRK5-mTTR-X2-rTALE respectively.

pRK5-CMV-S1-rTALE, pRK5-CMV-S2-rTALE and pRK5-CMV-X2-rTALE were double digested with *Kpn* I and *Nhe* I restriction enzymes according to the manufacturer's instructions (Thermo Scientific, CA, USA). Each reaction was carried out at 37 °C for 2 hours and contained 1 µg of each pRK5-CMV-rTALE plasmid individually digested with 1 U *Kpn* I enzyme and 2 U of *Nhe* I enzyme in 2 µl of 1× Buffer Tango in a final volume of 40 µl made up with ddH₂O. The restriction digests were resolved on a 1% agarose gel stained with 0.5 µg/ml ethidium bromide and viewed with a GBOX UV transilluminator (Syngene, Cambridge, UK) (Appendix 5.2.1). The 2584 bp band representing the insert fragment (Figure 6.5 and 6.6) was excised from the gel and purified using the MinElute™ Gel Extraction Kit (Qiagen, Hilden, Germany) (Appendix 5.2.2). DNA recovery was confirmed with gel electrophoresis (Appendix 5.2.1) and the purity and yields were determined spectrophotometrically.

To generate the pRK5-mTTR backbone for cloning, the TALE DNA binding domain represented by the 4723 bp bands (Appendix, Figure 5.7) was excised from the pRK5-mTTR-control-rTALE plasmid (Appendix, Figure 5.2) by double digestion with *Kpn* I and *Nhe* I restriction enzymes as described above.

The rTALE inserts were ligated to the vector backbone by T4 DNA ligase (New England Biolabs, NJ, USA) as described previously. Ten microlitres of the ligation mix was used to

transform 100 µl of chemically competent *E. coli* cells (XL10-Gold, Thermo Scientific, CA, USA) (Appendix 5.2.3). Positive clones containing the correct sized insert were screened using *Bam* HI restriction enzyme digestion.

An additional screening test using *Bgl* I restriction enzyme digestion was performed. The restriction digest reactions contained 1 µg of pRK5-mTTR plasmid DNA, 10× NEB buffer (New England Biolabs, NJ, USA), 1 U *Bgl* I enzyme (New England Biolabs, NJ, USA) made to a final volume of 20 µl with ddH₂O. The restriction digests were resolved on a 0.5% agarose gel stained with 0.5 µg/ml ethidium bromide and viewed with a GBOX UV transilluminator (Syngene, Cambridge, UK) (Appendix 5.2.1).

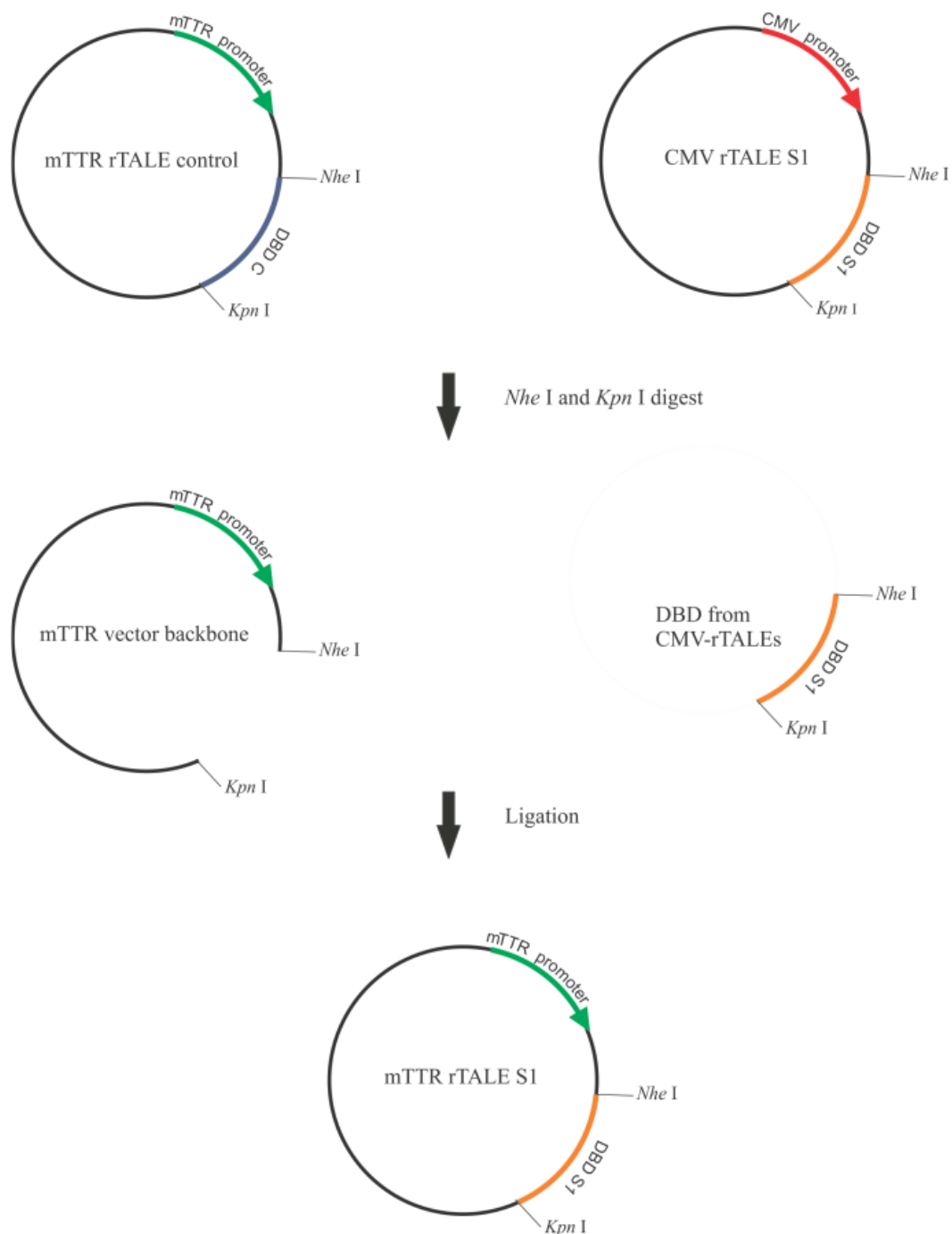


Figure 2.3: Schematic diagram of the cloning strategy used to generate the pRK5-mTTR-plasmids. The successfully cloned pRK5-mTTR-control-rTALE plasmid was double digested with *Kpn* I and *Nhe* I to remove the TALE DNA-binding domain (DBD) and yield the mTTR rTALE backbone. The CMV-driven rTALEs; pRK5-CMV-S1-rTALE, pRK5-CMV-S2-rTALE and pRK5-CMV-X2-rTALE, were separately double digested with *Kpn* I and *Nhe* I to excise and extract their respective DBDs. Each DBD was separately ligated into the mTTR rTALE backbone to create the pRK5-mTTR-S1-rTALE, pRK5-mTTR-S2-rTALE and pRK5-mTTR-X2-rTALE plasmids.

2.3 Plasmid preparation

All plasmids were prepared with the Plasmid Maxi Kit (Qiagen, Hilden, Germany) according to the manufacturer's instructions, and resuspended in 200 µl of sterile H₂O (Appendix 5.2.5).

2.4 Mammalian cell culture

The liver-derived, human hepatoma 7 (Huh 7) and the kidney derived, human embryonic kidney 293T (HEK293T) cell lines were maintained using routine cell culture methodologies. The cells were cultured in CellStar® 75 cm² cell culture flasks (Greiner Bio-One, Frickenhausen, Germany) and were maintained in low glucose (1 g/L) Gibco™ Dulbecco's Modified Eagle's Medium (DMEM) (Thermo Scientific, CA, US), supplemented with 10% foetal calf serum (FCS), penicillin (100 000 U/ml) and streptomycin (100 µg/ml), in a humidified incubator at 37 °C and 5% CO₂. Cells were routinely tested for mycoplasma contamination using a MycoAlert™ Mycoplasma Detection Kit (Lonza, Basel, Switzerland) according to the manufacturer's instructions (Appendix 5.2.6). Cells were monitored using an Olympus CKX31 light microscope (Olympus, Tokyo, Japan). Once the cells reached 80% confluency, the media was discarded, the cells washed with, and incubated in saline at 37 °C for 3 minutes. The saline was removed and the cells were incubated with 1 ml of 1× TrypLE Express (Thermo Scientific, CA, USA) at 37 °C for 3 minutes. The cells were dislodged from the surface by gently tapping the flask and resuspended in growth media. The cells were subsequently transferred to a new 75 cm² tissue culture flask. Huh 7 cells were grown in conditioned media prepared by combining an equal volume of fresh media and spent media. The flasks were incubated at 37 °C and 5% CO₂ until the next passage.

2.5 Determination of rTALE expression in cell culture

2.5.1 Transient transfection of cultured mammalian cells with rTALE expression vectors

A day prior to transfection, the Huh 7 and HEK293T cells were seeded at a density of 30% and 40% respectively in CellStar® 48-well plates (Greiner Bio-One, Frickenhausen Germany) in 250 µl of complete DMEM. Using jetPRIME® transfection reagent (Polyplus-transfection, Illkirch, France) (Appendix 5.2.7) or Lipofectamine™ 3000 (Thermo Scientific, CA, USA) (Appendix 5.2.8), cultured cells were transfected with 200 ng of each of the CMV- and mTTR-driven rTALE plasmids according to the manufacturer's instructions. A mock transfection where 200 ng of pTZ57R was transfected was included as a negative control. To assess transfection efficiency, a transfection containing 200 ng of pCI-neo-eGFP was performed separately. All the transfections were carried out in triplicate. Forty-eight hours after transfection immunofluorescence staining was carried out on the transfected cells.

2.4.5.1.1 Immunofluorescence staining

Forty-eight hours post-transfection, the efficiency of the transfection was assessed by analysing GFP expression through a Fluorescein isothiocyanate (FITC) filter using a fluorescence microscope (Axiovert 100M, Zeiss, Germany). Spent medium was removed from wells and the cells were washed with 500 µl of 1× phosphate buffered saline (PBS) (Sigma-Aldrich, MO, USA). The cells were subsequently fixed in 500 µl of 4 % paraformaldehyde (PFA) at room temperature for 15 minutes. The fixed cells were washed twice with 500 µl of 1× PBS and incubated with 500 µl of 0.1% Triton-X (Sigma-Aldrich, MO, USA) in PBS for 10 minutes at room temperature to permeabilise the cells. The cells were then washed twice with 500 µl of 1× PBS and blocked in 100 µl of 1% bovine serum albumin (BSA) (Roche Applied Science, Mannheim, Germany), in 1× PBS at room

temperature for 1 hour in a humidity chamber. After the blocking process, the cells were incubated for 1 hour at room temperature in a humidity chamber with 100 μ l of mouse anti-HA primary antibody (Abcam, MA, UK) diluted 1:200 in 1% BSA in PBS. After the incubation period, the cells were washed twice with 500 μ l of 1 \times PBS, and incubated in the dark at room temperature in a humidity chamber for 40 minutes with 100 μ l of rabbit anti-mouse Alexa Fluor 488 labelled secondary antibody that was diluted 1:200 in 1% BSA in PBS. The cells were then washed twice with 500 μ l of 1 \times PBS followed by counterstaining the cell nuclei with 100 μ l of 1 \times 4,6-diamidino-2-phenylindole chloride (DAPI) for 5 minutes at room temperature. The DAPI was removed by washing the cells with 500 μ l of 1 \times PBS and the fluorescent labelling of the cells viewed using a fluorescence microscope (Axiovert 100M, Zeiss, Germany) equipped with filters for the detection of FITC and DAPI signal.

2.6 Assessing rTALE-mediated HBV gene knockdown

2.6.1 Transient transfection of cultured mammalian cells with rTALE expression vectors

A day prior to transfection, Huh 7 and HEK293T cells were seeded at a density of 30% and 40% respectively in CellStar® 6-well plates (Greiner Bio-One, Frickenhausen, Germany) in 2 ml of complete DMEM. Using jetPRIME® transfection reagent (Polyplus-transfection, Illkirch, France) (Appendix 5.2.7) or Lipofectamine™ 3000 (Thermo Scientific, CA, USA) (Appendix 5.2.8), the cultured cells were transfected with each of the CMV- and mTTR-driven rTALE plasmids according to the manufacturer's instructions. The transfections were performed in triplicate and the DNA mixes were prepared as follows: 100 ng of pCI-neo-eGFP, 180 ng of pCH-9/3091 and 1800 ng of either rTALE. A mock transfection where 1800 ng of pTZ57R was substituted for the rTALE DNA in the

mixes was also included. All the transfections were carried out in triplicate and forty-eight hours after transfection ELISA and qPCR was carried out.

2.6.1.1 ELISA

Forty-eight hours post transfection, HBsAg levels were measured using the Monolisa™ HBs Ag ULTRA kit (Bio-Rad, CA, USA) according to the manufacturer's instructions. Briefly, 100 µl of the cell supernatant was added to the wells of a microplate coated with mouse monoclonal anti HBsAg antibody. Fifty microlitres of the conjugate working solution, containing mouse monoclonal and polyclonal anti HBsAg antibodies bound to a peroxidase, was added to the wells, the plate covered with adhesive film and incubated for 1 hour and 30 minutes at 37 °C. After the incubation, the wells were washed 5 times in an Immuno Wash™ 1575 Microplate Washer (Bio-Rad, CA, USA) using the supplied washing solution to remove any unbound conjugate. Thereafter, 100 µl of a development solution containing the substrate and a chromogen was added to the wells and the plate incubated in the dark for 30 minutes at room temperature. After the incubation, the reaction was terminated using 100 µl of stopping solution and 4 minutes later the optical densities of the samples in the wells were measured at 490/700 nm using a Model 680 Microplate Reader (Bio-Rad, CA, USA).

2.6.1.2 Relative quantification of HBV gene expression

Forty-eight hours post transfection, total RNA was extracted from the transfected cells using TRIzol® Reagent (Thermo Scientific, CA, USA) according to the manufacturer's instructions. Briefly, the spent media was removed and 1 ml of TRIzol® Reagent was added to each well to lyse the cells. The lysate was transferred to a microcentrifuge tube and incubated at room temperature for 5 minutes. Two hundred microlitres of chloroform was added to the lysates, the samples were mixed and then incubated for 3 minutes at room

temperature followed by centrifugation at 12 000 ×g for 15 minutes at 4 °C. The aqueous phase, which contains the RNA, was transferred to a clean microcentrifuge tube, to which 0.5 ml of 100% isopropanol was added and the mixture incubated for 10 minutes at room temperature. The samples were centrifuged at 12 000 ×g for 10 minutes at 4 °C. The supernatant was discarded and the RNA pellet was washed by adding 0.5 ml of 75 % ethanol, followed by brief vortexing and centrifugation at 7500 ×g for 5 minutes at 4 °C. The RNA pellet was air dried for 10 minutes, and re-suspended in 30 µl of RNase-free water. The purity and concentration of samples were assessed by spectrophotometry.

Using the QuantiTect reverse transcription kit (Qiagen, Hilden, Germany), the extracted RNA was reversed transcribed to cDNA according to manufacturer's instructions. First, the extracted RNA was treated to remove any genomic DNA (gDNA). The gDNA elimination reaction consisted of 1 µg of the extracted RNA, 2 µl of 7× gDNA Wipeout Buffer and made to a final volume of 14 µl with RNase-free water. The reactions were incubated at 42 °C for 5 minutes. After the incubation period, 1 µl of QuantiTect reverse transcriptase, 4 µl of 5× QuantiTect reverse transcription (RT) buffer and 1 µl of RT primer mix were added to the RNA samples and incubated at 42 °C for 30 minutes. Negative control reactions were included where the reverse transcriptase enzyme was omitted from the reaction. To deactivate the Quantitect reverse transcriptase the samples were then incubated at 95 °C for 3 minutes.

For the relative quantitation of the HBV *surface* mRNA and pgRNA as well as the human *glyceraldehyde-3-phosphate dehydrogenase* (hGAPDH) mRNA, separate quantitative PCR (qPCR) mixes were prepared. The qPCR reaction mixes contained 10 µl of 2× concentrated FastStart Essential DNA Green Master (Roche Applied Science, Mannheim, Germany), 10 pmol each of the respective forward and reverse primers, 5 µl of template cDNA and

RNase-free water to make a final volume of 20 μ l. The primers used for the amplification of the genes of interest are indicated in Table 2.3. The qPCR reactions were carried out using the Bio-Rad CFX96™ RealTime System (Bio-Rad, CA, USA) with the following thermal cycling conditions: 1 pre-incubation cycle for initial denaturation of DNA and activation of polymerase at 95 °C for 3 minutes; followed by 45 cycles of denaturation for 10 seconds at 95 °C, annealing for 10 seconds at 58 °C and extension for 10 seconds at 72 °C. mRNA expression of HBV genes was normalised to h*GAPDH* mRNA expression, and the relative amounts were calculated using the comparative Ct method.

Table 2.3: Sequences of the primers used in qPCR to amplify the HBV and h*GAPDH* genes.

The expected amplicon sizes are also displayed

Primer name	Primer sequence	Expected amplicon size
HBV <i>Surface</i> forward	5'- TGC ACC TGT ATT CCC ATC -3'	142 bp
HBV <i>Surface</i> reverse	5'- CTG AAA GCC AAA CAG TGG -3'	
HBV <i>Core</i> forward	5'- ACC ACC AAA TGC CCC TAT -3'	125 bp
HBV <i>Core</i> reverse	5'- TTC TGC GAG GCG GCG A -3'	
h <i>GAPDH</i> forward	5'- GAA GGT GAA GGT CGG AGT C -3'	226 bp
h <i>GAPDH</i> reverse	5'- GAA GAT GGT GAT GGG ATT TC -3'	

2.4 Assessment of potential cellular toxicity

2.4.1 Examining potential rTALE-mediated cell toxicity

2.4.1.1 Transient transfection of cultured mammalian cells with rTALE expression vectors

A day prior to transfection, Huh 7 cells were seeded at a density of 30% in CellStar® 96-well plates (Greiner Bio-One, Frickenhausen, Germany) in 0.1 ml of complete DMEM. Using jetPRIME® transfection reagent (Polyplus-transfection, Illkirch, France) (Appendix 5.2.7) or Lipofectamine™ 3000 (Thermo Scientific, CA, USA) (Appendix 5.2.8), the cultured cells were transfected according to manufacturer's instructions with 10 ng of pCI-neo-eGFP, 8 ng of pCH-9/3091 and 80 ng of each of the rTALE plasmids. A mock transfection with 80 ng of pTZ57R substituted for the rTALE DNA was included as a control. An untransfected control consisting of cells receiving no DNA was included. Additionally, wells receiving DMEM but no cells were included as blank controls. All the transfections were carried out in triplicate. Forty-eight hours after transfection an MTT assay was carried out.

2.4.1.1.1 MTT assay

Forty-eight hours post transfection, 20 µl of 3-(4,5-Dimethylthiazol-2-yl)-2,5-diphenyltetrazolium bromide (MTT) solution (5 mg/mL dissolved in 1× PBS) was added into each well and mixed by shaking for 5 minutes. Thereafter the plate was incubated for 4 hours at 37 °C and 5% CO₂. Culture medium was gently aspirated from the wells and the formazan crystals formed were resuspended in 200 µl DMSO by pipetting up and down for 5 minutes. Optical density was measured at 570 and 650 nm using a Model 680 Microplate Reader (BioRad, CA, USA).

2.4.2 Examining potential off-target binding

Potential rTALE off-target binding sites in the *Homo sapiens* genome were determined using the TALE-NT 2.0 TAL target finder (175) for the S1 and S2 rTALEs. Primers were designed to amplify the *prostate androgen-regulated transcript 1 (PART1)* and *phosphodiesterase 4D (PDE4D)* genes as they lie near the potential off-target site. Multiple alternatively spliced transcript variants have been described for these genes (176, 177) and as such a qPCR assay that simultaneously detected all the of transcripts using different sets of primers was designed.

2.4.2.1 Transient transfection of cultured mammalian cells with rTALE expression vectors

A day prior to transfection, Huh7 cells were seeded at a density of 30% in CellStar® 6-well plates (Greiner Bio-One, Frickenhausen, Germany) in 2 ml of complete DMEM. Using jetPRIME® transfection reagent (Polyplus-transfection, Illkirch, France) (Appendix 5.2.7) or Lipofectamine™ 3000 (Thermo Scientific, CA, USA) (Appendix 5.2.8), the cultured cells were transfected according to manufacturer's instructions with 1900 ng of the CMV- and mTTR-driven rTALEs and 100 ng of pCI-neo-eGFP. A transfection with 1900 ng of pTZ57R and 100 ng of pCI-neo-eGFP was included as a negative control. All the transfections were performed in triplicate and 48 hours after the transfection qPCR was carried out.

2.4.2.1.2 Quantitative PCR analysis of potential rTALE off-target binding genes

Forty-eight hours post transfection a qPCR reaction was carried out as described in section 2.6.1.2. The primers used for the amplification of the genes of interest are indicated in Table 2.4

Table 2.4: Sequences of the primers used in qPCR to amplify the potential rTALE off-target binding sites. The expected amplicon sizes are also displayed

Primer name	Primer sequence	Expected amplicon size
PART1-A forward	5'- GAA AAC GCA GCT ACA CCT G -3'	148 bp
PART1-A reverse	5'- CTC ATA TAG TCA CCG AAG GCA G -3'	
PART1-B forward	5'- TGC CTT CCA GGA GTT TCA C -3'	148 bp
PART1-B reverse	5'- TGC TTC AAT TTA CCC GTC CAG -3'	
PART1-C forward	5'- CCG TCC CAG AAA CCA AAG G -3'	80 bp
PART1 C reverse	5'- CTC CTG CTT GCC AAA TCT TG -3'	
PDE4D A forward	5'- GCC AGT GAT ATA CAC GGA GAT G -3'	133 bp
PDE4D A reverse	5'- TGG GTG ATC TTT TGC TAG GTG -3'	
PDE4D B forward	5'- ATG TTT TCA GAA TAG CAG AGT TGT C -3'	150 bp
PDE4D B reverse	5'- CAT GGT AAT GGT CTT CGA GAG TC -3'	
PDE4D C forward	5'- CCT GTG ATT TGC TTT CTC GG -3'	133 bp
PDE4D C reverse	5'- GGA AGC TGA ATA TTG CGA CAT G -3'	

2.5 Statistical analysis

Data is represented as the mean (n=3) \pm the standard error of the mean (SEM). GraphPad Prism software package version 4.03 (GraphPad, CA, USA) was used to perform two-tailed paired student's t tests. Statistical differences were regarded as significant for p values < 0.05 .

Chapter 3

3. Results

3.1 Successful generation of mTTR-driven rTALE vectors

Four mTTR-driven rTALEs were constructed to target the HBV genome and transcriptionally repress viral gene expression. These rTALEs contain a DBD that has been engineered to bind specific sequences of HBV cccDNA, a KRAB domain for transcriptional silencing and an mTTR promoter to ensure liver-specific expression. An additional rTALE, targeted against an unrelated sequence, was constructed and used as a negative control. The rTALEs were generated from existing CMV-driven rTALEs (unpublished data), using restriction enzyme digestion and ligation methods, as discussed in Section 2.2.

pRK5-mTTR-control-rTALE and pRK5-mTTR-X1-rTALE were successfully generated by removing the CMV promoter of the respective plasmids and replacing it with the mTTR promoter sequence. Initially the same cloning strategy was used for the generation of pRK5-mTTR-S1-rTALE, pRK5-mTTR-S2 and pRK5-mTTR-X2. This was unsuccessful necessitating an alternative approach which entailed replacing the DBD of pRK-mTTR-control-rTALE with the S1, S2 or X2 DBD encoding sequence. Positive clones were identified using *Bam* HI digestion which would cut in the insert and vector backbone sequences. Based on the vector map and the agarose gel, all the clones proved to be positive for the correct insert as they yielded the expected 3128 and 4179 bp band sizes (Figure 3.1). Additionally, *Bgl* I restriction enzyme was carried out which generates specific banding patterns from the DBD and allows the CMV-driven rTALEs to be

distinguished from each other and the mTTR-driven rTALEs to be distinguished from each other (Figure 3.2).

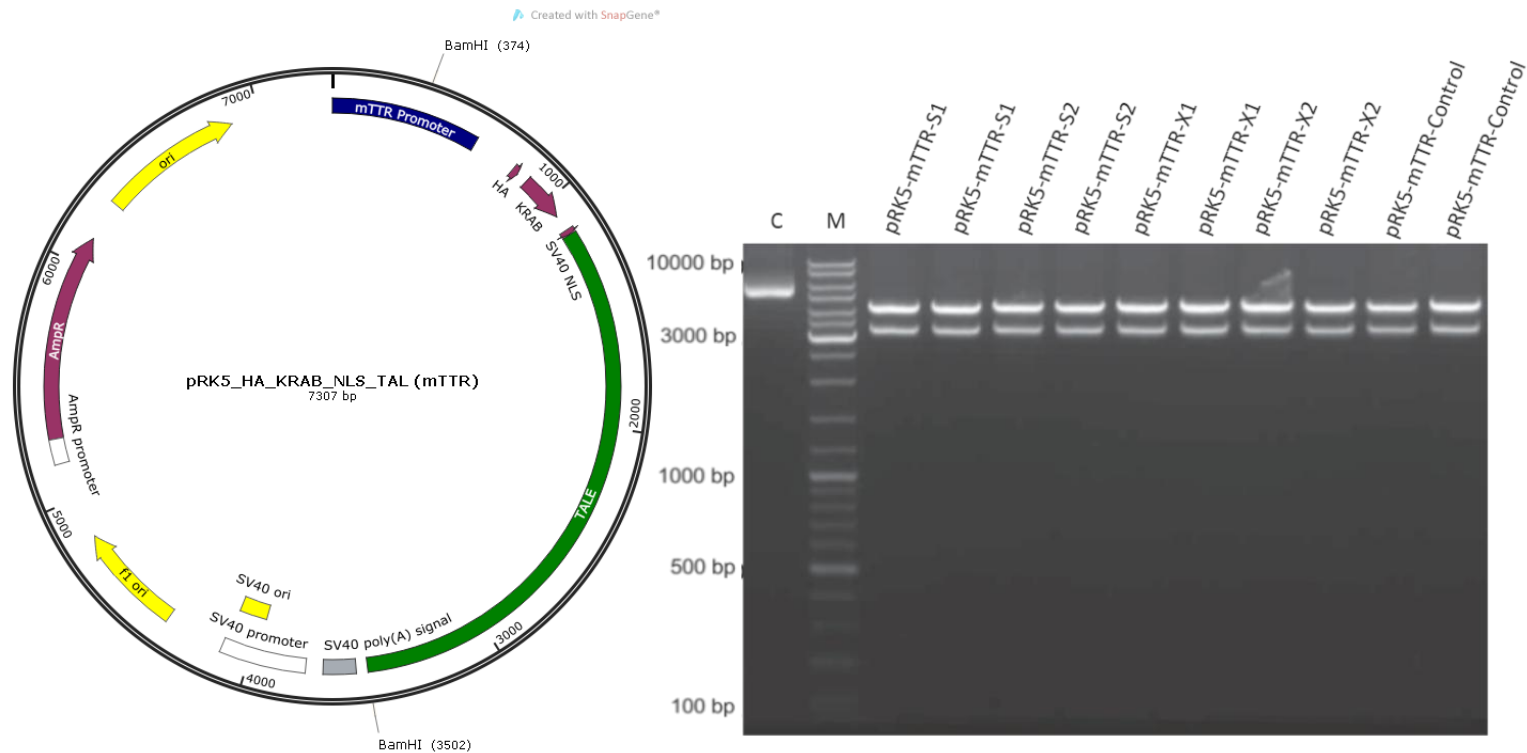


Figure 3.1: Confirmation of complete pRK5-mTTR-rTALEs assembly. mTTR-driven rTALE plasmids were generated by replacing the CMV promoter sequence of CMV-driven rTALEs with that of an mTTR promoter. The final mTTR-driven rTALE vector map with *Bam* HI restriction sites is shown on the left and agarose gel electrophoresis restriction digestion migration patterns of selected rTALE clones is shown on the right. Clones were screened with a *Bam* HI restriction enzyme digest, indicating successfully generated clones with a 3128 and 4179 bp band. All the clones of pRK5-mTTR-S1, pRK5-mTTR-S2, pRK5-mTTR-X1, pRK5-mTTR-X2 and pRK5-mTTR-control yielded the correct banding patterns. (M: O'GeneRuler 1 kb DNA Ladder (Thermo Scientific, CA, USA); C1: undigested control).

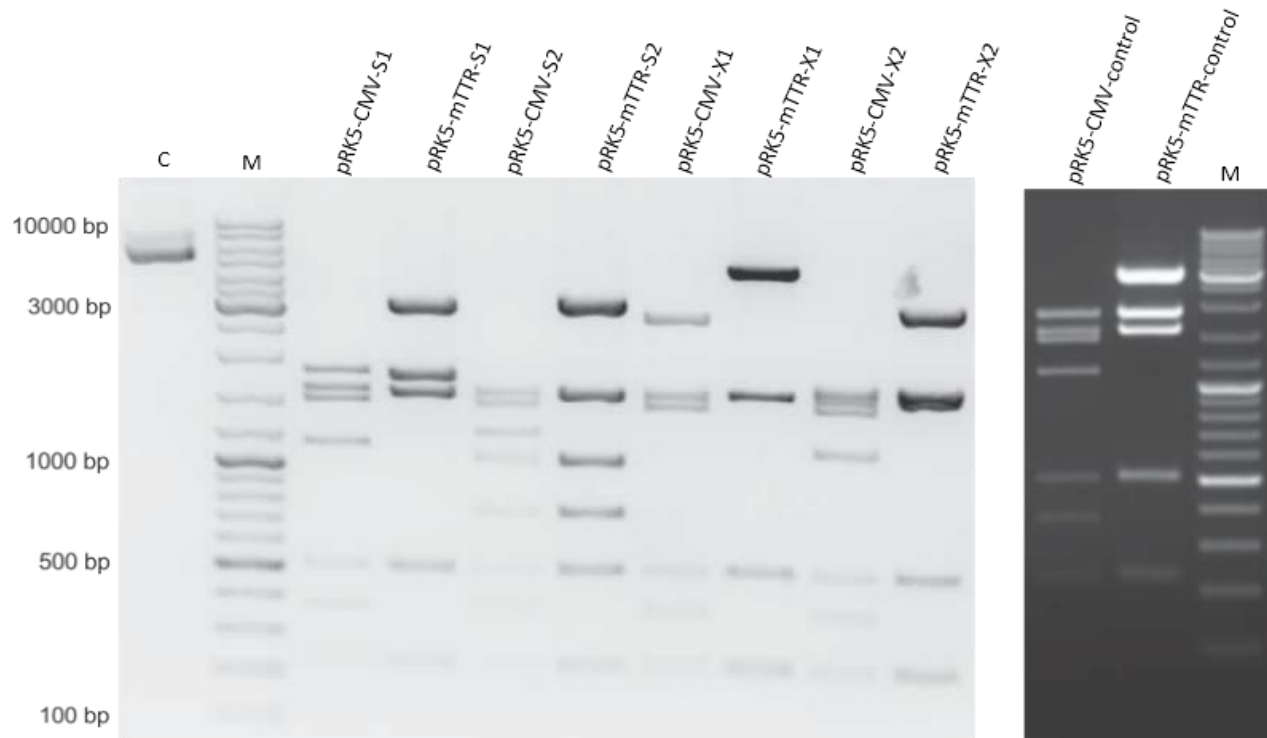


Figure 3.2: Confirmation of rTALE identity. mTTR-driven rTALE plasmids were generated by replacing the CMV promoter sequence of CMV-driven rTALEs with that of an mTTR promoter. Restriction enzyme digestion of the mTTR rTALEs with *Bgl* I produces banding patterns that allows the CMV-driven rTALEs to be distinguished from each other and the mTTR-driven rTALEs to be distinguished from each other (M: O'GeneRuler 1 kb DNA Ladder (Thermo Scientific, CA, USA); C1: undigested control).

3.2 Liver-specific expression of mTTR rTALEs *in vitro*

The mTTR promoter sequence contains binding sites for liver-specific factors which are required to initiate mTTR promoter activity, thereby permitting tissue-specific expression from the promoter (171). To determine whether the cloned mTTR promoter drives liver-specific expression of the rTALE sequences, Huh 7 and HEK293T cells were transiently transfected with each of the CMV- and mTTR-driven rTALE vectors. Expression of the rTALEs was assessed by immunofluorescence (IF) staining of the transfected cells using a monoclonal primary antibody to the HA epitope of the rTALEs, and a fluorescently labelled secondary antibody. A mock transfection with pTZ57R plasmid was used as a negative control. Transfections were performed in triplicate to ensure reproducibility. Successful transfections of the cells were determined by GFP expression in the control wells.

In both Huh 7 and HEK293T cells, GFP expression in the control wells reveals that transfection with the pCI-neo-eGFP plasmid was successful (Figure 3.3). This further suggested that the transfections in the experimental wells were successful. Green fluorescence signal from the IF staining indicate that the mTTR-driven rTALEs are detected in the liver derived Huh 7 cells only (Figure 3.4 - 3.8). Whereas the CMV-driven rTALEs were detected in both the Huh 7 and HEK293T cells (Figure 3.4 - 3.8). The negative control which is cells transfected with pTZ57R only, had no green fluorescence signal as this plasmid does not express an HA-tag (Figure 3.3). The data confirms that the mTTR promoter is functional as it expresses the rTALE proteins, and in stark contrast to the CMV promoter, exhibits tissue-specificity as rTALE expression was only detected in the liver-derived cells.

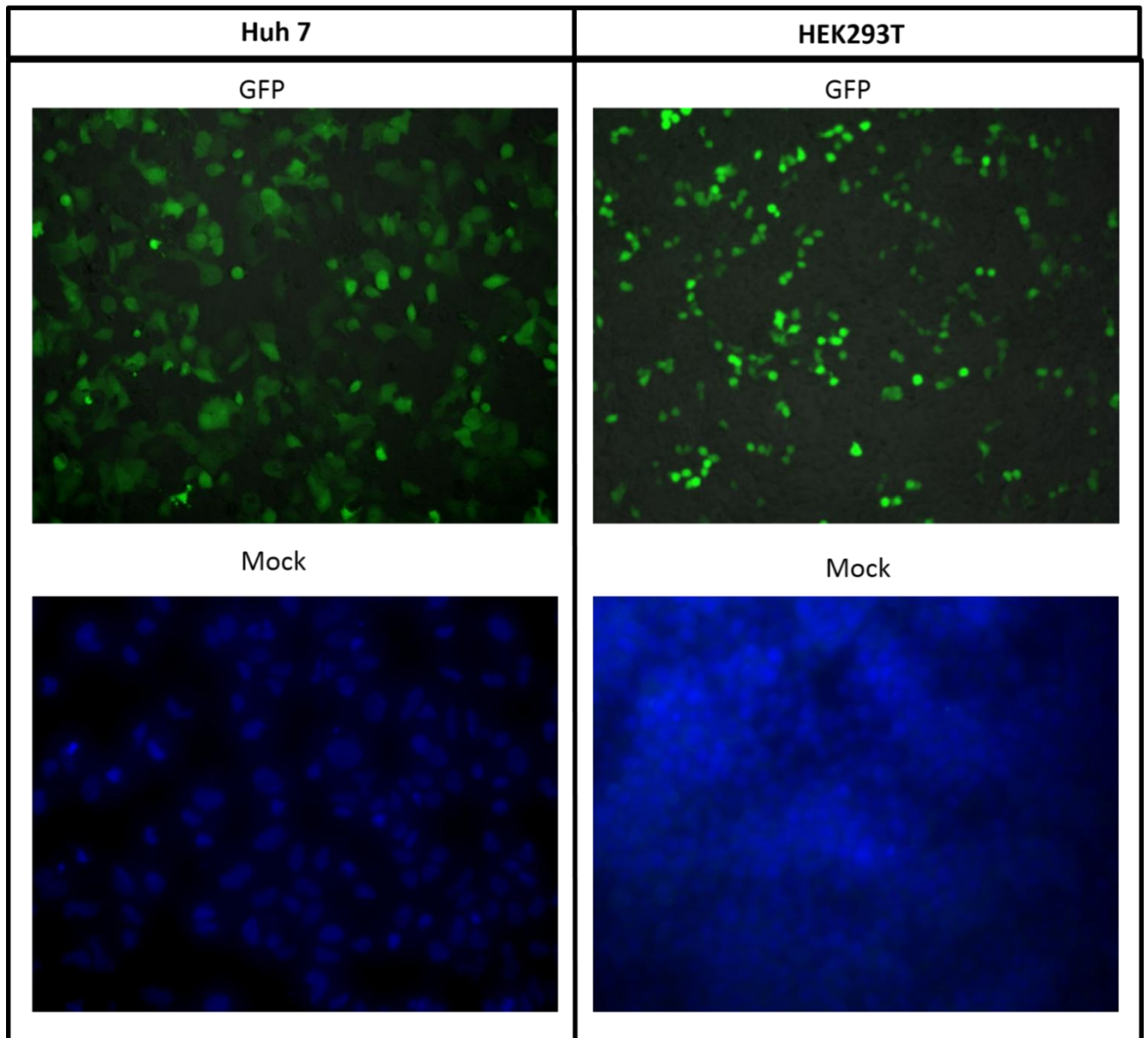


Figure 3.3: Immunofluorescence detection of rTALEs *in vitro*. Immunofluorescence staining was performed to detect rTALE expression in cell culture. Huh 7 and HEK293T cells were transfected with pTZ57R as a mock transfection and separately with pCI-neo-eGFP plasmid to assess transfection efficiency. An anti-HA primary antibody together with a fluorescently labelled secondary antibody was used to detect the HA tag on the rTALEs and fluorescence imaged by microscopy. DAPI was used to stain the nuclei. GFP analysis show good transfection efficiency in both cell lines. No IF signal was detected in the mock transfections. Cells were visualised using a fluorescence microscope at 20× magnification for HEK293T cells and at 40×magnification for Huh 7 cells.

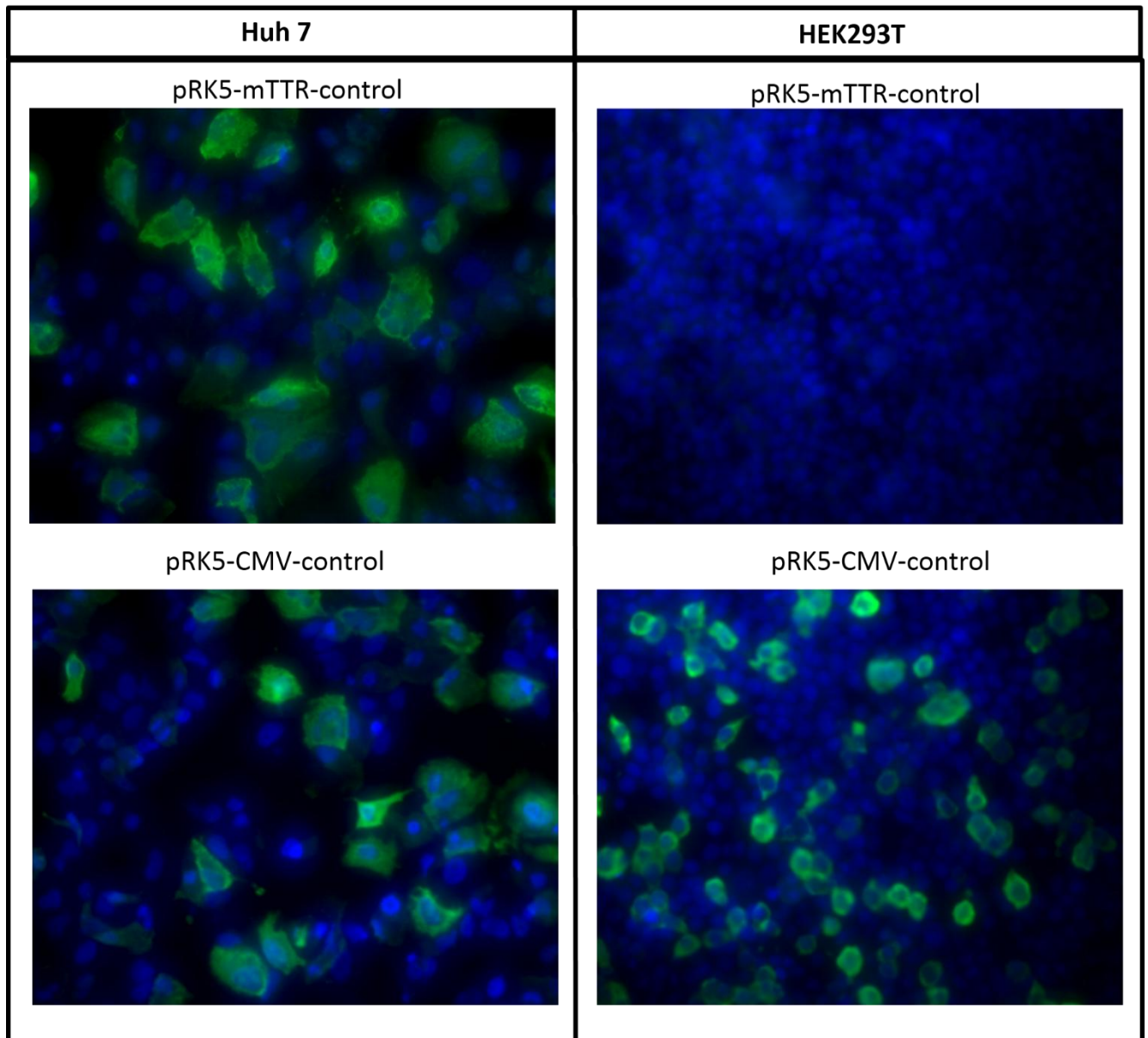


Figure 3.4: Immunofluorescence detection of control rTALEs *in vitro*. Immunofluorescence staining was performed to detect rTALE expression in cell culture. Huh 7 and HEK293T cells were transfected with the CMV- and mTTR-control rTALE plasmids. An anti-HA primary antibody together with a fluorescently labelled secondary antibody was used to detect the HA tag on the rTALEs and fluorescence imaged by microscopy. DAPI was used to stain the nuclei. The CMV-control rTALE was detected in both cell lines, whereas the mTTR-control rTALE was only detected in the Huh 7 cells. Cells were visualised using a fluorescence microscope at 20× magnification for HEK293T cells and at 40× magnification for Huh 7 cells.

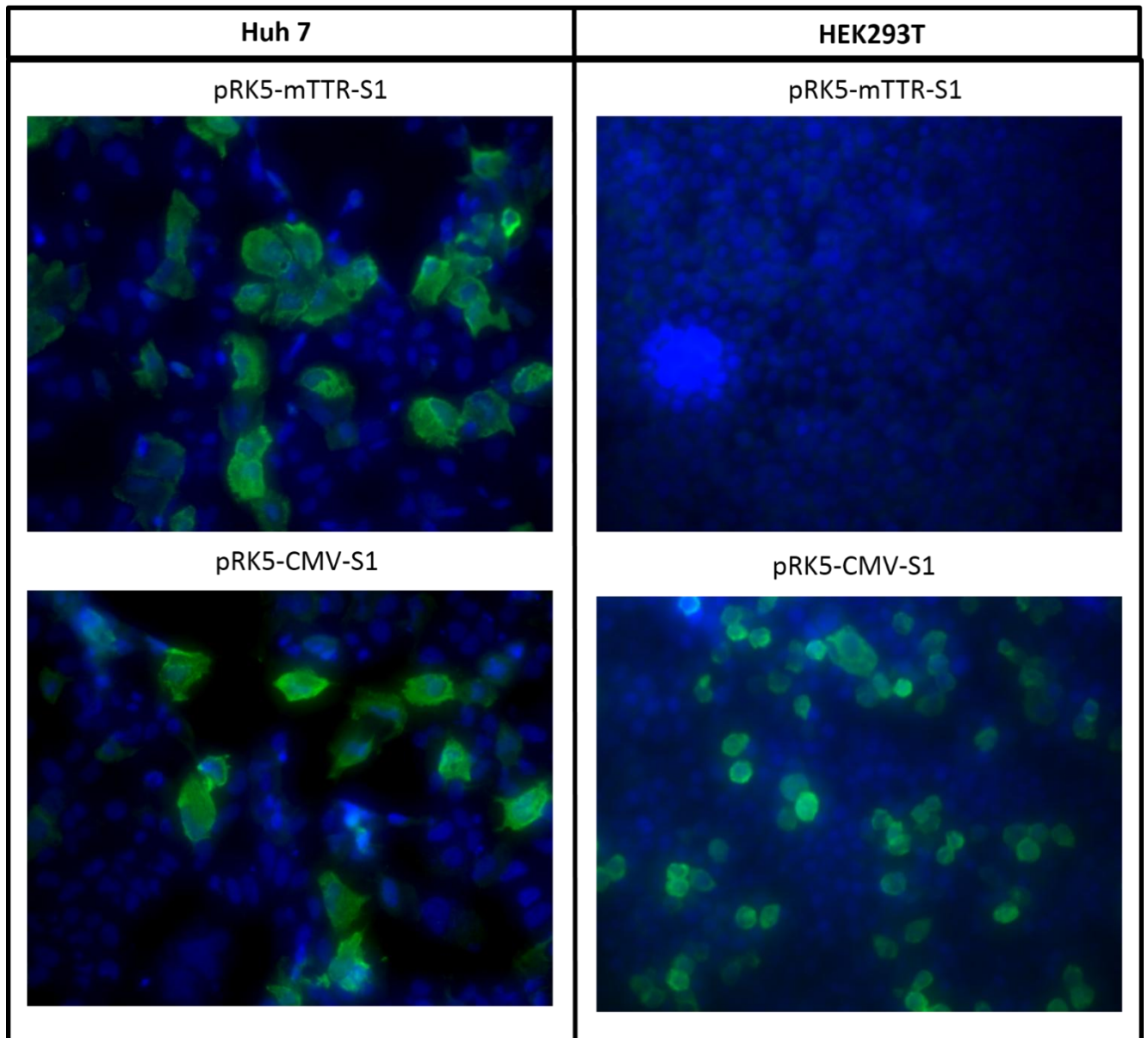


Figure 3.5: Immunofluorescence detection of S1 rTALEs *in vitro*. Immunofluorescence staining was performed to detect rTALE expression in cell culture. Huh 7 and HEK293T cells were transfected with the CMV- and mTTR-S1 rTALE plasmids. An anti-HA primary antibody together with a fluorescently labelled secondary antibody was used to detect the HA tag on the rTALEs and fluorescence imaged by microscopy. DAPI was used to stain the nuclei. The CMV-S1 rTALE was detected in both cell lines, whereas the mTTR-S1 rTALE was only detected in the Huh 7 cells. Cells were visualised using a fluorescence microscope at 20× magnification for HEK293T cells and at 40× magnification for Huh 7 cells.

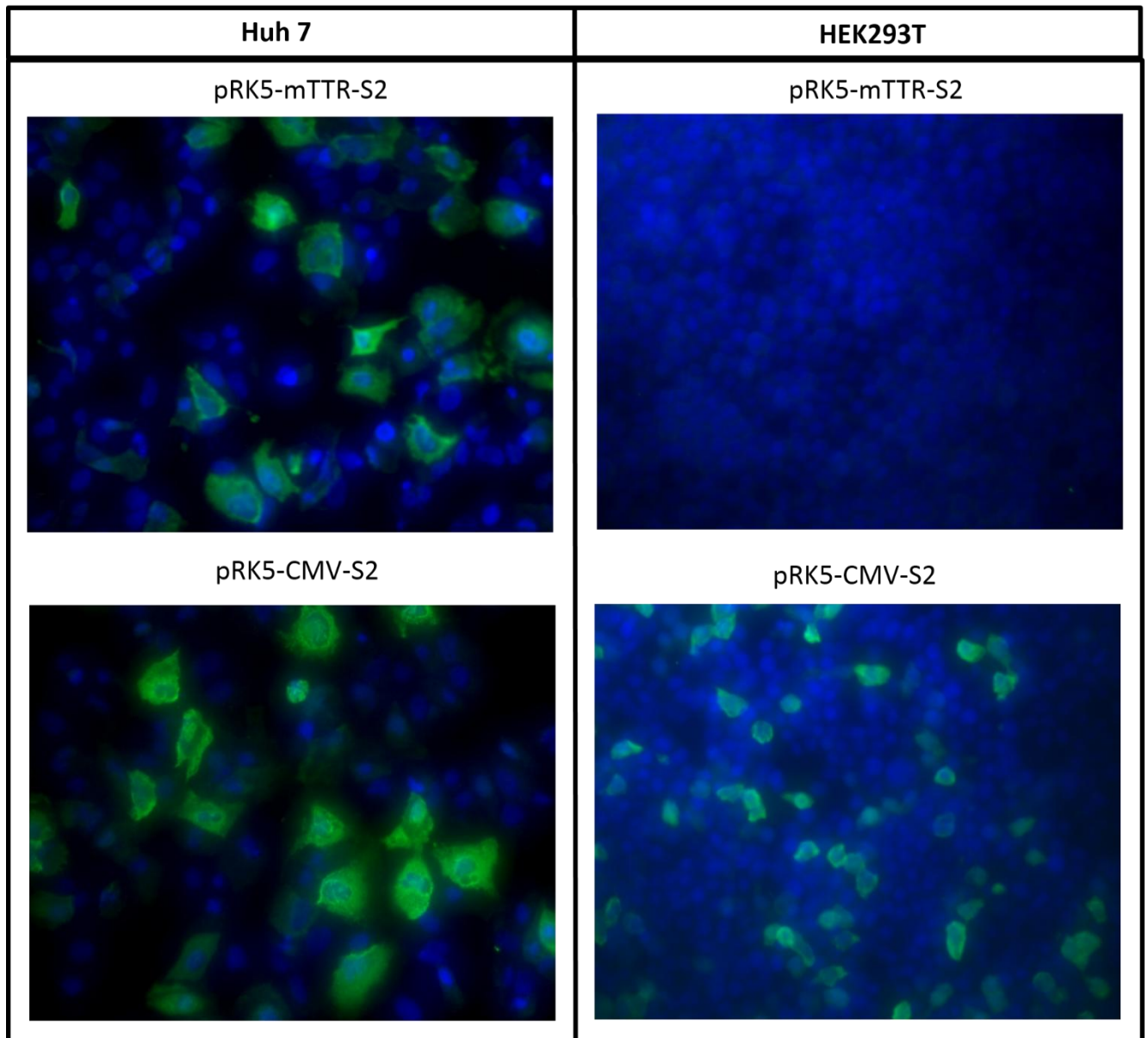


Figure 3.6: Immunofluorescence detection of S2 rTALEs *in vitro*. Immunofluorescence staining was performed to detect rTALE expression in cell culture. Huh 7 and HEK293T cells were transfected with the CMV- and mTTR-S2 rTALE plasmids. An anti-HA primary antibody together with a fluorescently labelled secondary antibody was used to detect the HA tag on the rTALEs and fluorescence imaged by microscopy. DAPI was used to stain the nuclei. The CMV-S2 rTALE was detected in both cell lines, whereas the mTTR-S2 rTALE was only detected in the Huh 7 cells. Cells were visualised using a fluorescence microscope at 20× magnification for HEK293T cells and at 40× magnification for Huh 7 cells.

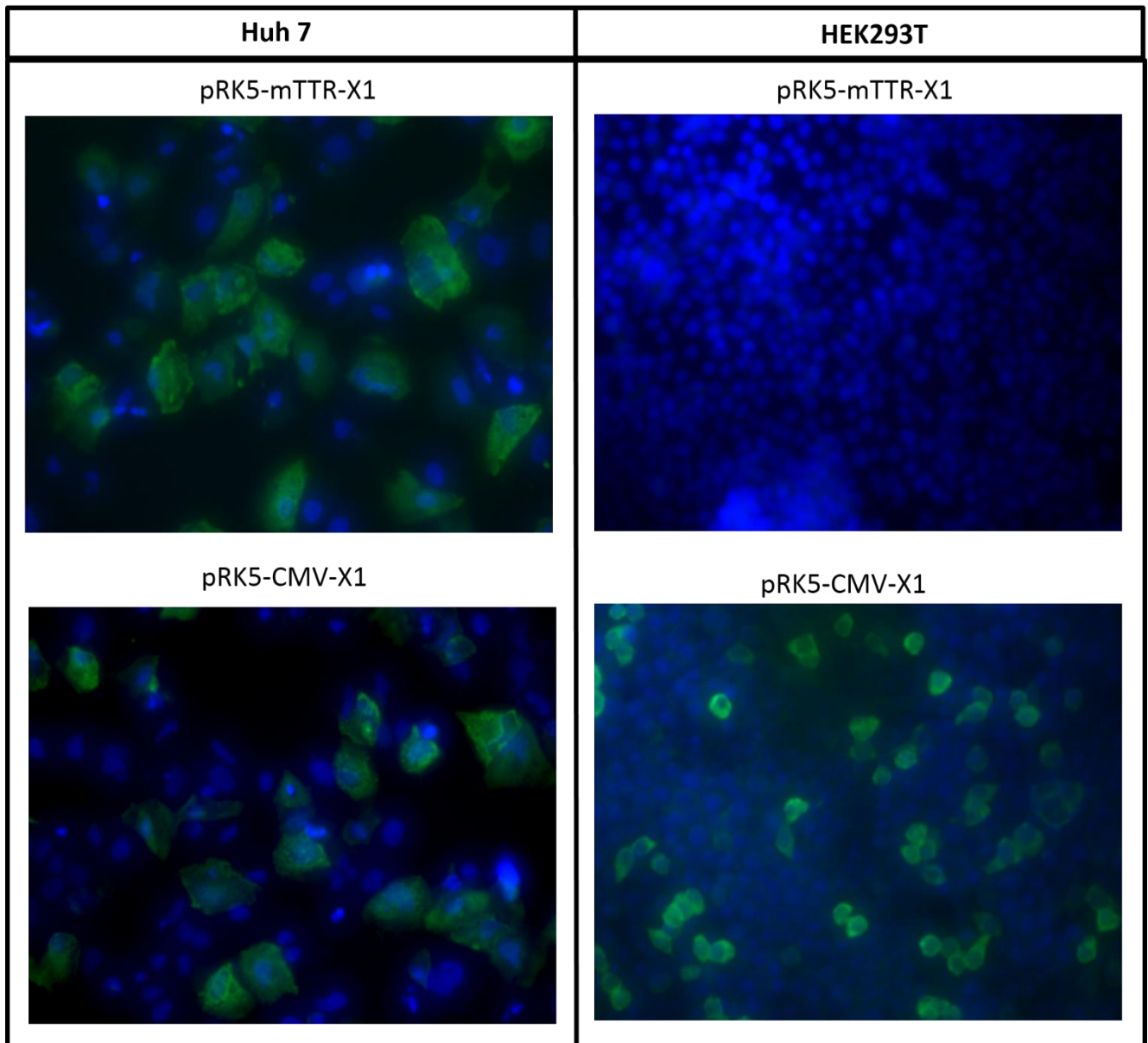


Figure 3.7: Immunofluorescence detection of X1 rTALEs *in vitro*. Immunofluorescence staining was performed to detect rTALE expression in cell culture. Huh 7 and HEK293T cells were transfected with the CMV- and mTTR-X1 rTALE plasmids. An anti-HA primary antibody together with a fluorescently labelled secondary antibody was used to detect the HA tag on the rTALEs and fluorescence imaged by microscopy. DAPI was used to stain the nuclei. The CMV-X1 rTALE was detected in both cell lines, whereas the mTTR-X1 rTALE was only detected in the Huh 7 cells. Cells were visualised using a fluorescence microscope at 20× magnification for HEK293T cells and at 40× magnification for Huh 7 cells.

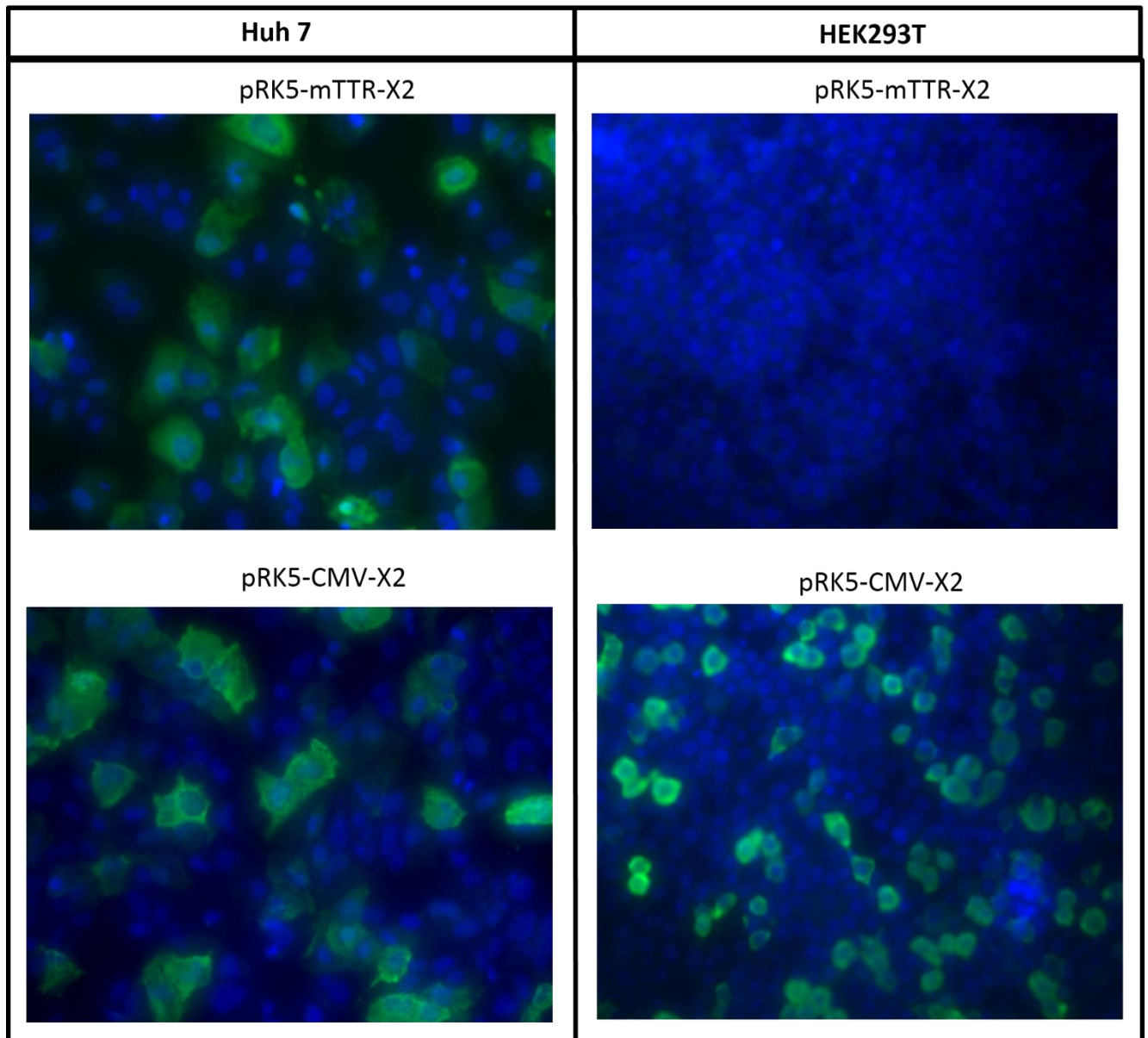


Figure 3.8: Immunofluorescence detection of X2 rTALEs *in vitro*. Immunofluorescence staining was performed to detect rTALE expression in cell culture. Huh 7 and HEK293T cells were transfected with the CMV- and mTTR-X2 rTALE plasmids. An anti-HA primary antibody was together with a fluorescently labelled secondary antibody used to detect the HA tag on the rTALEs and fluorescence imaged by microscopy. DAPI was used to stain the nuclei. The CMV-X2 rTALE was detected in both cell lines, whereas the mTTR-X2 rTALE was only detected in the Huh 7 cells. Cells were visualised using a fluorescence microscope at 20× magnification for HEK293T cells and at 40× magnification for Huh 7 cells.

3.3 Anti-HBV rTALEs mediate efficient transcriptional silencing of viral gene expression

3.3.1 rTALE-mediated inhibition of HBsAg expression *in vitro*

Following demonstration of tissue-specific expression, the effects of the mTTR-driven rTALEs on viral replication was assessed. This was done by measuring the levels of secreted HBsAg which is used as a marker of HBV replication. Mammalian cells were transiently transfected with rTALE and the pCH-9/3091 plasmid DNA. This target plasmid is a greater-than-genome-length HBV sequence which expresses viral RNAs essential for HBV replication. Cells were transfected with pCH-9/3091 and pTZ57R plasmid DNA as a negative control, which provided baseline HBsAg expression. Transfections were performed in triplicate to ensure reproducibility and successful transfections were established by GFP expression (Appendix, Figure 5.8). Forty-eight hours post transfection, secreted HBsAg levels in the growth media of transfected HEK293T and Huh 7 cells were measured using an HBsAg ELISA assay. The data obtained were averaged and normalised to the negative control.

Transfection of the Huh7 cells with the mTTR- and CMV-driven rTALEs significantly knocked down HBsAg expression compared to the mock transfection (Figure 3.9; $p < 0.01$). In contrast, in HEK293T cells, the CMV-driven rTALEs significantly knocked down HBsAg expression compared to the mock transfection ($p < 0.01$) whereas the mTTR-driven rTALEs did not ($p > 0.05$). The absence of significant knockdown of HBsAg expression by the mTTR rTALEs in kidney-derived cells further serves to demonstrate that the mTTR promoter is liver-specific. Furthermore, mTTR-X1, -X2, -S1 and -S2 rTALEs significantly reduced HBsAg expression by 63 %, 66 %, 87 % and 92 % respectively compared to the mTTR-control rTALE. This was comparable to the CMV-X1, -X2, -S1 and -S2 rTALEs

which significantly reduced HBsAg expression by 42 %, 54 %, 82 % and 90 % respectively. These results indicate that the S rTALEs, which targets the viral *surface* ORF, are more efficient in inhibiting HBsAg expression than the X rTALEs. This trend was also seen in the HEK293T cells as the S rTALEs decreased HBsAg expression to a greater extent than the X rTALEs (Figure 3.9). Therefore, while the S and X rTALEs do not directly bind the Pre-S1 and Pre-S2 promoters, but rather the *surface* ORF and *HBx* promoter, they are both still able to repress HBsAg expression. This suggests that the KRAB domain has an effect over relatively long distances. It is possible that the X1 and X2 rTALEs are binding to their target sequence in the *HBx* promoter and via the KRAB domain repress *HBx* expression. As *HBx* is necessary for expression of viral sequences its inhibition may explain the reduction in secreted HBsAg levels. Control rTALEs were used to assess the effect of transfection on HBsAg levels and the specificity of the rTALEs. The control rTALEs caused no significant changes in HBsAg expression ($p>0.05$), compared to the mock transfection, which was expected as the control rTALEs do not target any sequences in the HBV genome (Figure 3.9). Together the data demonstrates that the rTALEs are sequence-specific and any HBsAg knockdown observed can be attributed to the repressors. Overall the results demonstrate that the mTTR-driven rTALEs can cause potent liver-specific silencing of HBsAg expression.

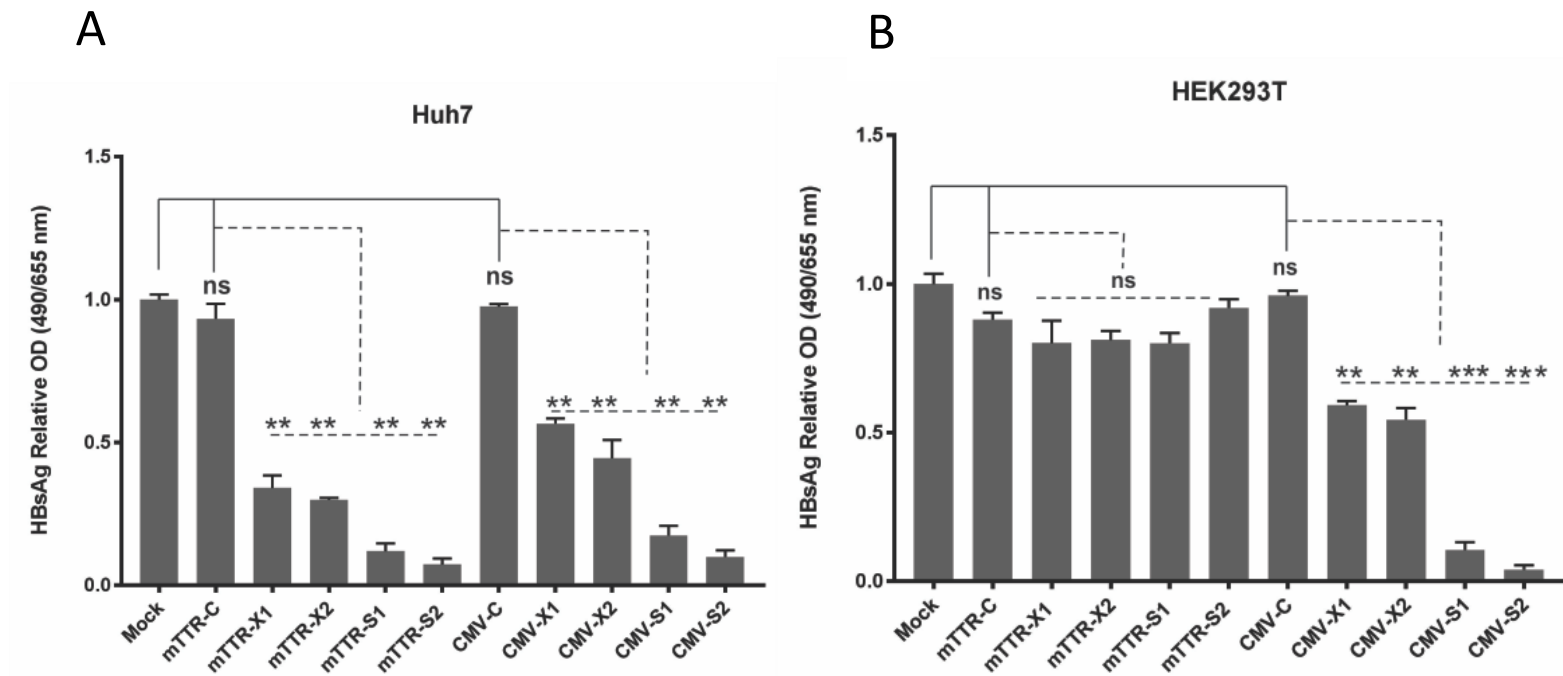


Figure 3.9: Assessment of rTALE-mediated knockdown of HBsAg in Huh 7 (A) and HEK293T (B) cells. To assess rTALE efficiency, HBsAg levels in the culture supernatants were measured. Transient co-transfections were performed in Huh 7 and HEK293T cells with pCH9/3091 and individual rTALE plasmids or pTZ57R (mock). Forty-eight hours post transfection HBsAg levels in the culture supernatants were measured by ELISA. The readings were averaged and the values displayed are relative to the mock transfection. Error bars indicate the normalised standard deviation (n=3). (**: p<0.01; ***: p<0.001; ns: not significant)

3.3.2 rTALE-mediated repression of HBV transcription *in vitro*

To determine if the rTALEs were capable of transcriptional repression of viral replication, intracellular HBV *surface* and *core* transcript levels were measured using reverse transcriptase quantitative PCR (RT-qPCR). pCH-9/3091 was individually co-transfected with each of the CMV- and mTTR-driven rTALE plasmids into Huh 7 and HEK293T cells. pCH-9/3091 co-transfected with pTZ57R was used as the mock transfection. Transfections were performed in triplicate to ensure reproducibility and successful transfections were determined by GFP expression (Appendix, Figure 5.9). Forty-eight hours post transfection, RNA was isolated from the transfected cells, converted to cDNA, and used in a RT-qPCR reaction to measure the levels of HBV *surface* mRNA and pgRNA relative to hGAPDH mRNA.

Transfection of the Huh7 cells with the mTTR- and CMV- driven rTALEs significantly knocked down HBV RNA levels compared to the mock transfection (Figure 3.10; $p < 0.05$). In contrast, knockdown of viral RNA in HEK293T cells was only observed for the CMV-driven rTALEs (Figure 3.11). As the mTTR-driven rTALE vector does not express the repressor in non-liver-derived cells there was no knockdown observed in HEK293T cells (Figure 3.11). Transfections in the Huh 7 cells demonstrate that mTTR-X1, -X2, -S1 and -S2 rTALEs reduced *surface* mRNA levels by 65 %, 75 %, 83 % and 81% respectively, and pgRNA levels by 60 %, 63 %, 78 % and 76% respectively. Whereas the CMV-X1, -X2, -S1 and -S2 rTALEs reduced *surface* mRNA levels by 27 %, 53 %, 76 % and 72 % respectively and, pgRNA levels by 38 %, 45 %, 61 % and 66 % respectively. The reduction in pgRNA levels, which is expressed exclusively from the basic core promoter, suggests that the S and X rTALEs suppress transcription from the basic core promoter. Similarly, the reduction in *surface* mRNA levels suggests that the S and X rTALEs suppress transcription from the Pre-S1 and/or the Pre-S2 promoters. This data further

confirms that the rTALEs can exert their effect over a long distance. Furthermore, the control rTALEs did not alter HBV RNA levels significantly ($p>0.05$) when compared to the mock transfection (Figure 3.10 and 11). Again, this was expected as the control rTALEs do not target regions in the HBV genome. As before the S rTALEs seem to be more efficient than the X rTALEs, as they caused greater knockdown of pgRNA from the basic core promoter and *surface* mRNA from the Pre-S1 and/or the Pre-S2 promoters (Figure 3.10 and 3.11). This data corroborates the ELISA results, and overall it demonstrates that the mTTR-driven rTALEs function at a transcriptional level to tissue specifically inhibit viral replication.

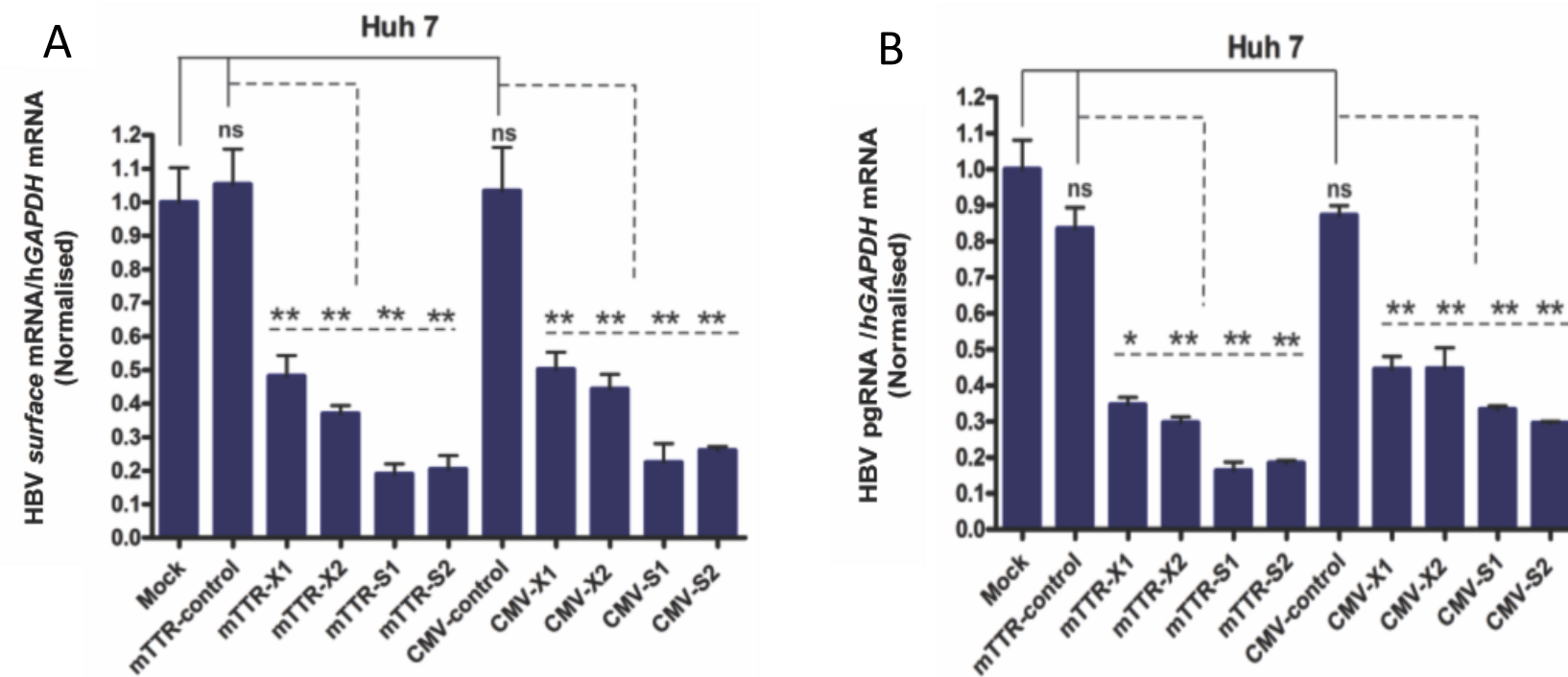


Figure 3.10: Assessment of rTALE-mediated knockdown of HBV mRNA *in vitro*. To assess rTALE efficiency, HBV mRNA levels were measured following transfection of Huh 7 cells with rTALE plasmids and pCH-9/3091. Using primers against the *surface* (A) and *core* (B) ORFs, RT-qPCR was performed to determine the relative levels of viral mRNA relative to *hGAPDH*, forty-eight hours' post transfection. The readings were averaged and the values displayed are normalised to the mock transfection. Error bars indicate the normalised standard deviation (n=3). (*: p<0.05; **: p<0.01; ns: not significant).

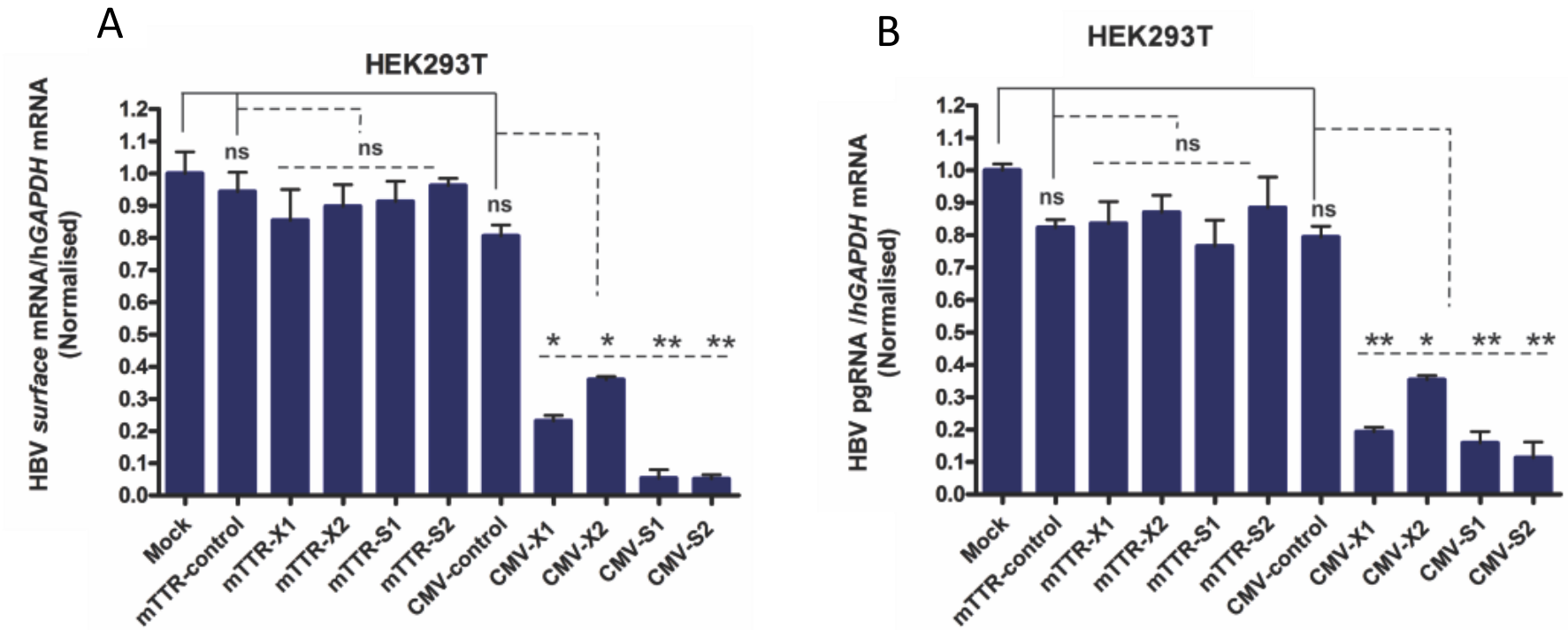


Figure 3.11: Assessment of rTALE-mediated knockdown of HBV mRNA *in vitro*. To assess rTALE efficiency, HBV mRNA levels were measured following transfection of HEK293T cells with rTALE plasmids and pCH-9/3091. Using primers against the *surface* (A) and *core* (B) ORFs, RT-qPCR was performed to determine the relative levels of viral mRNA relative to hGAPDH, forty-eight hours' post transfection. The readings were averaged and the values displayed are normalised to the mock transfection. Error bars indicate the normalised standard deviation (n=3). (*: p<0.05; **: p<0.01; ns: not significant).

3.4 Evaluation of potential rTALE-mediated cytotoxicity

3.4.1 rTALE expression does not alter cell viability

To ensure the decrease in HBV transcripts and protein expression was not due to rTALE-induced toxicity, a thiazolyl blue tetrazolium bromide (MTT) assay was performed. This assay measures metabolic activity as only the mitochondria of viable cells can reduce the MTT tetrazolium dye to an insoluble formazan purple product (178). Cells were transfected with either rTALE plasmid or pTZ57R DNA (control). A blank control consisting of wells that did not receive any cells was included. An untransfected control consisting of cells receiving transfection reagents and no DNA was included to rule out the possibility of the transfection reagent being toxic. Transfections were performed in triplicate to ensure reproducibility and successful transfections of the cells were determined by GFP expression (Appendix, Figure 5.10). The MTT assay was carried out 48 hours post transfection.

Compared to the untransfected control cells, the optical density (OD) readings of the rTALEs do not significantly differ ($p > 0.05$) (Figure 3.12). This suggests that the metabolic activity of the cells transfected with the rTALEs were comparable to the untransfected cells and therefore these rTALEs do not exhibit any cytotoxic effects. However, the OD readings of the rTALEs were higher than the blank control wells (Figure 3.12). This is expected as there were no cells in the wells and thus it reinforces the point that the transfected cells were viable. Overall the data demonstrates that the rTALEs do not have cytotoxic effects and confirms that the suppression of viral replication observed in the cells treated with rTALEs was due to KRAB induced repression as opposed to cytotoxic effects.

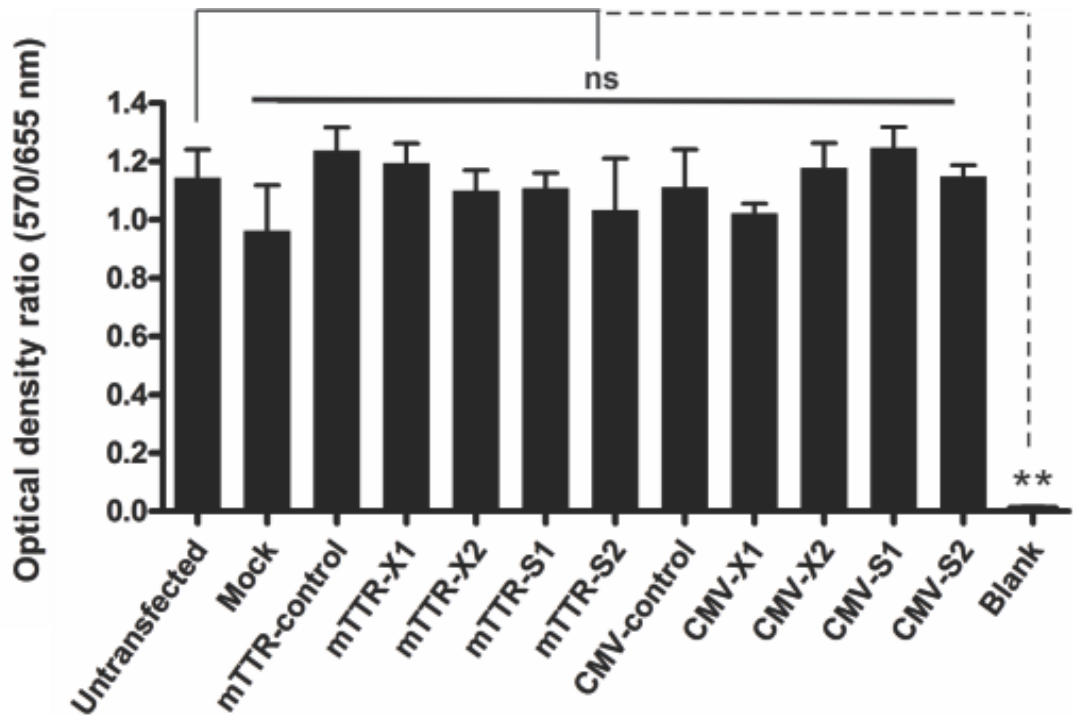


Figure 3.12: Assessment of cell viability. To determine if there is any toxicity associated with the rTALEs, cell viability was assessed by an MTT assay forty-eight hours after co-transfecting cells with pCH-9/3091 and each individual rTALE-expressing plasmid or pTZ57R. The values displayed are the means and standard deviation (n=3). (**: p<0.01; ns: not significant).

3.4.2 rTALEs do not interfere with expression of potential off-target genes

To further characterise the safety of these rTALEs potential off-target binding and subsequent gene silencing was investigated. As the S1 and S2 rTALEs were shown to be the most efficient repressors and represent possible lead candidates the off-target binding of these rTALEs was characterised further. The TALE-NT 2.0 TAL target finder (175) was used to search the human genome for any potential off-target binding sites for rTALEs S1 and S2. Based on bioinformatic analysis several potential binding sites were identified for the rTALEs (Table 3.1).

Mobility shift assays (unpublished data) demonstrated that these rTALEs bind an oligonucleotide that represents the off-target site on Chromosome 5 (Table 3.1). qPCR primers were designed for genes found closest to this off-target site. The genes identified were *prostate androgen-regulated transcript 1 (PART1)* and *phosphodiesterase 4D (PDE4D)*. Located on Chromosome 5, *PART 1* is an androgen-induced gene in prostate cells that may have a role in prostate carcinogenesis (177), whereas *PDE4D* is part of a protein family with a role in modulating intracellular signalling by cyclic nucleotides (179). Multiple alternatively spliced transcript variants have been described for these genes (5, 6). qPCR assay designed to simultaneously detect all the transcripts using 3 different sets of primers for each gene was used.

Cells were transfected with pCH-9/3091 and either pTZ57R or the rTALE-expression constructs. Transfections were performed in triplicate to ensure reproducibility. Successful transfections of the cells were determined by GFP expression (Appendix, Figure 5.11). Forty-eight hours post transfection, RNA was isolated from the transfected cells, converted

to cDNA, and then used in a qPCR reaction to measure the levels of the off-target mRNA relative to h*GAPDH* mRNA.

Table 3.1: Potential rTALE binding sites. Displayed are the potential binding sites identified by TALE-NT 2.0 TAL target finder for each rTALE.

Mismatches between the target sequence and potential binding sites are underlined.

rTALE:	Target sequence	Potential site sequence	Chromosome	Nucleotides
S1	TGCGTCAGCAAACACTTGG	T <u>C</u> CGTCAGCAAACACTT <u>A</u> G	2	241953249 – 241953266
		T <u>C</u> CATCAGCAAACACTT <u>A</u> G	X	55615772 - 55615789
		T <u>C</u> CATCAGCAAACACTT <u>A</u> G	2	120408657 - 120408674
		T <u>C</u> CATCAGCAAACACTT <u>A</u> G	2	129770494 - 129770511
		TGCA <u>A</u> CAGCAAACACTTGG	10	121028175 -121028192
		T <u>A</u> CA <u>A</u> CAGCAAACACTTGG	12	59584156 - 59584173
		TGCTTCA <u>A</u> CAAACACTT <u>A</u> G	18	944741 - 944758
		T <u>T</u> CATCAGCAAACACTT <u>A</u> G	8	2655658 - 2655675
		TG <u>A</u> GTCA <u>A</u> CAAACACTTGG	2	62695067 - 62695084
		TG <u>A</u> GTCA <u>A</u> CAAACACTTGG	8	146220808 - 146220825
S2	TACCCCGTTGCCCGGCAAC	T <u>C</u> CCCGTTGCCCGGCAAC	14	89882580 - 89882597
		TACCC <u>A</u> GTTGCC <u>C</u> AGCAAC	X	65927522 - 65927539
		TACCC <u>A</u> CGTTGCC <u>C</u> AGCAAC	7	103304981 - 103304998
		TACCC <u>A</u> CATTGCC <u>C</u> AGCAAC	10	43622387 - 43622404
		TACCC <u>A</u> TCACCC <u>A</u> ACAAC	5	59831800 - 59831817
		TACCC <u>A</u> TTACCC <u>A</u> AC <u>C</u> C	X	63011453 - 63011470
		TACCC <u>A</u> TTACCC <u>A</u> AC <u>C</u> C	HG1437_PATCH	63011043 - 63011060
		TACCCCGTTGCC <u>C</u> AC <u>C</u> C	8	130210005 - 130210022
		TACCC <u>A</u> C <u>C</u> TTGCCCGGCAAC	14	65814423 - 65814440
		TACCC <u>A</u> CTGCC <u>C</u> ACAAC	9	109120776 - 109120793

Melt curve analysis from the qPCR of *PART 1* demonstrated that amplification did not occur (Appendix, Figure 5.12). The qPCR product was analysed by agarose gel electrophoresis which revealed that there are only primer dimers present (Appendix, Figure 5.13). Primer dimers indicate non-existent or low levels of the target sequence and suggests that *PART 1* is not expressed in Huh 7 cells. This is in accordance with a study that showed *PART 1* is mostly expressed in the prostate and could not be detected in the liver (177). This highlights the improved safety profile of liver-specific expression of rTALEs as limiting expression of the therapeutic to a specific tissue prevents inhibition of potential off-target genes that are normally expressed in a different tissue.

In contrast to *PART 1*, *PDE4D* expression was detected the liver-derived Huh 7 cell line, but was unaffected by rTALE activity. Compared to mock transfected cells, the relative amount of *PDE4D* mRNA levels were not significantly different in Huh 7 cells transfected with rTALEs ($p > 0.05$) (Figure 3.13). This suggests that transcription of the gene is not repressed in the presence of the rTALEs. The transcription start site of the *PDE4D* gene is located approximately 800 000 bp upstream of the predicted off-target binding site of the rTALEs. The data suggest that the repressors either do not bind the potential off-target site, or bind and are too far from the *PDE4D* promoter to effect transcriptional inhibition. Importantly the data demonstrate that rTALEs are safe and do not cause undesirable effects on host gene expression.

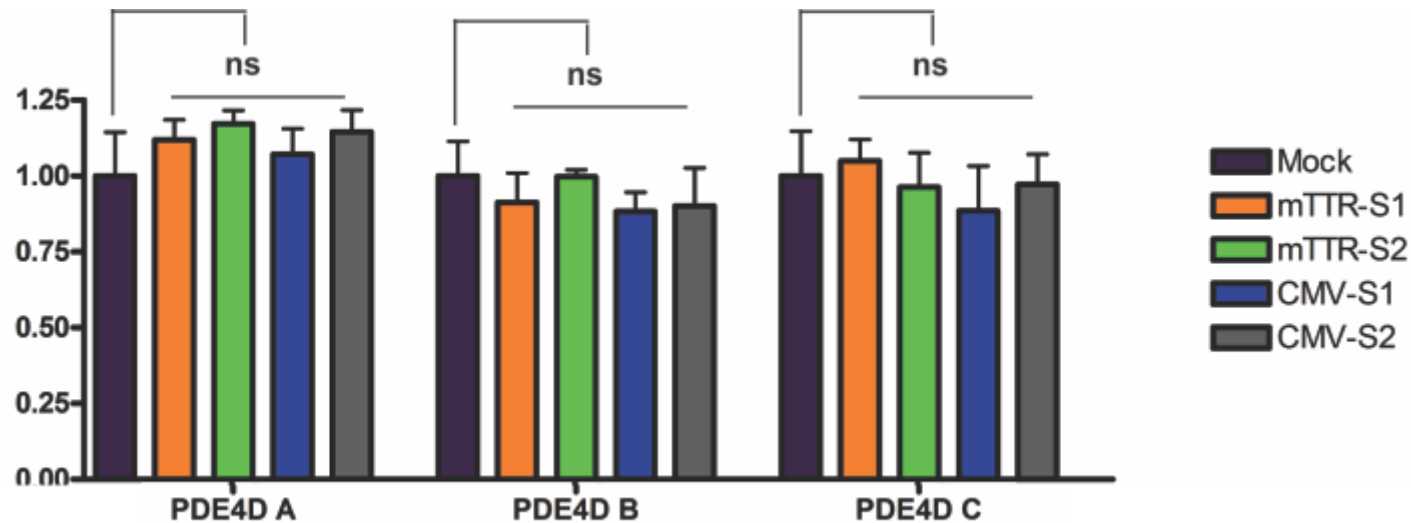


Figure 3.13: Evaluation of rTALE off-target activity. Bioinformatic analysis identified potential off-target binding sites for rTALEs S1 and S2. To determine if the rTALEs bind to the off-target sites and cause repression, qPCR was performed to determine the relative levels of the *27 phosphodiesterase 4D (PDE4D)* transcript variants. PDE4D A covers transcripts *PDE4D-001, -003, -012, -013, -014, -015, -016, -017, -018, -019, -020, -022* and *-201*. PDE4D B covers all the PDE4D A transcripts except *PDE4D-017* and includes *PDE4D-011, -024, -025, -026*. PDE4D C covers transcripts *PDE4D-004, -005, -006, -007, -008, -009, -010, -021, -023* and *-025*. The readings were averaged and the values displayed are relative to the mock transfection. Error bars indicate the normalised standard deviation (n=3). (ns: not significant).

Chapter 4

4. Discussion

HBV infection continues to be a global health threat, particularly for hyper-endemic regions such as sub-Saharan Africa and Asia (2). Current treatment options are unable to diminish HBV cccDNA, which is the cause of persistent HBV infection, and therefore novel treatment strategies which can target the viral cccDNA reservoirs are required (18). Artificial repressor transcription factors such as a KRAB repressor domain fused to a designer TALE provides a promising approach to specifically target and transcriptionally silence HBV cccDNA expression.

4.1 Tissue-specificity

The HBV cccDNA minichromosome serves as the template for viral RNA synthesis and is associated with histone and non-histone proteins (180). It has been established that HBV replication is regulated by the acetylation status of cccDNA bound H3 and H4 histones (181). Acetylation of the bound H3 and H4 histones is associated with HBV replication, whereas lower HBV viral replication was associated with reduced acetylation of histones H3 and H4 (181). By exploiting the chromatin remodelling process of cccDNA, sequence-specific DNA-binding proteins can be used to direct repressor domains to target sites to achieve chromatin based repression of HBV gene expression.

In this study, the anti-HBV potential of KRAB-based rTALEs designed to target HBV cccDNA was assessed. In contrast to current treatment strategies, this technology can directly target HBV cccDNA, as the simple TALE DNA recognition code permits

adaptable sequence-specific DNA interaction (117). A critical factor for gene therapy strategies is the control of exogenous gene expression to prevent unwanted activity in non-targeted tissue. Since HBV primarily affects hepatocytes (1), the design of previously generated anti-HBV rTALEs (unpublished data) was optimised by replacing the ubiquitous CMV promoter with the liver-specific mTTR promoter to ensure hepato-specific rTALE activity. Assessment of mTTR promoter tissue-specificity and functionality, demonstrated that the promoter is capable of driving liver-specific expression of rTALEs. This hepatotropic expression is facilitated by the binding requirement of at least four different cell-specific factors: hepatocyte nuclear factors (HNF) -1, -3, -4 and CCAAT/enhancer binding protein (C/EBP) for mTTR activity (171). C/EBP and HNF 4 are essential for mTTR enhancer activity whilst HNF-1, -3, and -4 are required for the promoter activity (171). Although the HNF transcription factors are also found in other cells, the combination of the 4 essential factors are exclusive to liver cells, thus limiting extrahepatic expression from a mTTR promoter (171). While kidney cells express HNF-1 (182) and HNF-4 (183) this is not sufficient for mTTR promoter activity. As a consequence, immunofluorescence staining was unable to detect rTALE expression in HEK293T cells transfected with the mTTR-driven rTALEs vectors. The tissue-specificity conferred by the mTTR promoter ensures that rTALE activity is limited to hepatocytes thereby significantly reducing the potential of off-target effects.

4.2 Anti-HBV activity

The rTALEs generated in this study were designed to specifically bind a region in the *surface* ORF and the HBx promoter region of HBV cccDNA to direct KRAB mediated repression of viral transcription. This study demonstrated that the mTTR-driven rTALEs were shown to reduce liver-specifically secreted HBsAg levels by 63-92 % *in vitro*.

Additionally, a significant liver-specific reduction in HBV *surface* mRNA (65-81%) and pgRNA (60-76%) levels was observed. The data indicates that the rTALEs cause transcriptional silencing of HBV genes.

HBV transcription is regulated by four individual promoters, which in turn is regulated by the binding of several liver-specific and ubiquitous transcriptional factors (26). Transcription of the pre-S1 and pre-S2 promoters yield pre-S1 and pre-S2 mRNAs which encode the HBV surface proteins (11). Whereas the basic core promoter initiates transcription of the pgRNA which is reverse transcribed into rcDNA (10). Here we show that the S rTALEs and the X rTALEs silence HBsAg secretion and reduce the levels of RNAs amplified by the surface primers and the pgRNA primers. The surface primers amplify Pre-S1 and Pre-S2 mRNA as well as pgRNA. The data indicate that the S and the X rTALEs are likely repressing activity of one or all three of the promoters producing these transcripts. On the other hand, the core primers only amplify pgRNA. Therefore, both S and X rTALEs are clearly inhibiting transcription from the basic core promoter. Furthermore, HBsAg secretion decreases in cells receiving S and X rTALEs. Since HBsAg can only be translated from the Pre-S1 and Pre-S2 mRNA this indicates that the S and X rTALEs decrease Pre-S1 and/or Pre-S2 mRNA. Taken together the data show that pgRNA and Pre-S1 and/or Pre-S2 mRNA levels are decreased indicating in turn that the rTALEs suppress transcription from the basic core promoter and the Pre-S1 and/or the Pre-S2 promoters.

A possible mechanism of HBV gene silencing exhibited by these rTALEs is that binding of the target sequences is followed by recruitment of KRAB-associated protein 1 (KAP1), which in turn recruits heterochromatin-inducing factors (165). This leads to localised chromatin remodelling, histone deacetylation and methylation, thereby forming facultative heterochromatin that extends from the binding site to the basic core, Pre-S1 and Pre-S2

promoters. This is consistent with a study that demonstrated the ability of the KRAB domain to induce heterochromatin spreading across long ranges of DNA (168). The heterochromatin formation at the promoters would inhibit binding of the aforementioned transcription factors which are necessary for transcription initiation of the basic core, Pre-S1 and Pre-S2 promoters, thereby suppressing gene transcription. The data also demonstrates that the S rTALEs caused a greater knockdown of HBV mRNA than the X rTALEs. The observation that some TALE proteins exhibit lower activity than others has been reported before and could possibly be due to the differences in binding efficiency, chromatin state or conformation of their target sites (184). If low binding efficiency is a cause it could be attributed to the design of the rTALEs which contain the so-called weak NK RVD to bind G nucleotides (137). Compared to the S rTALEs, the binding sites of the X rTALEs contains more G nucleotides, therefore due to the presence of weak RVDs, there would be less efficient binding of the X rTALEs to their site. This could ultimately lead to lower repression activity. Moreover TALE design guidelines are available to ensure that the choice of RVDs and target site are sufficient to provide efficient TALE activity (119, 184, 185). Nonetheless, the X and S rTALEs were able to exhibit significant silencing of viral replication. Together this data indicates that the rTALEs generated repress expression from the HBV replication competent plasmid at a transcriptional level, resulting in a decrease of viral mRNA production and subsequently a decrease in viral protein production. It is worth noting that since the X rTALEs bind at the HBx promoter and near the Enhancer I sequence, through heterochromatin formation silencing of HBx may also occur. HBx promotes viral replication by targeting the structural maintenance of chromosomes' (Smc) complex Smc5/6 for ubiquitin-mediated degradation (35). Smc5/6 is a restrictive factor which inhibits cccDNA transcription, thus when HBx expression is repressed, Smc5/6 remains functional and as a result, HBV transcription is silenced.

The ability of these rTALEs to cause silencing of HBV gene expression is in agreement with conceptually similar studies, involving a different DBD protein, where KRAB-based ZFPs targeted to HBV sequences demonstrated efficient silencing of viral gene expression (154, 186). Another study demonstrated that dCas9-KRAB can mediate transcriptional silencing via methylation of the lysine at the position 9 of histone 3 (H3K9me3) (152). Based on comparative studies between the effect of dCas9 and dCas9-KRAB, it was demonstrated that the formation of repressive histone modifications was indeed due to KRAB domain activity (152). This supports our hypothesis that our rTALEs silence gene activity through KRAB-mediated induction of heterochromatin. Since KRAB domains induce heterochromatin formation over a distance, it raises a concern about the specificity of KRAB-based repressor activity. However a study investigating this point demonstrated that KRAB-ZFPs did not alter expression of neighbouring genes of the target site (187). Nonetheless further studies are warranted to investigate the extent of the rTALE-mediated epigenome modifications observed in this study.

Although rTALE-mediated silencing of HBV DNA has not been demonstrated before, there are several studies that demonstrate rTALEs targeted to enhancer and promoter regions can cause potent transcriptional repression of genes in mammalian cells (118, 147, 157, 161, 188). Other methods to transcriptionally silence genes have been explored. These include using a DBD with no effector which is targeted to regulatory sequences of a gene. The DBD would competitively bind transcription activator sites thereby inhibiting the initiation of transcription (189). The efficacy of fusing a DBD to epigenome editing effectors such as DNA methyltransferases or histone demethylase to achieve gene silencing has also been investigated (190, 191). However with a KRAB domain, the efficiency of gene repression is derived from the incorporation of different histone modifiers, instead of producing a single type of histone modification as with other

epigenome modifiers (149, 152, 169, 192, 193). This study and others demonstrate that the versatility of a KRAB repressor domain coupled with the specificity of a TALE DBD presents a promising platform for gene therapy applications (118, 147, 161, 188).

4.3 Cytotoxicity

The simple TALE recognition code allows for any DNA sequence to be targeted, and unlike ZFPs there are fewer constraints with regards to site selection, thus making it a favourable tool to adapt for precise genome targeting (194). However, a major concern with developing gene therapy strategies is the possible toxic effects of introducing exogenous DNA to the cell. In this study, the MTT assay demonstrated that the rTALEs do not negatively affect the cell viability of transfected cells. This confirms that the expression of rTALEs is not toxic to cells. Additionally, we show that driving expression of these rTALEs from a liver-specific promoter restricted rTALE activity to liver-derived cells thereby reducing the likelihood of causing toxic effects from unwanted activity in non-targeted tissue. Furthermore, DBD proteins have a risk of binding to off-target sequences leading to off-target activity which consequently can be cytotoxic to the cell. Although binding assays in cell culture has demonstrated that TALE proteins primarily bind their intended sequences (195), off-target binding of TALE derivatives has been reported (196-198). In addition, increased off-target binding when a KRAB domain was added to a ZFP as compared to a ZFP alone has been demonstrated (199). Thus, in this study the potential of these rTALEs to bind off-target sites and alter their gene expression was evaluated by determining the mRNA levels of potential off-target genes. Our results show that levels of the off-target gene were not altered by the rTALEs. Thus, demonstrating that the rTALEs were not repressing gene activity at the off-target site but preferred their intended viral target sequences. To ensure adequate specificity and thus safety of the rTALEs, an 18

nucleotide sequence was targeted as the probability of this target sequence occurring within the human genome is estimated to be 0.041 (95). This ensures that possible off-target binding is reduced. Off-target binding sites can be predicted using computational tools which can scan genomic sequences to identify potential off-target binding sites which have similar homology to a dTALE target sequence (175, 200). In addition there are TALE protein assembly protocols which can facilitate the design and generation of efficient TALEs with adequate specificity for its intended sequence (159, 185, 201, 202). There are several ways to assess off target binding and activity by artificial repressors. Chromatin immunoprecipitation (ChIP) followed by high-throughput DNA sequencing has been extensively used to assess genome-wide binding of proteins on DNA thereby giving an indication of any off-target binding (152). Transcriptome profiling by either microarray or RNA-seq can be used to assess expression levels of RNA to determine any unintended gene silencing (203). Alternatively, global H3K9me3 patterns can be measured by ChIP-seq to assess if there are unintended histone modifications (152). Off-target activity of artificial repressors is a concern as it could lead to unintended silencing of critical genes. The risk of off-target binding will always exist for DNA binding proteins as large genomes present an array of potential binding sites. To ensure safety of this approach, it is important to design the rTALE proteins appropriately to ensure efficient specificity with minimal off-target binding, and to assess potential off-target activity.

4.4 Challenges facing anti-HBV gene therapy

Transcriptional repression of HBV genes presents an alternative approach as an anti-HBV therapy. However, some challenges still need to be addressed to ensure rTALEs are fit for clinical application, such as determining efficacy and safety of rTALE-mediated repression of cccDNA *in vivo*, and finding a safe and efficient delivery agent. The use of small animal

models such as woodchucks, HBV-transgenic mice, or the urokinase plasminogen activator SCID (uPA-SCID) mice have been instrumental in testing the preclinical efficacy and safety of anti-HBV agents *in vivo* (204-207). However as the woodchuck hepatitis virus only shares 70% nucleotide identity to HBV, it poses a challenge as anti-HBV agents would need to be adapted to target a very different sequence (205). The transgenic mice contain an integrated HBV replication-competent sequence which permits continuous expression of viral proteins for new virion assembly and secretion (204). The limitation of this model is that cccDNA is not formed in the livers of these mice highlighting a significant shortcoming when evaluating antivirals. The uPA-SCID mouse model has an ablated liver repopulated with human hepatocytes and as a consequence is susceptible to HBV infection, maintains a productive infection and, importantly, establishes a cccDNA reservoir (206). However, this model lacks a functional adaptive immune system making it unsuitable for studying immune responses to HBV, evaluating efficacy of vaccines, or assessing the role of the immune system in studies of therapeutic efficacy (208). Nonetheless, these mice are a major improvement in the development of suitable mouse models and remain the popular model to evaluate anti-HBV agents (209-211). Since these mice establish and maintain cccDNA, the model provides a promising platform for evaluating the effects, safety, and efficacy of rTALE-mediated transcriptional silencing of the cccDNA replicative intermediate. cccDNA has been identified as a critical target for effective HBV therapeutic strategies and as such chimeric mice will play a critical role in studying and developing drugs against the molecular mechanisms which regulate cccDNA stability and activity (208, 212). Developments in anti-HBV therapeutics include agents which directly target the virus life cycle, and indirect acting agents that target host functions, therefore a good HBV animal model should closely resemble the HBV infection and replication process that occurs in humans to better characterise anti-HBV agents (213).

Despite the advancements made in gene therapy against HBV, a major hurdle is its delivery into animal models.

The delivery of therapeutic genes into cells is fraught with problems which include the degradation by intra and extra-cellular enzymes, and inability to cross the cell membrane because of size and negative charge (214, 215). Both viral and non-viral vectors have emerged as promising candidates for the delivery of therapeutic nucleic acids sequences (216). The use of viral vectors as delivery agents is based on their efficient mechanisms of entering a cell and delivering their genetic sequences for expression (217). As such, the use of lentiviral, adenoviral and adeno-associated viral (AAV) vectors has been successfully utilised for the delivery of gene modifiers (161, 217). The lentivirus is an integrating vector and therefore the therapeutic sequence gets integrated into the host DNA permitting long-term transgene expression (218). AAVs and adenoviral vectors are non-integrating vectors that confer long-term transgene expression with minimal risk of insertional mutagenesis and can be modified to allow liver-specific expression of transgenes (216, 219, 220). However AAVs are non-pathogenic vectors, and are therefore widely used as delivery vectors however, a packaging limit of approximately 4.5 kb limits its application (221). Non-viral methods of delivering gene editing tools were developed in an attempt to overcome limitations that viral vectors present (219). These methods deliver therapeutic sequences into the cell using synthetic or natural compounds, such as lipid- or polymer-based vectors and cell-penetrating peptides, or by physical forces such as electric pulses (222). Advantages of non-viral vectors include large loading capacity, low toxicity, low host immunogenicity and the ability of repeated administration (223). TALE proteins have been successfully delivered through the conjugation of cell-penetrating TAT peptides (224) and recently TALE-transcription factors were successfully delivered into cells using extracellular vesicles (225). Non-viral vectors are known to be less effective than viral

vectors however, and, some methods such as lipoplexes and polyplexes are associated with cytotoxicity (222). Both types of gene delivery methods have their own advantages and disadvantages and a good choice of delivery system should provide safe and efficient delivery to target cells. To meet this requirement, hybrid systems are being investigated that can exploit the advantages of both systems overcoming their limitations thereby producing vectors with high efficacy and low toxicity (226-229).

4.5 Potential antiviral combinatorial therapy

An interesting avenue for rTALE technology would be to investigate the potential for combinatorial strategies with other therapeutic modalities. RNAi technology has been extensively used to silence HBV gene expression by acting post transcriptionally, but does not affect the cccDNA reservoirs (100, 102, 103). In contrast the rTALEs generated in this study silence HBV gene expression by acting directly on the cccDNA at a transcriptional level. A study assessing the effects of the combination of rTALE and shRNA demonstrated double repression of target protein levels to near background levels (147). Based on this it will be interesting to assess if such combined activity can enhance repression against HBV replication. It will also be worth investigating the possibility of complete transcriptional inhibition of the entire viral genome through the synergistic effect of multiple rTALEs designed to target the regulatory elements of the HBV genome. Additionally, the availability of rTALEs simultaneously targeted to different regions of the HBV genome could prevent the possibility of rTALE resistance occurring from a mutation at one rTALE target site (230). With this approach, several critical issues arise such as the increased potential for off-target effects, the method of delivering multiple rTALEs, and possible cytotoxic effects.

Conclusion

4.6 Conclusion

The work presented here provides a proof-of-concept study demonstrating the potential of KRAB-based rTALEs to cause potent HBV gene silencing through the epigenetic modification of cccDNA. Significant knockdown of HBsAg including HBV mRNA was observed demonstrating that the rTALEs silence HBV at a transcriptional level. By engineering the TALE DBD to target specific cccDNA sequences KRAB-mediated inhibition of transcription was achieved without causing mutations in the genome. In addition, silencing of viral promoters that were not directly targeted demonstrated the ability of the KRAB domain to act over long stretches of DNA. Furthermore, using the liver-specific mTTR promoter, expression of the rTALEs was limited to liver-derived cells, the primary site of HBV infection. Importantly the observed knockdown of HBV viral transcription was not associated with any cytotoxic effects or off-target activity. The high specificity, efficient activity and absence of cytotoxicity make rTALEs an ideal approach for targeting HBV. Considerations should be made to further characterise this molecular tool *in vivo*.

Chapter 5

5. Appendix

5.1 Additional figures

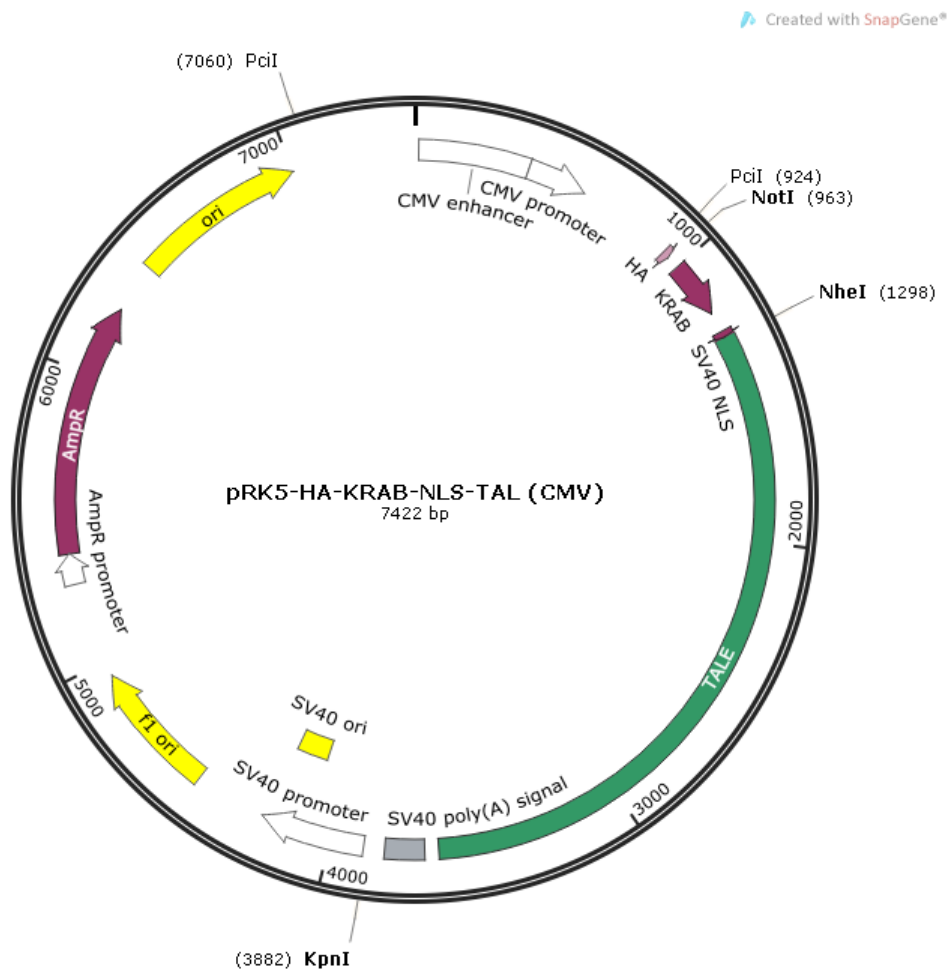


Figure 5.1: CMV-driven rTALE plasmid map. This vector sequence encodes a CMV promoter to drive rTALE transcription, a TALE DNA binding domain, a haemagglutinin (HA) epitope as a protein tag for rTALE expression, a KRAB repressor domain for gene suppression and a nuclear localisation signal to facilitate transport into the nucleus once translated. This rTALE plasmid was used to generate mTTR-driven rTALEs. The restriction sites used in the cloning strategy are displayed. Map was created with SnapGene® software (from GSL Biotech; available at snapgene.com).

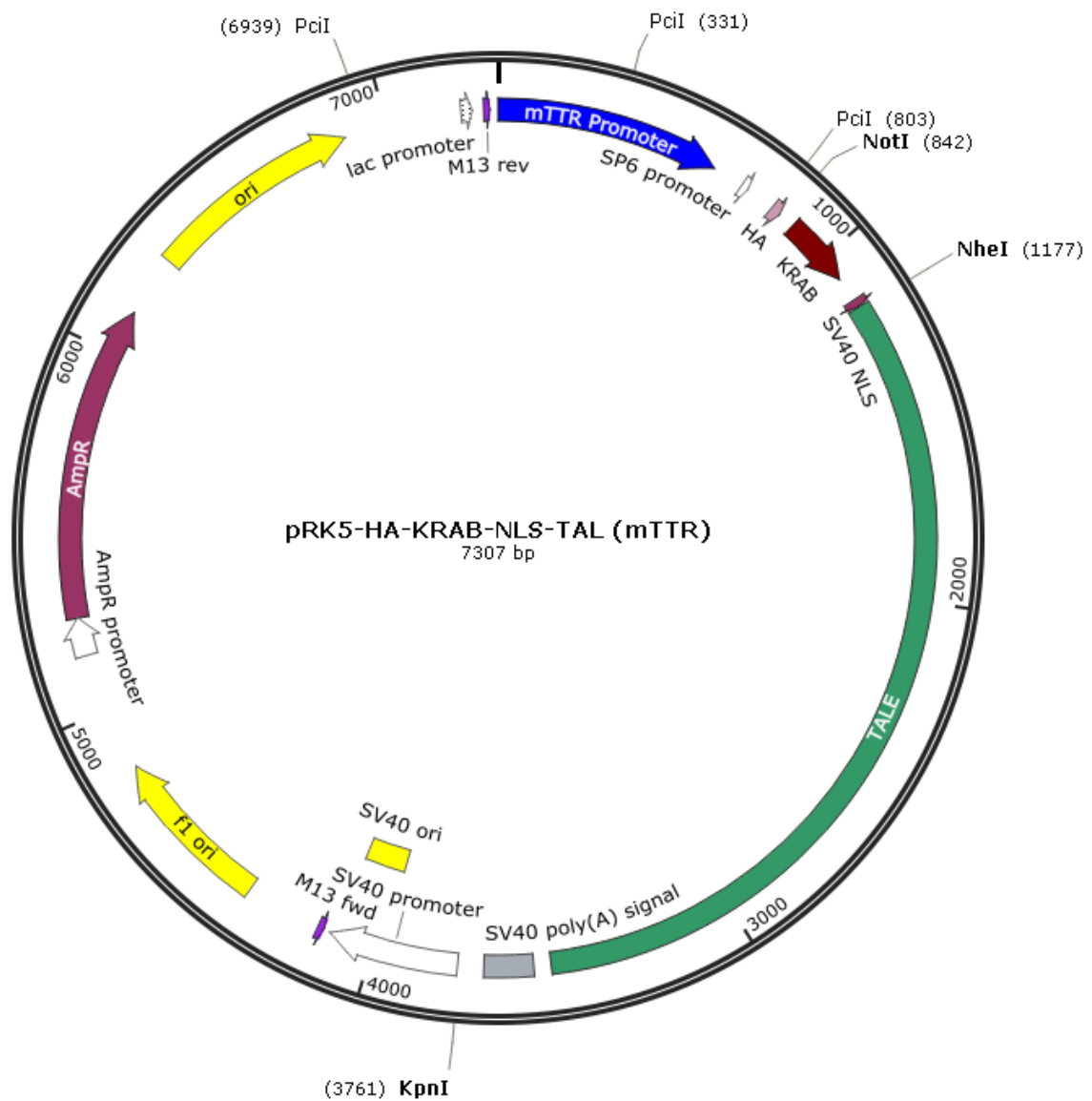


Figure 5.2: mTTR-driven rTALE plasmid map. The pRK5-HA-KRAB-NLS-TAL (mTTR) vector sequence encodes an mTTR promoter to drive rTALE transcription, a TALE DNA binding domain, a haemagglutinin (HA) epitope as a protein tag for rTALE expression, a KRAB repressor domain for gene suppression and a nuclear localisation signal to facilitate transport into the nucleus once translated. Map was created with SnapGene® software (from GSL Biotech; available at snapgene.com).

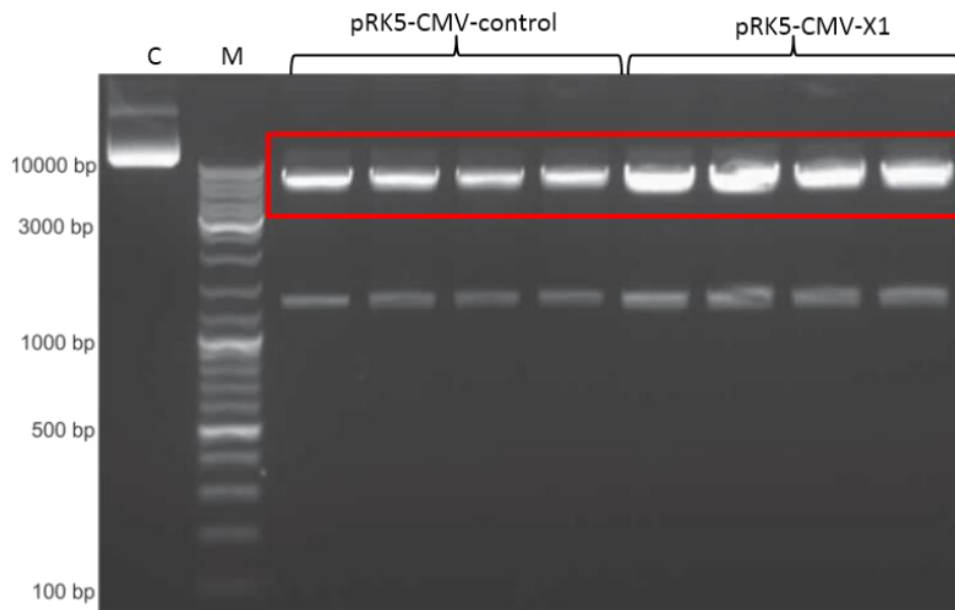


Figure 5.3: Agarose gel electrophoresis of the digested plasmids for backbone preparation.

Pci I and *Not* I restriction enzyme digestion was carried out to excise the rTALE vector backbones of pRK5-CMV-control and pRK5-CMV-X1. The rTALE vector backbones are represented by the 6097 bp bands (Red rectangle). (C: undigested control, M: O'GeneRuler 1 kb DNA Ladder (Thermo Scientific, CA, USA)).

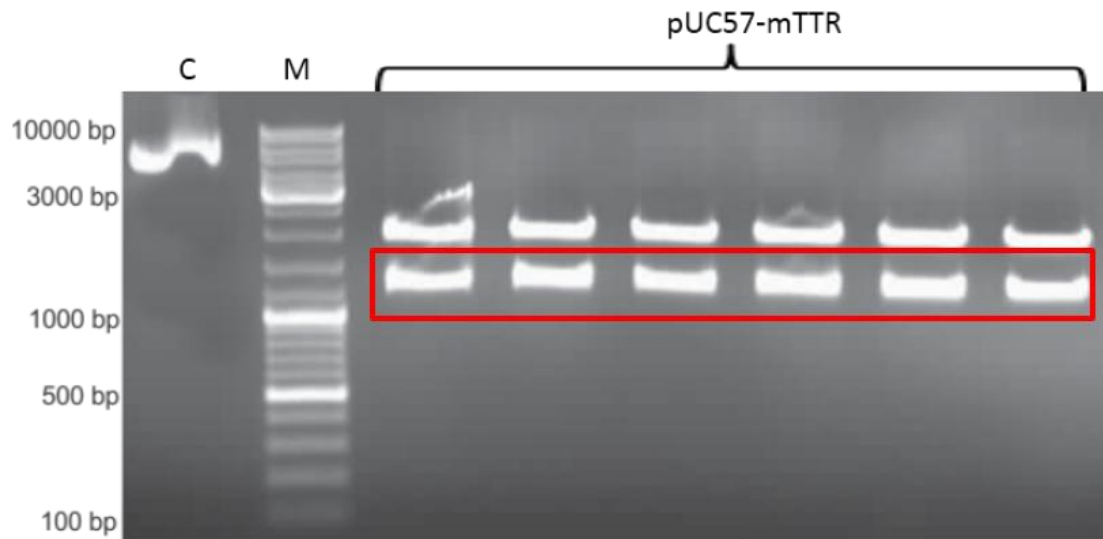


Figure 5.4: Agarose gel electrophoresis of *Bpi* I digested pUC57-mTTR. *Bpi* I restriction enzyme digestion was carried out to excise the mTTR promoter sequence from the pUC57-mTTR plasmid. The mTTR promoter sequence is represented by the 1210 bp bands (Red rectangle). (C: undigested control, M: O'GeneRuler 1 kb DNA Ladder (Thermo Scientific, CA, USA)).

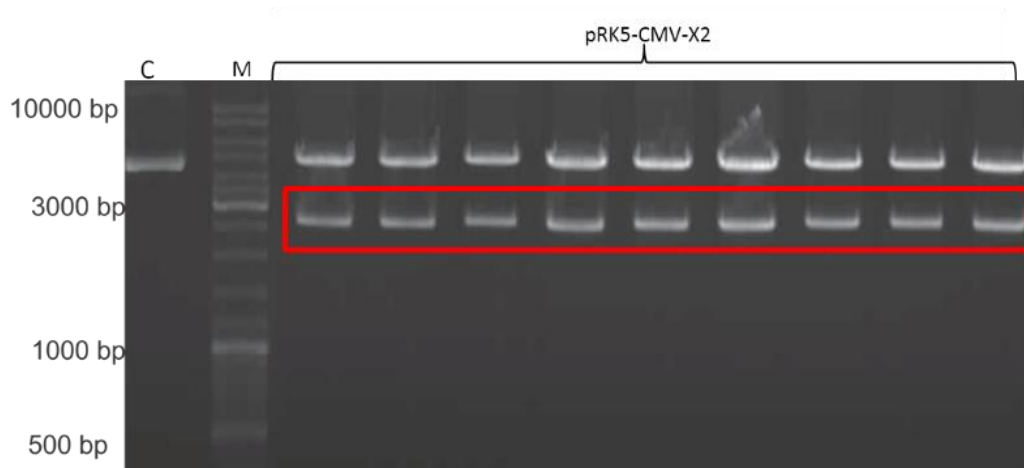


Figure 5.5: Agarose gel electrophoresis of digested pRK5-CMV-X2-rTALE for insert extraction. *Kpn* I and *Nhe* I restriction enzyme digestion was carried out to extract the TALE DBD sequence from the pRK5-CMV-X2 plasmid. The TALE DBD sequence is represented by the 2584 bp bands (Red rectangle). (C: undigested control, M: O'GeneRuler 1 kb DNA Ladder (Thermo Scientific, CA, USA)).

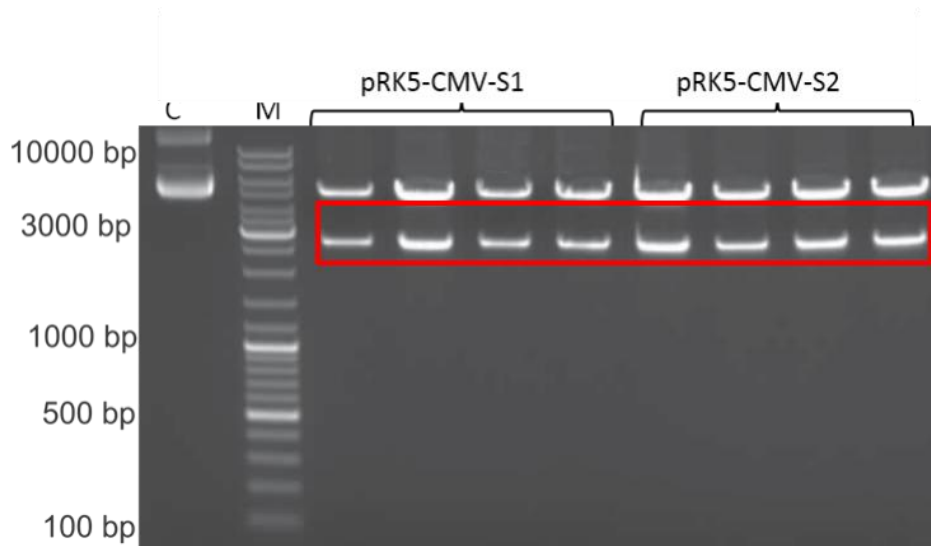


Figure 5.6: Agarose gel electrophoresis of digested pRK5-CMV-S1-rTALE and pRK5-CMV-S2-rTALE for insert extraction. *Kpn* I and *Nhe* I restriction enzyme digestion was carried out to extract the TALE DBD sequences from the pRK5-CMV-S1 and pRK5-CMV-S2 plasmids. The TALE DBD sequences are represented by the 2584 bp bands (Red rectangle). (C: undigested control, M: O'GeneRuler 1 kb DNA Ladder (Thermo Scientific, CA, USA)).

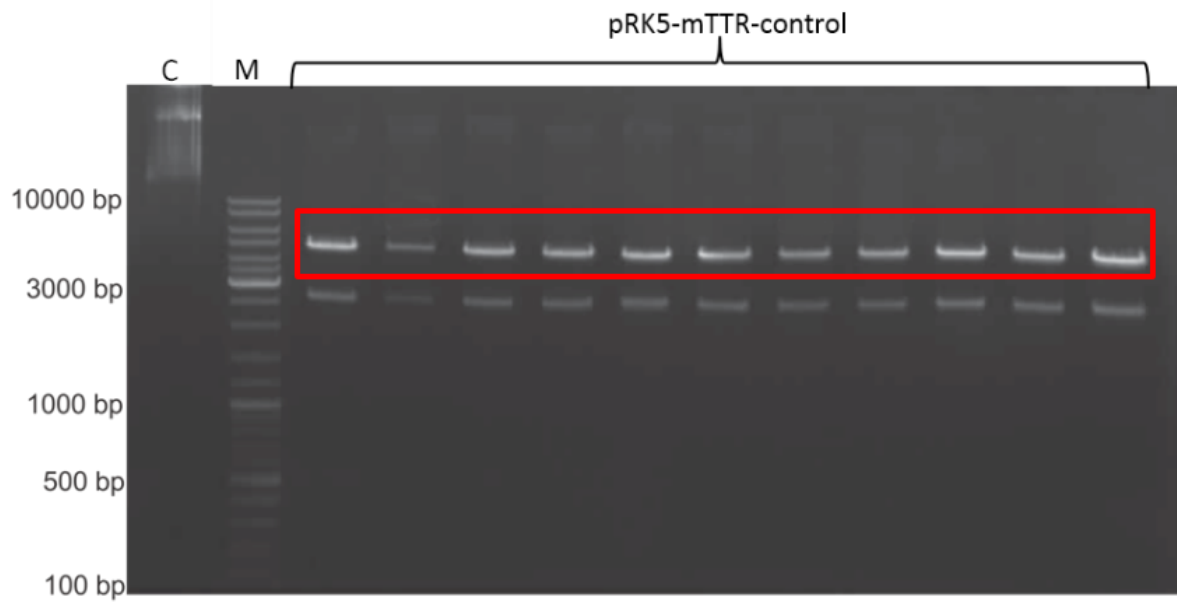


Figure 5.7: Agarose gel electrophoresis of the digested plasmids for backbone extraction. *Kpn* I and *Nhe* I restriction enzyme digestion was carried out to extract the rTALE vector backbone of pRK5-mTTR-control. The mTTR vector backbone is represented by the 4723 bp bands (Red rectangle). (C: undigested control, M: O'GeneRuler 1 kb DNA Ladder (Thermo Scientific, CA, USA)).

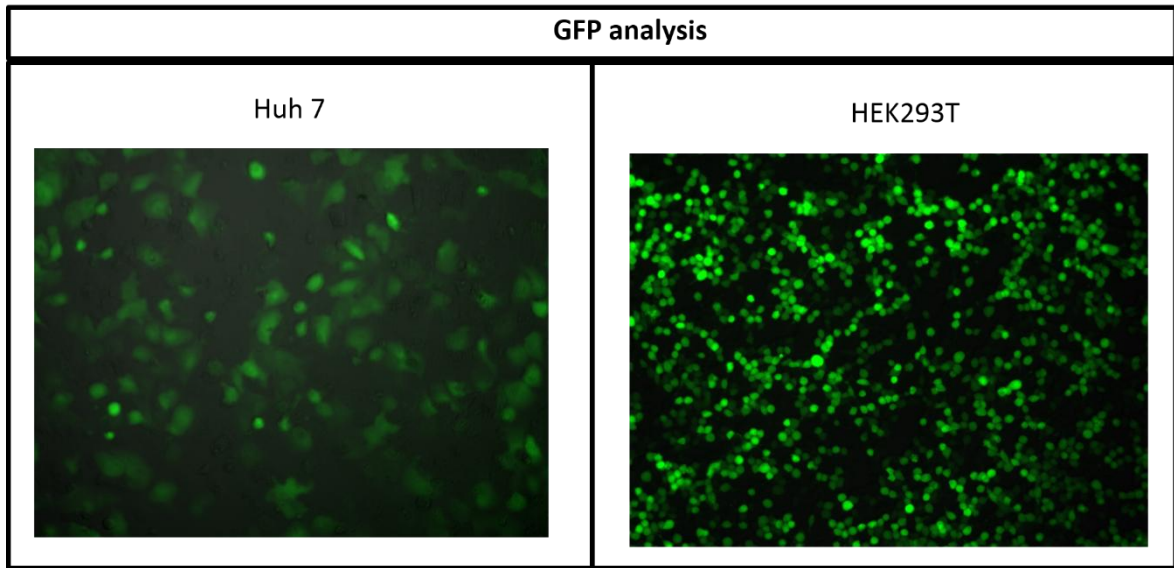


Figure 5.8: Transfection efficiency of Huh 7 and HEK293T cells (ELISA). To assess the efficiency of transfections performed for an ELISA assay, pCI-neo-eGFP was added to the transfection DNA mix. Forty-eight hours post transfection, GFP expression was analysed using a fluorescence microscope. Representative images of transfected cells are shown.

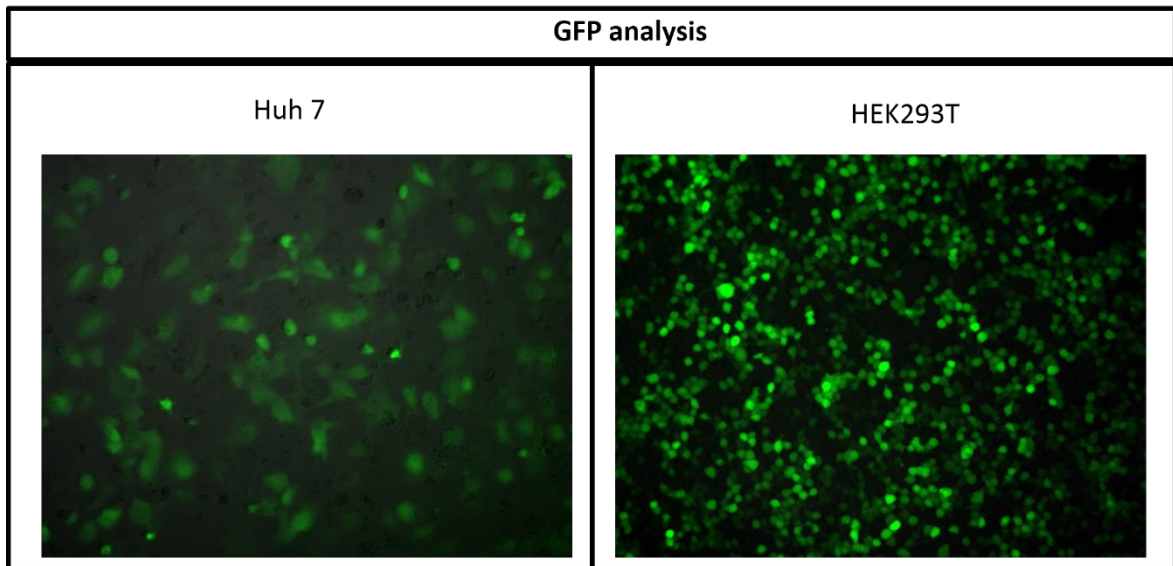


Figure 5.9: Transfection efficiency of Huh 7 and HEK293T cells (HBV RT-qPCR). To assess the efficiency of transfections performed for RNA extraction, pCI-neo-eGFP was added to the transfection DNA mix. Forty-eight hours post transfection, GFP expression was analysed using a fluorescence microscope. Representative images of transfected cells are shown.

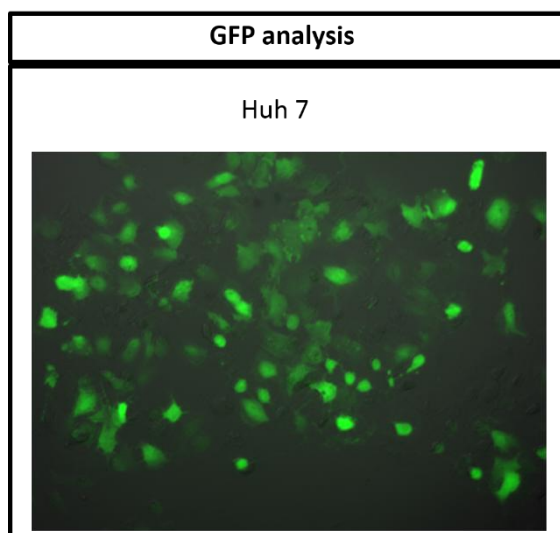


Figure 5.10: Transfection efficiency of Huh 7 cells (MTT assay). To assess the efficiency of transfections performed for a MTT assay, pCI-neo-eGFP was added to the transfection DNA mix. Forty-eight hours post transfection, GFP expression was analysed using a fluorescence microscope. A representative image of transfected cells is shown.

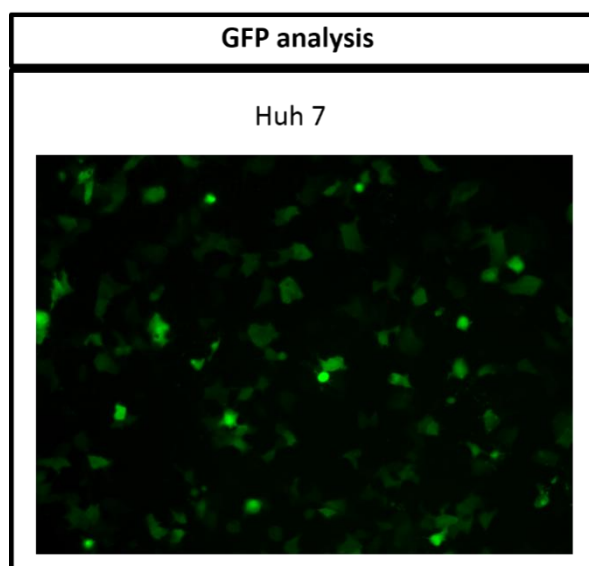


Figure 5.11: Transfection efficiency of Huh 7 cells (Off-target RT-qPCR). To assess the efficiency of transfections performed for RNA extraction, pCI-eGFP was added to the transfection DNA mix. Forty-eight hours post transfection, GFP expression was analysed using a fluorescence microscope. A representative image of transfected cells is shown.

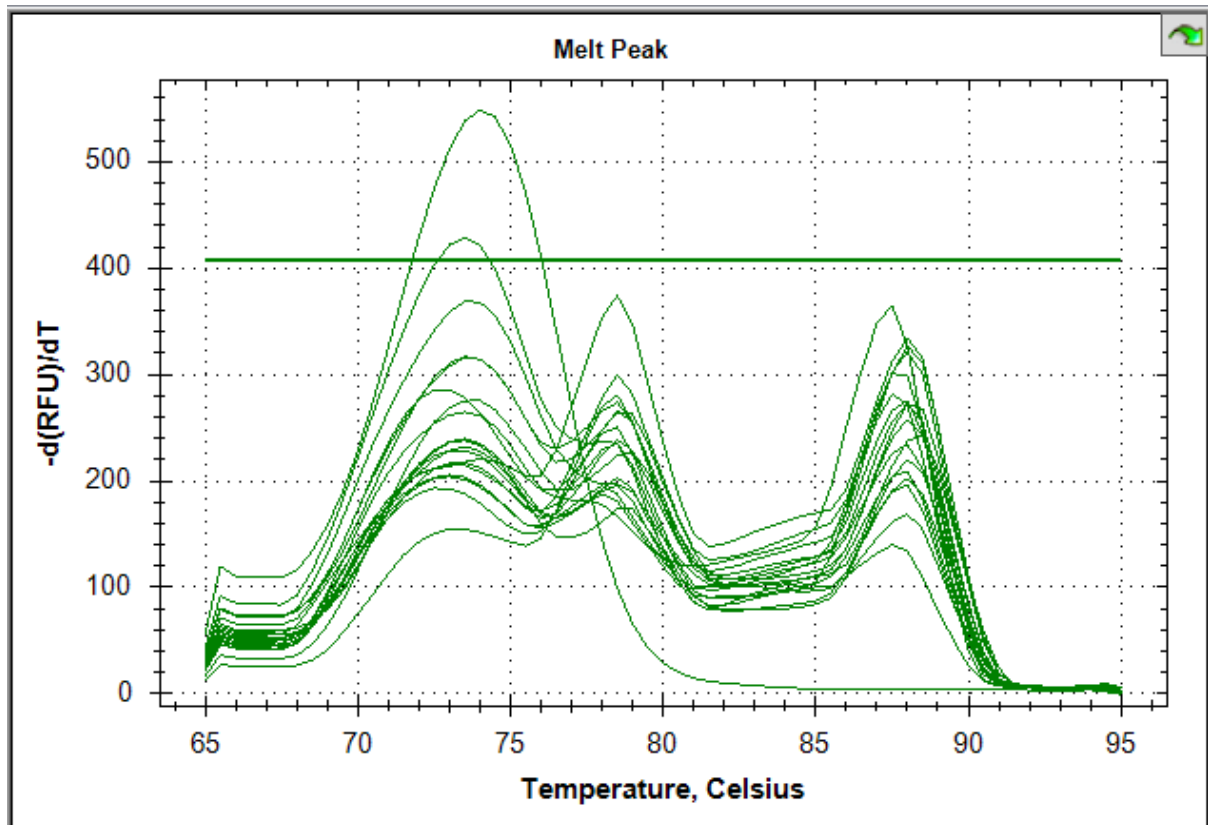


Figure 5.12: Melting curve analysis from qPCR of the *prostate androgen-regulated transcript 1 (PART1)* gene. Relative qPCR was performed to determine levels of *PART 1* mRNA. Depicted are the multiple temperature peaks observed for the reaction indicating nonspecific amplification. Image obtained from CFX Manager™ Software (Bio-Rad, CA, USA).

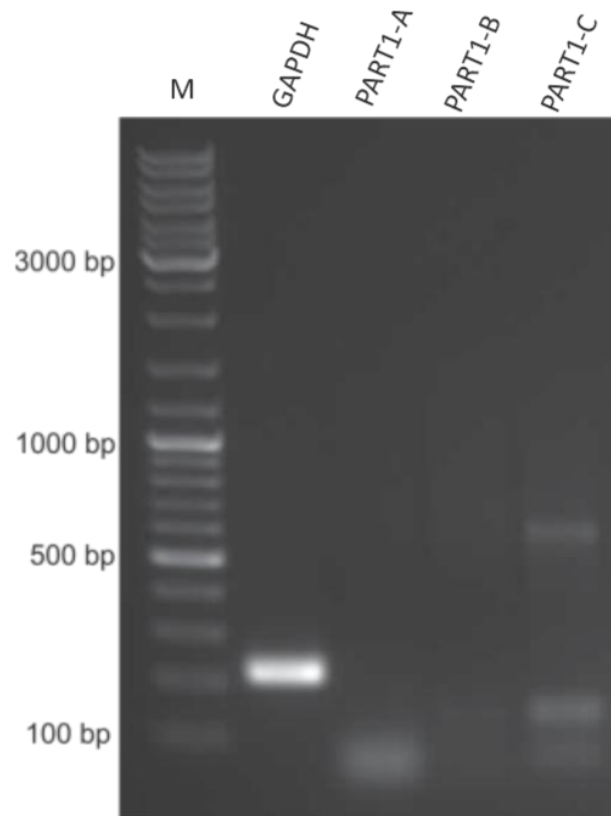


Figure 5.13: Agarose gel electrophoresis of qPCR products. Analysis of qPCR amplicons on an agarose gel stained with ethidium bromide shows a single band representing amplification of the *hGAPDH* gene. In contrast a low molecular weight band (~ 90 bp) representing primer dimers is observed for the different transcripts of the *prostate androgen-regulated transcript 1 (PART1)* gene. (M: O'GeneRuler 1 kb DNA Ladder (Thermo Scientific, CA, USA)).

5.2 Laboratory techniques

5.2.1 Gel Electrophoresis

Reagents

- ***50× Tris Acetate EDTA (TAE) Buffer***

Two hundred and forty-two grams of Tris base, 57.1 ml glacial acetic acid and 100 ml of 0.5 M EDTA was added to 800 ml of ddH₂O. The pH was adjusted to 8.0 and the solution was made to a total volume of 1 L with ddH₂O.

- ***Ethidium Bromide (10 mg/ml)***

Protocol

To prepare a 1% gel, 1 g of agarose was mixed with 100 ml of 1× TAE and dissolved by heating in a microwave for 2-4 minutes. The agarose mixture was cooled at room temperature before 5 µl of Ethidium Bromide solution was added. The mixture was then poured into a gel chamber and allowed to solidify. Once solid, the gel was placed in 1× TAE buffer in an electrophoresis chamber. The gel was run at 80 volts until the loading dyes (Loading dye 6×, Thermo Scientific, CA, USA) reached the bottom of the gel. The DNA was visualised by a GBOX UV transilluminator (Syngene, Cambridge, UK).

5.2.2 Gel extraction

Reagents

- *Qiagen® MinElute Gel Extraction kit (Qiagen, Hilden, Germany)*
- *Isopropanol*

Protocol

The DNA fragment of interest was excised from the agarose gel and placed in a microcentrifuge tube. The fragments were weighed and 3 volumes of Buffer QG was added to 1 volume of gel. The tube was incubated at 50 °C for 10 minutes to dissolve the gel slice. One gel volume of isopropanol was added to the samples and mixed. A QIAquick spin column was inserted into a 2 ml collection tube, the samples transferred to the column and centrifuged for 1 minute at maximum speed in a standard bench top microcentrifuge. The flow-through was discarded and the column was placed back into the collection tube, 500 µl of Buffer QG was added to the column and centrifuged at maximum speed for 1 minute. The flow-through was discarded and the DNA washed by adding 750 µl of Buffer PE and centrifuging the tube at maximum speed for 1 minute. The flow-through was discarded and the tube was centrifuged for an additional 1 minute. The column was transferred to a sterile 1.7 ml microcentrifuge tube. Fifty microlitres of Buffer EB was added to the membrane of the column to elute the DNA by centrifugation at maximum speed for 1 minute.

5.2.3 Preparation and transformation of chemically competent *E. coli*

Chemically competent *E. coli*

Reagents:

- *Luria-Bertani (LB) media*

To one litre of deionised water, 10 g Bacto-tryptone (Oxoid, UK), 5 g Yeast extract (Oxoid, UK), and 5 g NaCl were added and the solution was autoclaved for 30 minutes at 121 °C and 1 kg/cm². The media was stored at room temperature.

- *Transformation buffer (100 mM CaCl₂, 10 mM PIPES-HCl, 15% glycerol)*

Transformation buffer was prepared by adding 1.4702 g CaCl₂·2H₂O, 0.3024 g PIPES and 15 ml glycerol to 80 ml of ddH₂O. The pH of the solution was adjusted to 7.0 with NaOH, the solution made up to 100 ml and then autoclaved for 20 minutes at 121 °C and 1 kg/cm². The buffer was stored at -20 °C.

Protocol

Ten millilitres of LB media was inoculated with a 100 µl of untransformed XL10-Gold *E. coli*. The inoculum was placed at 37 °C in a shaking incubator until it reached an A₆₀₀ of approximately 0.4. The cells were centrifuged at 3000 ×g for 15 minutes. Thereafter the pellet was resuspended in 10 ml of transformation buffer and incubated for 20 minutes on ice. The suspension was centrifuged at 1000 ×g for 10 minutes and the pellet was resuspended in 2 ml transformation buffer, aliquoted, and stored at -70 °C.

Transformation

Reagents

- *1000 × Ampicillin*

One hundred milligrams of ampicillin (Roche Applied Science, Mannheim, Germany) was dissolved in 1 ml of 50% ethanol.

- *Ampicillin positive Luria Bertani agar plates*

LB agar plates were prepared by mixing 1% (w/v) Agar (Oxoid, UK) in LB medium. The solution was autoclaved for 20 minutes at 121 °C and 1 kg/cm². The agar solution was cooled to 50 °C and ampicillin was added to a final concentration of 100 µg/ml of Luria Bertani agar solution. The agar solution was poured into petri dishes and allowed to solidify at room temperature. The agar plates were stored at 4 °C.

Protocol

Ten microlitres of ligation mix was used to transform 100 µl of chemically competent XL10-Gold cells. The mixture was incubated on ice for 30 minutes followed by a heat shock treatment at 42 °C for 90 seconds. The sample was placed on ice for 5 minutes and then spread on an agar plate. The plate was sealed and incubated upside down at 37 °C overnight.

5.2.4 High Pure Plasmid Isolation

Reagents

- *Roche High Pure Plasmid Isolation Kit (Roche Applied Science, Mannheim Germany)*
- *LB media (Appendix 5.2.3)*

Protocol

A single bacterial colony containing the plasmid of interest was used to inoculate 10 ml of LB media supplemented with 10 µl of 1000 × ampicillin. The broth was placed in a shaking incubator at 37 °C overnight. Thereafter, the bacterial culture was centrifuged at 4000 ×g for 20 minutes followed by resuspending the pellet in 250 µl suspension buffer. The bacterial cells were lysed by adding 250 µl lysis buffer, gently mixed and incubated at room temperature for 5 minutes. Three hundred and fifty microlitres of chilled binding buffer was added to the sample, followed by gentle mixing and then incubation on ice or 5 minutes. The sample was centrifuged at 4000 ×g for 20 minutes and the supernatant was transferred to a High Pure column that was placed in a collection tube. Using a standard bench top centrifuge the sample was centrifuged at maximum speed for 1 minute. The flow-through in the collection tube was discarded and 700 µl of wash buffer II was added to the column. The sample was centrifuged at 13 000 ×g for 1 minute, the flow-through was discarded and the sample was centrifuged for 1 minute to remove excess wash buffer. The column was placed in a sterile microcentrifuge tube and 100 µl of elution buffer was added to the filter tube followed by centrifugation at 13 000 ×g for 1 minute. The eluted plasmid DNA was stored at - 70°C.

5.2.5 Plasmid Maxi preparation

Reagents

- *Luria-Bertani media (Appendix 5.2.3)*
- *Plasmid Maxi Kit (Qiagen, Hilden, Germany)*
- *1000× ampicillin*

Protocol

A single bacterial colony containing the plasmid of interest was used to inoculate 100 ml of LB media supplemented with 100 µl of 1000 × ampicillin. The broth was placed in a shaking incubator at 37 °C overnight. Thereafter, the bacterial culture was centrifuged at 4000 ×g for 30 minutes at 4 °C followed by resuspending the pellet in 10 ml buffer P1. The bacterial cells were lysed by adding 10 ml buffer P2, mixed by inverting the tube 4-6 times and incubated at room temperature for 5 minutes. Ten millilitres of chilled buffer P3 was added to the tube and the sample mixed by inverting the tube. The solution was incubated for 20 minutes on ice followed by centrifugation at 20 000 ×g for 30 minutes at 4 °C. The supernatant was transferred to a sterile tube and centrifuged at 20 000 ×g for 20 minutes at 4 °C. Simultaneously a QIAGEN-tip 500 was equilibrated by adding 10 ml buffer QBT to the column and allowing it to empty. After the centrifugation, the supernatant from the sample was added to the QIAGEN-tip and allowed to enter the resin by gravity. Thereafter the QIAGEN-tip was washed twice with 30 ml of buffer QC. The QIAGEN-tip was transferred to a sterile collection tube and subsequently 15 ml of buffer QF was added to elute the DNA. The eluted plasmid DNA was precipitated by adding 10.5 ml of room temperature isopropanol, followed by mixing and centrifugation at 15 000 ×g for 30 minutes at 4 °C. The isopropanol was discarded and the DNA pellet was washed by adding room temperature 70 % ethanol and centrifuging the sample at 4000 ×g for 10 minutes at 4

°C. The ethanol was discarded, the pellet was left to air dry for 5 minutes and then re-suspended in 200 µl of distilled water and stored at -20 °C.

5.2.6 Mycoplasma detection

Reagents

- *MycoAlert™ mycoplasma detection kit (Lonza, Basel, Switzerland)*

Protocol

Two millilitres of cell culture supernatant was centrifuged at 200 ×g for 5 minutes. Thereafter a 100 µl of the supernatant was placed into a well of a luminometer plate. One hundred microlitres of MycoAlert™ reagent was added to the sample in the well and left for 5 minutes at room temperature before measuring the luminescence (Reading A) in a Veritas™ Microplate Luminometer (Promega, WI, USA). Next, 100 µl of MycoAlert™ substrate was added to the sample and left for 10 minutes before measuring the luminescence (Reading B). A ratio of Reading B/Reading A was calculated.

5.2.7 jetPRIME® transfection

Reagents

- *jetPRIME® Transfection Reagent kit (Polyplus-transfection, Illkirch, France)*

Protocol

Twenty-four hours prior to transfections, HEK293T cells were seeded to be 60 to 80 % confluent at the time of transfections. For the transfections, the DNA mix was diluted with jetPRIME® buffer and mixed well by vortexing for 10 seconds followed by brief centrifugation. Thereafter, jetPRIME® reagent was added to the diluted DNA mix, which was then vortexed for 10 seconds, centrifuged briefly and incubated at room temperature for 10 minutes at room temperature. The transfection mix was then added dropwise to the

cell culture medium per well and mixed by gentle agitation. The cells were incubated in a humidified incubator at 37 °C and 5% CO₂ for 48 hours. The volumes of reagents used for the different culture plates are displayed in Table 5.1.

Table 5.1: The DNA transfection amounts used for the different culture plates based on the jetPRIME® transfection guidelines. Volumes are given per well.

Culture plates	Amount of DNA used	Volume of jetPRIME® Buffer	Volume of jetPRIME® reagent
96 well	98 ng	5 µl	0.2 µl
48 well	200 ng	25 µl	0.4 µl
6 well	2080 ng	200 µl	4.16 µl

5.2.8 Lipofectamine® 3000 transfections

Reagents

- *Lipofectamine® 3000 Reagent (Thermo Scientific, CA, USA),*
- *Opti-MEM® Reduced Serum Medium*

Protocol

Twenty-four hours prior to transfections, Huh 7 cells were seeded to be 70 to 90% confluent at the time of transfections. For the transfections, the DNA mixes were diluted in the appropriate volume of Opti-MEM™ and P3000™ Reagent and thoroughly mixed. In a separate centrifuge tube Lipofectamine™ 3000 was diluted in Opti-MEM™ and thoroughly mixed. A volume of the diluted Lipofectamine™ 3000 Reagent was then mixed with the diluted DNA and incubated for 15 minutes at room temperature. The transfection mix was then added dropwise to the cell culture medium per well and mixed by gentle agitation. The cells were incubated in a humidified incubator at 37 °C and 5% CO₂ for 48 hours. The volumes of reagents used for the different culture plates are displayed in Table 5.2.

Table 5.2: The DNA transfection amounts used for the different culture plates based on the Lipofectamine® 3000 transfection guidelines. Volumes are given per well.

Culture plate	Volumes for dilution of DNA			Volumes for dilution of Lipofectamine® 3000 Reagent	
	DNA amount	Opti-MEM® Medium	P3000™ Reagent	Opti-MEM® Medium	Lipofectamine® 3000 Reagent
48 well	200 ng	12.5 µl	0.5 µl	12.5 µl	0.75 µl
6 well	2080 ng	125 µl	10 µl	125 µl	7.5 µl

6. References:

1. Seeger C, Mason WS. Hepatitis B virus biology. *Microbiology and molecular biology reviews* : MMBR. 2000 Mar;64(1):51-68.
2. World Health Organization. Hepatitis B virus Fact sheet No. 204. 2015 [updated July 2015; cited 2015]; Available from:
<http://www.who.int/mediacentre/factsheets/fs204/en/>.
3. Mast EE, Alter MJ, Margolis HS. Strategies to prevent and control hepatitis B and C virus infections: a global perspective. *Vaccine*. 1999 17(13-14):1730-3.
4. Chang M-H, Chen D-S. Prevention of hepatitis B. *Cold Spring Harbor perspectives in medicine*. 2015;5(3):a021493.
5. Gerlich WH. Prophylactic vaccination against hepatitis B: achievements, challenges and perspectives. *Medical microbiology and immunology*. 2015;204(1):39-55.
6. Burnett RJ, Kramvis A, Dochez C, Meheus A. An update after 16 years of hepatitis B vaccination in South Africa. *Vaccine*. 2012;30:C45-C51.
7. Kramvis A, Kew MC. Epidemiology of hepatitis B virus in Africa, its genotypes and clinical associations of genotypes. *Hepatology Research*. 2007;37:S9-S19.
8. Sunbul M. Hepatitis B virus genotypes: Global distribution and clinical importance. *World Journal of Gastroenterology* : WJG. 2014;20(18):5427-34.
9. Shepard CW, Simard EP, Finelli L, Fiore AE, Bell BP. Hepatitis B virus infection: epidemiology and vaccination. *Epidemiologic reviews*. 2006;28(1):112-25.
10. Papastergiou V, Lombardi R, MacDonald D, Tsochatzis EA. Global Epidemiology of Hepatitis B Virus (HBV) Infection. *Current Hepatology Reports*. [journal article]. 2015;14(3):171-8.
11. Hyams KC. Risks of chronicity following acute hepatitis B virus infection: a review. *Clinical Infectious Diseases*. 1995;20(4):992-1000.

12. Jung M-C, Pape GR. Immunology of hepatitis B infection. *The Lancet Infectious Diseases*. 2002 1//;2(1):43-50.
13. Sung J, Tsoi K, Wong V, Li K, Chan H. Meta-analysis: treatment of hepatitis B infection reduces risk of hepatocellular carcinoma. *Alimentary pharmacology & therapeutics*. 2008;28(9):1067-77.
14. European Association for the Study of the L. EASL Clinical Practice Guidelines: Management of chronic hepatitis B virus infection. *Journal of Hepatology*. 2012;57(1):167-85.
15. Zhang F, Wang G. A review of non-nucleoside anti-hepatitis B virus agents. *European Journal of Medicinal Chemistry*. 2014 3/21//;75(0):267-81.
16. Zhang Y, Wu Y, Ye S, Wang T, Zhao R, Chen F, et al. The response to interferon is influenced by hepatitis B virus genotype in vitro and in vivo. *Virus research*. 2013 Jan;171(1):65-70.
17. Shi YH. Correlation between hepatitis B virus genotypes and clinical outcomes. *Japanese journal of infectious diseases*. 2012;65(6):476-82.
18. Chen J, Wu M, Liu K, Zhang W, Li Y, Zhou X, et al. New insights into hepatitis B virus biology and implications for novel antiviral strategies. *National Science Review*. 2015;2(3):296-313.
19. Liang Y, Jiang J, Su M, Liu Z, Guo W, Huang X, et al. Predictors of relapse in chronic hepatitis B after discontinuation of anti-viral therapy. *Aliment Pharmacol Ther*. 2011 Aug;34(3):344-52.
20. Bloom K, Ely A, Mussolino C, Cathomen T, Arbuthnot P. Inactivation of hepatitis B virus replication in cultured cells and in vivo with engineered transcription activator-like effector nucleases. *Molecular therapy : the journal of the American Society of Gene Therapy*. 2013 Oct;21(10):1889-97.

21. Hu Z, Yu L, Zhu D, Ding W, Wang X, Zhang C, et al. Disruption of HPV16-E7 by CRISPR/Cas system induces apoptosis and growth inhibition in HPV16 positive human cervical cancer cells. *BioMed research international*. 2014;2014.
22. Ding W, Hu Z, Zhu D, Jiang X, Yu L, Wang X, et al. Zinc finger nucleases targeting the human papillomavirus E7 oncogene induce E7 disruption and a transformed phenotype in HPV16/18-positive cervical cancer cells. *Clinical Cancer Research*. 2014;20(24):6495-503.
23. Dampier W, Nonnemacher MR, Sullivan NT, Jacobson JM, Wigdahl B. HIV excision utilizing CRISPR/Cas9 technology: attacking the proviral quasispecies in reservoirs to achieve a cure. *MOJ immunology*. 2014;1(4).
24. Price AA, Sampson TR, Ratner HK, Grakoui A, Weiss DS. Cas9-mediated targeting of viral RNA in eukaryotic cells. *Proceedings of the National Academy of Sciences*. 2015;112(19):6164-9.
25. Fauquet CM, Mayo MA, Maniloff J, Desselberger U, Ball LA. *Virus taxonomy: VIIIth report of the International Committee on Taxonomy of Viruses*: Academic Press; 2005.
26. Seeger C, Mason WS. Molecular biology of hepatitis B virus infection. *Virology*. 2015;479:672-86.
27. Landers TA, Greenberg HB, Robinson WS. Structure of hepatitis B Dane particle DNA and nature of the endogenous DNA polymerase reaction. *Journal of virology*. 1977 Aug;23(2):368-76.
28. Summers J, Mason WS. Replication of the genome of a hepatitis B--like virus by reverse transcription of an RNA intermediate. *Cell*. 1982 Jun;29(2):403-15.
29. Tong S, Li J, Wands JR, Wen Y-m. Hepatitis B virus genetic variants: biological properties and clinical implications. *Emerging Microbes & Infections*. 2013;2(3):e10.

30. Watashi K, Urban S, Li W, Wakita T. NTCP and Beyond: Opening the Door to Unveil Hepatitis B Virus Entry. *International Journal of Molecular Sciences*. 2014;15(2):2892-905.
31. Liang TJ. Hepatitis B: the virus and disease. *Hepatology (Baltimore, Md)*. 2009 May;49(5 Suppl):S13-21.
32. Wang J, Lee A, Ou J-H. Proteolytic conversion of hepatitis B virus e antigen precursor to end product occurs in a postendoplasmic reticulum compartment. *Journal of virology*. 1991;65(9):5080-3.
33. Chen MT, Billaud J-N, Sällberg M, Guidotti LG, Chisari FV, Jones J, et al. A function of the hepatitis B virus precore protein is to regulate the immune response to the core antigen. *Proceedings of the National Academy of Sciences of the United States of America*. 2004 October 12, 2004;101(41):14913-8.
34. Moolla N, Kew M, Arbuthnot P. Regulatory elements of hepatitis B virus transcription. *J Viral Hepat*. 2002;9(5):323-31.
35. Decorsière A, Mueller H, Van Breugel PC, Abdul F, Gerossier L, Beran RK, et al. Hepatitis B virus X protein identifies the Smc5/6 complex as a host restriction factor. *Nature*. 2016;531(7594):386-0.
36. Nassal M. HBV cccDNA: viral persistence reservoir and key obstacle for a cure of chronic hepatitis B. *Gut*. 2015 Dec;64(12):1972-84.
37. Schulze A, Gripon P, Urban S. Hepatitis B virus infection initiates with a large surface protein-dependent binding to heparan sulfate proteoglycans. *Hepatology (Baltimore, Md)*. 2007 Dec;46(6):1759-68.
38. Yan H, Zhong G, Xu G, He W, Jing Z, Gao Z, et al. Sodium taurocholate cotransporting polypeptide is a functional receptor for human hepatitis B and D virus. *eLife*. 2012;1:e00049.

39. Rabe B, Glebe D, Kann M. Lipid-mediated introduction of hepatitis B virus capsids into nonsusceptible cells allows highly efficient replication and facilitates the study of early infection events. *Journal of virology*. 2006;80(11):5465-73.
40. Rabe B, Vlachou A, Panté N, Helenius A, Kann M. Nuclear import of hepatitis B virus capsids and release of the viral genome. *Proceedings of the National Academy of Sciences of the United States of America*. 2003;100(17):9849-54.
41. Xie Y, Zhai J, Deng Q, Tiollais P, Wang Y, Zhao M. Entry of hepatitis B virus: Mechanism and new therapeutic target. *Pathologie Biologie*. 2010 8//;58(4):301-7.
42. Summers J, Smith PM, Horwich AL. Hepadnavirus envelope proteins regulate covalently closed circular DNA amplification. *Journal of virology*. 1990;64(6):2819-24.
43. Luckenbaugh L, Kitrinou KM, Delaney WE, Hu J. Genome-free hepatitis B virion levels in patient sera as a potential marker to monitor response to antiviral therapy. *J Viral Hepat*. 2015 11/14;22(6):561-70.
44. Grimm D, Thimme R, Blum HE. HBV life cycle and novel drug targets. *Hepatology international*. 2011 Jun;5(2):644-53.
45. Chang J, Guo F, Zhao X, Guo J-T. Therapeutic strategies for a functional cure of chronic hepatitis B virus infection. *Acta Pharmaceutica Sinica B*. 2014 8//;4(4):248-57.
46. Lequin RM. Enzyme immunoassay (EIA)/enzyme-linked immunosorbent assay (ELISA). *Clinical chemistry*. 2005;51(12):2415-8.
47. Fatema K, Tabassum S, Nessa A, Jahan M. Development and evaluation of an in-house ELISA to detect hepatitis B virus surface antigen in resource-limited settings. *Bangladesh Medical Research Council bulletin*. 2013 Aug;39(2):65-8.
48. Urban S, Bartenschlager R, Kubitz R, Zoulim F. Strategies to inhibit entry of HBV and HDV into hepatocytes. *Gastroenterology*. 2014 Jul;147(1):48-64.

49. Volz T, Allweiss L, Ben MM, Warlich M, Lohse AW, Pollok JM, et al. The entry inhibitor Myrcludex-B efficiently blocks intrahepatic virus spreading in humanized mice previously infected with hepatitis B virus. *J Hepatol.* 2013 May;58(5):861-7.
50. Katen SP, Chirapu SR, Finn MG, Zlotnick A. Trapping of hepatitis B virus capsid assembly intermediates by phenylpropenamide assembly accelerators. *ACS chemical biology.* 2010 Dec 17;5(12):1125-36.
51. Xu YB, Yang L, Wang GF, Tong XK, Wang YJ, Yu Y, et al. Benzimidazole derivative, BM601, a novel inhibitor of hepatitis B virus and HBsAg secretion. *Antiviral research.* 2014 Jul;107:6-15.
52. Carmona S, Ely A, Crowther C, Moolla N, Salazar FH, Marion PL, et al. Effective inhibition of HBV replication in vivo by anti-HBx short hairpin RNAs. *Molecular Therapy.* 2006;13(2):411-21.
53. Loggi E, Vitale G, Conti F, Bernardi M, Andreone P. Chronic hepatitis B: Are we close to a cure? *Digestive and Liver Disease.* 2015 10//;47(10):836-41.
54. Maepa MB, Roelofse I, Ely A, Arbuthnot P. Progress and Prospects of Anti-HBV Gene Therapy Development. *Int J Mol Sci.* 2015 Aug;16(8):17589-610.
55. Kao J-H. Hepatitis B vaccination and prevention of hepatocellular carcinoma. *Best Practice & Research Clinical Gastroenterology.* 2015;29(6):907-17.
56. Walayat S, Ahmed Z, Martin D, Puli S, Cashman M, Dhillon S. Recent advances in vaccination of non-responders to standard dose hepatitis B virus vaccine. *World Journal of Hepatology.* 2015;7(24):2503-9.
57. Coates T, Wilson R, Patrick G, André F, Watson V. Hepatitis B vaccines: assessment of the seroprotective efficacy of two recombinant DNA vaccines. *Clinical therapeutics.* 2001;23(3):392-403.

58. Harpaz R, McMahon BJ, Margolis HS, Shapiro CN, Havron D, Carpenter G, et al. Elimination of new chronic hepatitis B virus infections: results of the Alaska immunization program. *Journal of infectious diseases*. 2000;181(2):413-8.
59. Goncalves L, Albarran B, Salmen S, Borges L, Fields H, Montes H, et al. The nonresponse to hepatitis B vaccination is associated with impaired lymphocyte activation. *Virology*. 2004 8/15/;326(1):20-8.
60. Averhoff F, Mahoney F, Coleman P, Schatz G, Hurwitz E, Margolis H. Immunogenicity of hepatitis B vaccines: implications for persons at occupational risk of hepatitis B virus infection. *American journal of preventive medicine*. 1998;15(1):1-8.
61. Tajiri K, Shimizu Y. Unsolved problems and future perspectives of hepatitis B virus vaccination. *World Journal of Gastroenterology : WJG*. 2015 05/04/accepted;21(23):7074-83.
62. Vitaliti G, Pratico AD, Cimino C, Di Dio G, Lionetti E, La Rosa M, et al. Hepatitis B vaccine in celiac disease: yesterday, today and tomorrow. *World journal of gastroenterology*. 2013 Feb 14;19(6):838-45.
63. Luongo M, Critelli R, Grottola A, Gitto S, Bernabucci V, Bevini M, et al. Acute hepatitis B caused by a vaccine-escape HBV strain in vaccinated subject: sequence analysis and therapeutic strategy. *Journal of clinical virology : the official publication of the Pan American Society for Clinical Virology*. 2015 Jan;62:89-91.
64. Huang X, Lu D, Ji G, Sun Y, Ma L, Chen Z, et al. Hepatitis B virus (HBV) vaccine-induced escape mutants of HBV S gene among children from Qidong area, China. *Virus research*. 2004 Jan;99(1):63-8.
65. Perrillo R. Benefits and risks of interferon therapy for hepatitis B. *Hepatology (Baltimore, Md)*. 2009;49(S5):S103-S11.

66. Dianzani F. Biological basis for the clinical use of interferon. *Gut*. 1993;34(2 Suppl):S74-6.
67. Cooksley WG, Piratvisuth T, Lee SD, Mahachai V, Chao YC, Tanwandee T, et al. Peginterferon alpha-2a (40 kDa): an advance in the treatment of hepatitis B e antigen-positive chronic hepatitis B. *J Viral Hepat*. 2003 Jul;10(4):298-305.
68. Abe H, Hayes CN, Chayama K. New insight into the enhanced effect of pegylated interferon- α . *Hepatology (Baltimore, Md)*. 2014;60(4):1435-7.
69. Rang A, Gunther S, Will H. Effect of interferon alpha on hepatitis B virus replication and gene expression in transiently transfected human hepatoma cells. *J Hepatol*. 1999 Nov;31(5):791-9.
70. Lau GKK, Piratvisuth T, Luo KX, Marcellin P, Thongsawat S, Cooksley G, et al. Peginterferon Alfa-2a, Lamivudine, and the Combination for HBeAg-Positive Chronic Hepatitis B. *New England Journal of Medicine*. 2005;352(26):2682-95.
71. Perrillo RP, Schiff ER, Davis GL, Bodenheimer HC, Jr., Lindsay K, Payne J, et al. A randomized, controlled trial of interferon alfa-2b alone and after prednisone withdrawal for the treatment of chronic hepatitis B. The Hepatitis Interventional Therapy Group. *N Engl J Med*. 1990;323(5):295-301.
72. Lin CC, Wu JC, Chang TT, Huang YH, Wang YJ, Tsay SH, et al. Long-term evaluation of recombinant interferon α 2b in the treatment of patients with hepatitis B e antigen-negative chronic hepatitis B in Taiwan. *J Viral Hepat*. 2001;8(6):438-46.
73. Papatheodoridis GV, Manesis E, Hadziyannis SJ. The long-term outcome of interferon- α treated and untreated patients with HBeAg-negative chronic hepatitis B. *Journal of Hepatology*. 2001;34(2):306-13.

74. Vlachogiannakos J, Papatheodoridis G. Hepatocellular carcinoma in chronic hepatitis B patients under antiviral therapy. *World Journal of Gastroenterology* : WJG. 2013;19(47):8822-30.
75. Osborn MK, Lok AS. Antiviral options for the treatment of chronic hepatitis B. *Journal of Antimicrobial Chemotherapy*. 2006;57(6):1030-4.
76. Buster EH, Flink HJ, Cakaloglu Y, Simon K, Trojan J, Tabak F, et al. Sustained HBeAg and HBsAg loss after long-term follow-up of HBeAg-positive patients treated with peginterferon alpha-2b. *Gastroenterology*. 2008 Aug;135(2):459-67.
77. Marcellin P, Bonino F, Lau GK, Farci P, Yurdaydin C, Piratvisuth T, et al. Sustained response of hepatitis B e antigen-negative patients 3 years after treatment with peginterferon alpha-2a. *Gastroenterology*. 2009 Jun;136(7):2169-79.e1-4.
78. Marcellin P, Lau GK, Bonino F, Farci P, Hadziyannis S, Jin R, et al. Peginterferon alfa-2a alone, lamivudine alone, and the two in combination in patients with HBeAg-negative chronic hepatitis B. *N Engl J Med*. 2004;351(12):1206-17.
79. Chae HB, Hann H-W. Time for an active antiviral therapy for hepatitis B: An update on the management of hepatitis B virus infection. *Therapeutics and Clinical Risk Management*. 2007;3(4):605-12.
80. Dienstag JL. Benefits and risks of nucleoside analog therapy for hepatitis B. *Hepatology (Baltimore, Md)*. 2009;49(S5):S112-S21.
81. Papatheodoridis GV, Dimou E, Papadimitropoulos V. Nucleoside analogues for chronic hepatitis B: antiviral efficacy and viral resistance. *Am J Gastroenterol*. 2002;97(7):1618-28.
82. Yuen MF, Seto WK, Chow DH, Tsui K, Wong DK, Ngai VW, et al. Long-term lamivudine therapy reduces the risk of long-term complications of chronic hepatitis B infection even in patients without advanced disease. *Antivir Ther*. 2007;12(8):1295-303.

83. Dienstag JL, Schiff ER, Wright TL, Perrillo RP, Hann H-WL, Goodman Z, et al. Lamivudine as Initial Treatment for Chronic Hepatitis B in the United States. *New England Journal of Medicine*. 1999;341(17):1256-63.
84. Lai C-L, Chien R-N, Leung NWY, Chang T-T, Guan R, Tai D-I, et al. A One-Year Trial of Lamivudine for Chronic Hepatitis B. *New England Journal of Medicine*. 1998;339(2):61-8.
85. Fischer KP, Gutfreund KS, Tyrrell DL. Lamivudine resistance in hepatitis B: mechanisms and clinical implications. *Drug Resist Updat*. 2001 2001/04//;4(2):118-28.
86. Xiong X, Flores C, Yang H, Toole JJ, Gibbs CS. Mutations in hepatitis B DNA polymerase associated with resistance to lamivudine do not confer resistance to adefovir in vitro. *Hepatology (Baltimore, Md)*. 1998;28(6):1669-73.
87. Lee JM, Kim HJ, Park JY, Lee CK, Kim Do Y KJ, Lee H, et al. Rescue monotherapy in lamivudine-resistant hepatitis B e antigen-positive chronic hepatitis B: adefovir versus entecavir. *Antivir Ther*. 2009;14(5):705-12.
88. Tenney DJ, Pokornowski KA, Rose RE, Baldick CJ, Eggers BJ, Fang J, et al. Entecavir maintains a high genetic barrier to HBV resistance through 6 years in naive patients. *Journal of Hepatology*. 2009;50:S10.
89. Marcellin P, Heathcote EJ, Buti M, Gane E, de Man RA, Krastev Z, et al. Tenofovir Disoproxil Fumarate versus Adefovir Dipivoxil for Chronic Hepatitis B. *New England Journal of Medicine*. 2008;359(23):2442-55.
90. Kitrinou KM, Corsa A, Liu Y, Flaherty J, Snow-Lampart A, Marcellin P, et al. No detectable resistance to tenofovir disoproxil fumarate after 6 years of therapy in patients with chronic hepatitis B. *Hepatology (Baltimore, Md)*. 2014;59(2):434-42.

91. Seignères B, Martin P, Werle B, Schorr O, Jamard C, Rimsky L, et al. Effects of Pyrimidine and Purine Analog Combinations in the Duck Hepatitis B Virus Infection Model. *Antimicrobial Agents and Chemotherapy*. 2003;47(6):1842-52.
92. Coffin CS, Mulrooney-Cousins PM, Peters MG, van Marle G, Roberts JP, Michalak TI, et al. Molecular characterization of intrahepatic and extrahepatic hepatitis B virus (HBV) reservoirs in patients on suppressive antiviral therapy. *J Viral Hepat*. 2011;18(6):415-23.
93. Delmas J, Schorr O, Jamard C, Gibbs C, Trepo C, Hantz O, et al. Inhibitory effect of adefovir on viral DNA synthesis and covalently closed circular DNA formation in duck hepatitis B virus-infected hepatocytes in vivo and in vitro. *Antimicrob Agents Chemother*. 2002 Feb;46(2):425-33.
94. Halegoua-De Marzio D, Hann H-W. Then and now: the progress in hepatitis B treatment over the past 20 years. *World journal of gastroenterology*. 2014;20(2):401-13.
95. Schiffer JT, Aubert M, Weber ND, Mintzer E, Stone D, Jerome KR. Targeted DNA Mutagenesis for the Cure of Chronic Viral Infections. *Journal of virology*. 2012 Sep;86(17):8920-36.
96. zu Putlitz J, Wieland S, Blum HE, Wands JR. Antisense RNA complementary to hepatitis B virus specifically inhibits viral replication. *Gastroenterology*. 1998;115(3):702-13.
97. Goodarzi G, Gross SC, Tewari A, Watabe K. Antisense oligodeoxyribonucleotides inhibit the expression of the gene for hepatitis B virus surface antigen. *J Gen Virol*. 1990;71(Pt 12):3021-5.
98. Asahina Y, Ito Y, Wu CH, Wu GY. DNA ribonucleases that are active against intracellular hepatitis B viral RNA targets. *Hepatology (Baltimore, Md)*. 1998;28(2):547-54.

99. Weinberg MS, Ely A, Passman M, Mufamadi SM, Arbuthnot P. Effective anti-hepatitis B virus hammerhead ribozymes derived from multimeric precursors. *Oligonucleotides*. 2007;17(1):104-12.
100. Arbuthnot P, Carmona S, Ely A. Exploiting the RNA interference pathway to counter hepatitis B virus replication. *Liver international*. 2005;25(1):9-15.
101. Fire A, Xu S, Montgomery MK, Kostas SA, Driver SE, Mello CC. Potent and specific genetic interference by double-stranded RNA in *Caenorhabditis elegans*. *Nature*. [10.1038/35888]. 1998;391(6669):806-11.
102. Marimani MD, Ely A, Buff MC, Bernhardt S, Engels JW, Scherman D, et al. Inhibition of replication of hepatitis B virus in transgenic mice following administration of hepatotropic lipoplexes containing guanidinopropyl-modified siRNAs. *J Control Release*. 2015;209:198-206.
103. Ely A, Naidoo T, Arbuthnot P. Efficient silencing of gene expression with modular trimeric Pol II expression cassettes comprising microRNA shuttles. *Nucleic Acids Res*. 2009;37(13):27.
104. McCaffrey AP, Nakai H, Pandey K, Huang Z, Salazar FH, Xu H, et al. Inhibition of hepatitis B virus in mice by RNA interference. *Nat Biotech*. [10.1038/nbt824]. 2003;21(6):639-44.
105. Starkey JL, Chiari EF, Isom HC. HBV-Specific shRNA is Capable of Reducing the Formation of Hepatitis B Virus Covalently Closed Circular DNA, but has No Effect on Established Covalently Closed Circular DNA in vitro. *The Journal of general virology*. 2009;90(Pt 1):115-26.
106. Cox DBT, Platt RJ, Zhang F. Therapeutic genome editing: prospects and challenges. *Nature medicine*. 2015;21(2):121-31.

107. Miller J, McLachlan AD, Klug A. Repetitive zinc-binding domains in the protein transcription factor IIIA from *Xenopus oocytes*: EMBO J. 1985 Jun;4(6):1609-14.; 1985.
108. Dreier B, Beerli RR, Segal DJ, Flippin JD, Barbas CF, 3rd. Development of zinc finger domains for recognition of the 5'-ANN-3' family of DNA sequences and their use in the construction of artificial transcription factors. The Journal of biological chemistry. 2001 Aug 3;276(31):29466-78.
109. Choo Y, Klug A. Toward a code for the interactions of zinc fingers with DNA: selection of randomized fingers displayed on phage. Proc Natl Acad Sci U S A. 1994 Nov 8;91(23):11163-7.
110. Mandell JG, Barbas CF. Zinc Finger Tools: custom DNA-binding domains for transcription factors and nucleases. Nucleic Acids Res. 2006 Jul 1;34(Web Server issue):W516-23.
111. Klug A. The discovery of zinc fingers and their applications in gene regulation and genome manipulation. Annual review of biochemistry. 2010;79:213-31.
112. Alwin S, Gere MB, Guhl E, Effertz K, Barbas CF, Segal DJ, et al. Custom Zinc-Finger Nucleases for Use in Human Cells. Molecular therapy : the journal of the American Society of Gene Therapy. 2005 10//print;12(4):610-7.
113. Liu PQ, Rebar EJ, Zhang L, Liu Q, Jamieson AC, Liang Y, et al. Regulation of an endogenous locus using a panel of designed zinc finger proteins targeted to accessible chromatin regions. Activation of vascular endothelial growth factor A. The Journal of biological chemistry. 2001 Apr 6;276(14):11323-34.
114. Snowden AW, Zhang L, Urnov F, Dent C, Jouvenot Y, Zhong X, et al. Repression of vascular endothelial growth factor A in glioblastoma cells using engineered zinc finger transcription factors. Cancer research. 2003 Dec 15;63(24):8968-76.

115. Boch J, Bonas U. Xanthomonas AvrBs3 family-type III effectors: discovery and function. *Annual review of phytopathology*. 2010;48:419-36.
116. Mak AN-S, Bradley P, Cernadas RA, Bogdanove AJ, Stoddard BL. The crystal structure of TAL effector PthXo1 bound to its DNA target. *Science (New York, NY)*. 2012;335(6069):716-9.
117. Boch J, Scholze H, Schornack S, Landgraf A, Hahn S, Kay S, et al. Breaking the code of DNA binding specificity of TAL-type III effectors. *Science (New York, NY)*. 2009;326(5959):1509-12.
118. Cong L, Zhou R, Kuo YC, Cunniff M, Zhang F. Comprehensive interrogation of natural TALE DNA-binding modules and transcriptional repressor domains. *Nature communications*. 2012;3:968.
119. Sanjana NE, Cong L, Zhou Y, Cunniff MM, Feng G, Zhang F. A transcription activator-like effector toolbox for genome engineering. *Nature protocols*. 2012 Jan;7(1):171-92.
120. Cong L, Ran FA, Cox D, Lin S, Barretto R, Habib N, et al. Multiplex Genome Engineering Using CRISPR/Cas Systems. *Science (New York, NY)*. 2013 01/03;339(6121):819-23.
121. Yang L, Mali P, Kim-Kiselak C, Church G. CRISPR-Cas-mediated targeted genome editing in human cells. *Methods in molecular biology (Clifton, NJ)*. 2014;1114:245-67.
122. Doudna JA, Charpentier E. Genome editing. The new frontier of genome engineering with CRISPR-Cas9. *Science (New York, NY)*. 2014 Nov 28;346(6213):1258096.
123. Horvath P, Barrangou R. CRISPR/Cas, the immune system of bacteria and archaea. *Science (New York, NY)*. 2010 Jan 8;327(5962):167-70.

124. Bortesi L, Fischer R. The CRISPR/Cas9 system for plant genome editing and beyond. *Biotechnology Advances*. 2015;33(1):41-52.
125. Barrangou R, Fremaux C, Deveau H, Richards M, Boyaval P, Moineau S, et al. CRISPR provides acquired resistance against viruses in prokaryotes. *Science (New York, NY)*. 2007;315(5819):1709-12.
126. Deltcheva E, Chylinski K, Sharma CM, Gonzales K, Chao Y, Pirzada ZA, et al. CRISPR RNA maturation by trans-encoded small RNA and host factor RNase III. *Nature*. [10.1038/nature09886]. 2011 03/31/print;471(7340):602-7.
127. Jinek M, Chylinski K, Fonfara I, Hauer M, Doudna JA, Charpentier E. A programmable dual-RNA-guided DNA endonuclease in adaptive bacterial immunity. *Science (New York, NY)*. 2012 Aug 17;337(6096):816-21.
128. Sander JD, Joung JK. CRISPR-Cas systems for editing, regulating and targeting genomes. *Nature biotechnology*. 2014;32(4):347-55.
129. Weber ND, Stone D, Sedlak RH, De Silva Felixge HS, Roychoudhury P, Schiffer JT, et al. AAV-mediated delivery of zinc finger nucleases targeting hepatitis B virus inhibits active replication. *PLoS ONE*. 2014;9(5).
130. Zhen S, Hua L, Liu YH, Gao LC, Fu J, Wan DY, et al. Harnessing the clustered regularly interspaced short palindromic repeat (CRISPR)/CRISPR-associated Cas9 system to disrupt the hepatitis B virus. *Gene Ther*. 2015;22(5):404-12.
131. Lin G, Zhang K, Li J. Application of CRISPR/Cas9 technology to HBV. *International Journal of Molecular Sciences*. 2015;16(11):26077-86.
132. Lee HJ, Kweon J, Kim E, Kim S, Kim JS. Targeted chromosomal duplications and inversions in the human genome using zinc finger nucleases. *Genome research*. 2012 Mar;22(3):539-48.

133. Bree RT, Neary C, Samali A, Lowndes NF. The switch from survival responses to apoptosis after chromosomal breaks. *DNA repair*. 2004;3(8):989-95.
134. Richardson C, Jasin M. Frequent chromosomal translocations induced by DNA double-strand breaks. *Nature*. 2000 Jun 8;405(6787):697-700.
135. Bloom K, Mussolino C, Arbuthnot P. Transcription Activator-Like Effector (TALE) Nucleases and Repressor TALEs for Antiviral Gene Therapy. *Current Stem Cell Reports*. 2015;1(1):1-8.
136. Mak AN, Bradley P, Bogdanove AJ, Stoddard BL. TAL effectors: function, structure, engineering and applications. *Curr Opin Struct Biol*. 2013;23(1):93-9.
137. Richter A, Streubel J, Boch J. TAL Effector DNA-Binding Principles and Specificity. *TALENs: Methods and Protocols*. 2016:9-25.
138. Streubel J, Blücher C, Landgraf A, Boch J. TAL effector RVD specificities and efficiencies. *Nature biotechnology*. 2012;30(7):593-5.
139. Lamb BM, Mercer AC, Barbas CF. Directed evolution of the TALE N-terminal domain for recognition of all 5' bases. *Nucleic Acids Research*. 2013;41(21):9779-85.
140. Kleinjan DA, van Heyningen V. Long-range control of gene expression: emerging mechanisms and disruption in disease. *The American Journal of Human Genetics*. 2005;76(1):8-32.
141. Smith AD, Sumazin P, Xuan Z, Zhang MQ. DNA motifs in human and mouse proximal promoters predict tissue-specific expression. *Proceedings of the National Academy of Sciences of the United States of America*. 2006 04/10 09/19/received;103(16):6275-80.
142. Ogbourne S, Antalis TM. Transcriptional control and the role of silencers in transcriptional regulation in eukaryotes. *The Biochemical journal*. 1998 Apr 1;331 (Pt 1):1-14.

143. Georgiev PG, Murav'eva EE, Golovnin AK, Gracheva EM, Belen'kaia T. [Insulators and interaction between long-distance regulatory elements in higher eukaryotes]. *Genetika*. 2000 Dec;36(12):1588-97.
144. Narlikar L, Ovcharenko I. Identifying regulatory elements in eukaryotic genomes. *Briefings in Functional Genomics*. 2009:elp014.
145. Gaston K, Jayaraman PS. Transcriptional repression in eukaryotes: repressors and repression mechanisms. *Cellular and molecular life sciences : CMLS*. 2003 Apr;60(4):721-41.
146. Reynolds L, Ullman C, Moore M, Isalan M, West MJ, Clapham P, et al. Repression of the HIV-1 5' LTR promoter and inhibition of HIV-1 replication by using engineered zinc-finger transcription factors. *Proc Natl Acad Sci U S A*. 2003;100(4):1615-20.
147. Garg A, Lohmueller JJ, Silver PA, Armel TZ. Engineering synthetic TAL effectors with orthogonal target sites. *Nucleic Acids Res*. 2012 Aug;40(15):7584-95.
148. Gilbert Luke A, Horlbeck Max A, Adamson B, Villalta Jacqueline E, Chen Y, Whitehead Evan H, et al. Genome-Scale CRISPR-Mediated Control of Gene Repression and Activation. *Cell*. 2014;159(3):647-61.
149. Schultz DC, Ayyanathan K, Negorev D, Maul GG, Rauscher FJ, 3rd. SETDB1: a novel KAP-1-associated histone H3, lysine 9-specific methyltransferase that contributes to HP1-mediated silencing of euchromatic genes by KRAB zinc-finger proteins. *Genes & development*. 2002 Apr 15;16(8):919-32.
150. Barde I, Laurenti E, Verp S, Groner AC, Towne C, Padrun V, et al. Regulation of episomal gene expression by KRAB/KAP1-mediated histone modifications. *Journal of virology*. 2009 Jun;83(11):5574-80.

151. Gilbert Luke A, Larson Matthew H, Morsut L, Liu Z, Brar Gloria A, Torres Sandra E, et al. CRISPR-Mediated Modular RNA-Guided Regulation of Transcription in Eukaryotes. *Cell*. 2013;154(2):442-51.
152. Thakore PI, D'Ippolito AM, Song L, Safi A, Shivakumar NK, Kabadi AM, et al. Highly specific epigenome editing by CRISPR-Cas9 repressors for silencing of distal regulatory elements. *Nat Meth*. [Article]. 2015;12(12):1143-9.
153. Kearns NA, Genga RMJ, Enuameh MS, Garber M, Wolfe SA, Maehr R. Cas9 effector-mediated regulation of transcription and differentiation in human pluripotent stem cells. *Development*. 2014 2014-01-01 00:00:00;141(1):219-23.
154. Zhao X, Zhao Z, Guo J, Huang P, Zhu X, Zhou X, et al. Creation of a six-fingered artificial transcription factor that represses the hepatitis B virus HBx gene integrated into a human hepatocellular carcinoma cell line. *J Biomol Screen*. 2013;18(4):378-87.
155. Eberhardy SR, Goncalves J, Coelho S, Segal DJ, Berkhout B, Barbas CF, 3rd. Inhibition of human immunodeficiency virus type 1 replication with artificial transcription factors targeting the highly conserved primer-binding site. *Journal of virology*. 2006;80(6):2873-83.
156. Mahfouz MM, Li L, Piatek M, Fang X, Mansour H, Bangarusamy DK, et al. Targeted transcriptional repression using a chimeric TALE-SRDX repressor protein. *Plant Molecular Biology*. 2012;78(3):311-21.
157. Werner J, Gossen M. Modes of TAL effector-mediated repression. *Nucleic Acids Res*. 2014;42(21):13061-73.
158. Gao X, Tsang JC, Gaba F, Wu D, Lu L, Liu P. Comparison of TALE designer transcription factors and the CRISPR/dCas9 in regulation of gene expression by targeting enhancers. *Nucleic Acids Res*. 2014;42(20):e155-e.

159. Zhang F, Cong L, Lodato S, Kosuri S, Church G, Arlotta P. Programmable Sequence-Specific Transcriptional Regulation of Mammalian Genome Using Designer TAL Effectors. *Nature biotechnology*. 2011 01/19;29(2):149-53.
160. Maeder ML, Linder SJ, Reyon D, Angstman JF, Fu Y, Sander JD, et al. Robust, synergistic regulation of human gene expression using TALE activators. *Nature methods*. 2013 02/10;10(3):243-5.
161. Zhang Z, Wu E, Qian Z, Wu W-S. A multicolor panel of TALE-KRAB based transcriptional repressor vectors enabling knockdown of multiple gene targets. *Scientific Reports*. 2014;4:7338.
162. Margolin JF, Friedman JR, Meyer WK, Vissing H, Thiesen HJ, Rauscher FJ, 3rd. Kruppel-associated boxes are potent transcriptional repression domains. *Proc Natl Acad Sci U S A*. 1994 May 10;91(10):4509-13.
163. Peng H, Begg GE, Harper SL, Friedman JR, Speicher DW, Rauscher FJ, 3rd. Biochemical analysis of the Kruppel-associated box (KRAB) transcriptional repression domain. *The Journal of biological chemistry*. 2000 Jun 16;275(24):18000-10.
164. Urrutia R. KRAB-containing zinc-finger repressor proteins. *Genome Biology*. 2003 09/23;4(10):231-.
165. Lupo A, Cesaro E, Montano G, Zurlo D, Izzo P, Costanzo P. KRAB-Zinc Finger Proteins: A Repressor Family Displaying Multiple Biological Functions. *Current Genomics*. 2013;14(4):268-78.
166. Friedman JR, Fredericks WJ, Jensen DE, Speicher DW, Huang XP, Neilson EG, et al. KAP-1, a novel corepressor for the highly conserved KRAB repression domain. *Genes & development*. 1996 Aug 15;10(16):2067-78.
167. Ryan RF, Schultz DC, Ayyanathan K, Singh PB, Friedman JR, Fredericks WJ, et al. KAP-1 corepressor protein interacts and colocalizes with heterochromatic and

euchromatic HP1 proteins: a potential role for Krüppel-associated box–zinc finger proteins in heterochromatin-mediated gene silencing. *Molecular and cellular biology*.

1999;19(6):4366-78.

168. Groner AC, Meylan S, Ciuffi A, Zangger N, Ambrosini G, Déneraud N, et al. KRAB–Zinc Finger Proteins and KAP1 Can Mediate Long-Range Transcriptional Repression through Heterochromatin Spreading. *PLoS Genet*. 2010;6(3):e1000869.

169. Ayyanathan K, Lechner MS, Bell P, Maul GG, Schultz DC, Yamada Y, et al. Regulated recruitment of HP1 to a euchromatic gene induces mitotically heritable, epigenetic gene silencing: a mammalian cell culture model of gene variegation. *Genes & development*. 2003;17(15):1855-69.

170. Hodel MR, Corbett AH, Hodel AE. Dissection of a nuclear localization signal. *Journal of Biological Chemistry*. 2001;276(2):1317-25.

171. Costa RH, Grayson DR. Site-directed mutagenesis of hepatocyte nuclear factor (HNF) binding sites in the mouse transthyretin (TTR) promoter reveal synergistic interactions with its enhancer region. *Nucleic Acids Res*. 1991 Aug 11;19(15):4139-45.

172. Nassal M, Junker-Niepmann M, Schaller H. Translational inactivation of RNA function: discrimination against a subset of genomic transcripts during HBV nucleocapsid assembly. *Cell*. 1990 Dec 21;63(6):1357-63.

173. Passman M, Weinberg M, Kew M, Arbuthnot P. In situ demonstration of inhibitory effects of hammerhead ribozymes that are targeted to the hepatitis Bx sequence in cultured cells. *Biochemical and biophysical research communications*. 2000;268(3):728-33.

174. Bloom K, Ely A, Mussolino C, Cathomen T, Arbuthnot P. Inactivation of Hepatitis B Virus Replication in Cultured Cells and In Vivo with Engineered Transcription Activator-Like Effector Nucleases. *Mol Ther*. [Original Article]. 2013;21(10):1889-97.

175. Doyle EL, Booher NJ, Standage DS, Voytas DF, Brendel VP, VanDyk JK, et al. TAL Effector-Nucleotide Targeter (TALE-NT) 2.0: tools for TAL effector design and target prediction. *Nucleic Acids Research*. 2012;40(W1):W117-W22.
176. Ricciarelli R, Fedele E. Phosphodiesterase 4D: an enzyme to remember. *British journal of pharmacology*. 2015;172(20):4785-9.
177. Lin B, White JT, Ferguson C, Bumgarner R, Friedman C, Trask B, et al. PART-1: a novel human prostate-specific, androgen-regulated gene that maps to chromosome 5q12. *Cancer research*. 2000;60(4):858-63.
178. Mosmann T. Rapid colorimetric assay for cellular growth and survival: application to proliferation and cytotoxicity assays. *Journal of immunological methods*. 1983;65(1-2):55-63.
179. Jørgensen C, Yasmeen S, Iversen HK, Kruuse C. Phosphodiesterase4D (PDE4D)—A risk factor for atrial fibrillation and stroke? *Journal of the neurological sciences*. 2015;359(1):266-74.
180. Bock CT, Schwinn S, Locarnini S, Fyfe J, Manns MP, Trautwein C, et al. Structural organization of the hepatitis B virus minichromosome. *Journal of molecular biology*. 2001;307(1):183-96.
181. Pollicino T, Belloni L, Raffa G, Pediconi N, Squadrito G, Raimondo G, et al. Hepatitis B virus replication is regulated by the acetylation status of hepatitis B virus cccDNA-bound H3 and H4 histones. *Gastroenterology*. 2006 Mar;130(3):823-37.
182. Baumhueter S, Mendel DB, Conley PB, Kuo CJ, Turk C, Graves M, et al. HNF-1 shares three sequence motifs with the POU domain proteins and is identical to LF-B1 and APF. *Genes & development*. 1990;4(3):372-9.

183. Sladek FM, Zhong W, Lai E, Darnell J. Liver-enriched transcription factor HNF-4 is a novel member of the steroid hormone receptor superfamily. *Genes & development*. 1990;4(12b):2353-65.
184. Thakore PI, Gersbach CA. Design, Assembly, and Characterization of TALE-Based Transcriptional Activators and Repressors. *TALENs: Methods and Protocols*. 2016:71-88.
185. Cermak T, Doyle EL, Christian M, Wang L, Zhang Y, Schmidt C, et al. Efficient design and assembly of custom TALEN and other TAL effector-based constructs for DNA targeting. *Nucleic Acids Res*. 2011 Jul;39(12):e82.
186. Li Z, Luo W, Fu Y, Jiang Q, Liu J, Wu Z. Inhibition of HBV replication by constructing an artificial transcription factor. *Xi bao yu fen zi mian yi xue za zhi= Chinese journal of cellular and molecular immunology*. 2015;31(10):1322-6, 31.
187. Garriga-Canut M, Agustín-Pavón C, Herrmann F, Sánchez A, Dierssen M, Fillat C, et al. Synthetic zinc finger repressors reduce mutant huntingtin expression in the brain of R6/2 mice. *Proceedings of the National Academy of Sciences*. 2012;109(45):E3136-E45.
188. Li Y, Moore R, Guinn M, Bleris L. Transcription activator-like effector hybrids for conditional control and rewiring of chromosomal transgene expression. *Scientific Reports*. 2012;2:897.
189. Zimmerman KA, Fischer KP, Joyce MA, Tyrrell DL. Zinc finger proteins designed to specifically target duck hepatitis B virus covalently closed circular DNA inhibit viral transcription in tissue culture. *Journal of virology*. 2008 Aug;82(16):8013-21.
190. Enríquez P. Focus: Epigenetics: CRISPR-Mediated Epigenome Editing. *The Yale Journal of Biology and Medicine*. 2016;89(4):471.

191. de Groote ML, Verschure PJ, Rots MG. Epigenetic editing: targeted rewriting of epigenetic marks to modulate expression of selected target genes. *Nucleic Acids Research*. 2012:gks863.
192. Sripathy SP, Stevens J, Schultz DC. The KAP1 corepressor functions to coordinate the assembly of de novo HP1-demarcated microenvironments of heterochromatin required for KRAB zinc finger protein-mediated transcriptional repression. *Molecular and cellular biology*. 2006;26(22):8623-38.
193. Reynolds N, Salmon-Divon M, Dvinge H, Hynes-Allen A, Balasooriya G, Leaford D, et al. NuRD-mediated deacetylation of H3K27 facilitates recruitment of Polycomb Repressive Complex 2 to direct gene repression. *The EMBO journal*. 2012;31(3):593-605.
194. Reyon D, Tsai SQ, Khayter C, Foden JA, Sander JD, Joung JK. FLASH assembly of TALENs for high-throughput genome editing. *Nature biotechnology*. 2012 May;30(5):460-5.
195. Miller JC, Tan S, Qiao G, Barlow KA, Wang J, Xia DF, et al. A TALE nuclease architecture for efficient genome editing. *Nature biotechnology*. 2011;29(2):143-8.
196. Morbitzer R, Römer P, Boch J, Lahaye T. Regulation of selected genome loci using de novo-engineered transcription activator-like effector (TALE)-type transcription factors. *Proceedings of the National Academy of Sciences*. 2010;107(50):21617-22.
197. Tesson L, Usal C, Ménoret S, Leung E, Niles BJ, Remy S, et al. Knockout rats generated by embryo microinjection of TALENs. *Nature biotechnology*. 2011;29(8):695-6.
198. Mussolino C, Morbitzer R, Lutge F, Dannemann N, Lahaye T, Cathomen T. A novel TALE nuclease scaffold enables high genome editing activity in combination with low toxicity. *Nucleic Acids Res*. 2011;39(21):9283-93.

199. Grimmer MR, Stolzenburg S, Ford E, Lister R, Blancafort P, Farnham PJ. Analysis of an artificial zinc finger epigenetic modulator: widespread binding but limited regulation. *Nucleic Acids Research*. 2014:gku708.
200. Grau J, Wolf A, Reschke M, Bonas U, Posch S, Boch J. Computational predictions provide insights into the biology of TAL effector target sites. *PLoS Comput Biol*. 2013;9(3):e1002962.
201. Rogers JM, Barrera LA, Reyon D, Sander JD, Kellis M, Joung JK, et al. Context influences on TALE-DNA binding revealed by quantitative profiling. *Nature communications*. 2015;6.
202. Morbitzer R, Elsaesser J, Hausner J, Lahaye T. Assembly of custom TALE-type DNA binding domains by modular cloning. *Nucleic Acids Res*. 2011;39(13):5790-9.
203. Perez-Pinera P, Kocak DD, Vockley CM, Adler AF, Kabadi AM, Polstein LR, et al. RNA-guided gene activation by CRISPR-Cas9-based transcription factors. *Nature methods*. 2013;10(10):973-6.
204. Guidotti LG, Matzke B, Schaller H, Chisari FV. High-level hepatitis B virus replication in transgenic mice. *Journal of virology*. 1995;69(10):6158-69.
205. Paronetto F, Tennant B. Woodchuck hepatitis virus infection: a model of human hepatic diseases and hepatocellular carcinoma. *Progress in liver diseases*. 1990;9:463-83.
206. Meuleman P, Leroux-Roels G. The human liver-uPA-SCID mouse: a model for the evaluation of antiviral compounds against HBV and HCV. *Antiviral research*. 2008;80(3):231-8.
207. Winer BY, Ding Q, Gaska JM, Ploss A. In vivo models of hepatitis B and C virus infection. *FEBS letters*. 2016;590(13):1987-99.
208. Inuzuka T, Takahashi K, Chiba T, Marusawa H. Mouse models of hepatitis B virus infection comprising host-virus immunologic interactions. *Pathogens*. 2014;3(2):377-89.

209. Tsuge M, Hiraga N, Takaishi H, Noguchi C, Oga H, Imamura M, et al. Infection of human hepatocyte chimeric mouse with genetically engineered hepatitis B virus. *Hepatology (Baltimore, Md)*. 2005;42(5):1046-54.
210. Dandri M, Burda MR, Zuckerman DM, Wursthorn K, Matschl U, Pollok JM, et al. Chronic infection with hepatitis B viruses and antiviral drug evaluation in uPA mice after liver repopulation with tupaia hepatocytes. *Journal of Hepatology*. 2005;42(1):54-60.
211. Petersen J, Dandri M, Mier W, Lütgehetmann M, Volz T, von Weizsäcker F, et al. Prevention of hepatitis B virus infection in vivo by entry inhibitors derived from the large envelope protein. *Nature biotechnology*. 2008;26(3):335-41.
212. Yang H-C, Kao J-H. Persistence of hepatitis B virus covalently closed circular DNA in hepatocytes: molecular mechanisms and clinical significance. *Emerging Microbes & Infections*. 2014;3(9):e64.
213. Kapoor R, Kottilil S. Strategies to eliminate HBV infection. *Future virology*. 2014;9(6):565-85.
214. Schreier H. The new frontier: gene and oligonucleotide therapy. *Pharmaceutica Acta Helvetiae*. 1994;68(3):145-59.
215. Coura RdS, Nardi NB. A role for adeno-associated viral vectors in gene therapy. *Genetics and Molecular Biology*. 2008;31(1):1-11.
216. Mali S. Delivery systems for gene therapy. *Indian journal of human genetics*. 2013;19(1):3.
217. Maggio I, Goncalves MA. Genome editing at the crossroads of delivery, specificity, and fidelity. *Trends in biotechnology*. 2015;33(5):280-91.
218. Dropulić B. Lentiviral vectors: their molecular design, safety, and use in laboratory and preclinical research. *Human gene therapy*. 2011;22(6):649-57.

219. Wang L, Li F, Dang L, Liang C, Wang C, He B, et al. In vivo delivery systems for therapeutic genome editing. *International Journal of Molecular Sciences*. 2016;17(5):626.
220. Mowa MB, Crowther C, Arbuthnot P. Therapeutic potential of adenoviral vectors for delivery of expressed RNAi activators. *Expert opinion on drug delivery*. 2010;7(12):1373-85.
221. Gupta RM, Musunuru K. Expanding the genetic editing tool kit: ZFNs, TALENs, and CRISPR-Cas9. *J Clin Invest*. 2014;124(10):4154-61.
222. Al-Dosari MS, Gao X. Nonviral gene delivery: principle, limitations, and recent progress. *The AAPS journal*. 2009;11(4):671.
223. Gardlík R, Pálffy R, Hodosy J, Lukács J, Turna J, Celec P. Vectors and delivery systems in gene therapy. *Medical Science Monitor*. 2005;11(4):RA110-RA21.
224. Ru R, Yao Y, Yu S, Yin B, Xu W, Zhao S, et al. Targeted genome engineering in human induced pluripotent stem cells by penetrating TALENs. *Cell Regeneration*. 2013;2(1):5.
225. Lainšček D, Lebar T, Jerala R. Transcription activator-like effector-mediated regulation of gene expression based on the inducible packaging and delivery via designed extracellular vesicles. *Biochemical and Biophysical Research Communications*. 2017;484(1):15-20.
226. Cevher E, Sezer AD, Çağlar EŞ. Gene delivery systems: recent progress in viral and non-viral therapy: INTECH Open Access Publisher; 2012.
227. Keswani RK, Lazebnik M, Pack DW. Intracellular trafficking of hybrid gene delivery vectors. *Journal of Controlled Release*. 2015;207:120-30.
228. Hodgson CP, Solaiman F. Virosomes: cationic liposomes enhance retroviral transduction. *Nature biotechnology*. 1996;14(3):339-42.

229. Keswani R, Su K, Pack DW. Efficient in vitro gene delivery by hybrid biopolymer/virus nanobiovectors. *Journal of Controlled Release*. 2014;192:40-6.
230. Arbuthnot P. *Gene therapy for viral infections*: Academic Press; 2015.